TIA/EIA/IS-69.5

TIA/EIA INTERIM STANDARD

Enhanced Digital Access Communications System IMBE™ Implementation

TIA/EIA/IS-69.5

APRIL 2000

TELECOMMUNICATIONS INDUSTRY ASSOCIATION

Representing the telecommunications industry in association with the Electronic Industries Alliance

NOTICE

TIA/EIA Engineering Standards and Publications are designed to serve the public interest through eliminating misunderstandings between manufacturers and purchasers, facilitating interchangeability and improvement of products, and assisting the purchaser in selecting and obtaining with minimum delay the proper product for his particular need. Existence of such Standards and Publications shall not in any respect preclude any member or nonmember of TIA/EIA from manufacturing or selling products not conforming to such Standards and Publications, nor shall the existence of such Standards and Publications preclude their voluntary use by those other than TIA/EIA members, whether the standard is to be used either domestically or internationally.

Standards and Publications are adopted by TIA/EIA in accordance with the American National Standards Institute (ANSI) patent policy. By such action, TIA/EIA does not assume any liability to any patent owner, nor does it assume any obligation whatever to parties adopting the Standard or Publication.

TIA/EIA INTERIM STANDARDS

TIA/EIA Interim Standards contain information deemed to be of technical value to the industry, and are published at the request of the originating Committee without necessarily following the rigorous public review and resolution of comments which is a procedural part of the development of a TIA/EIA Standard.

TIA/EIA Interim Standards should be reviewed on an annual basis by the formulating Committee and a decision made on whether to proceed to develop a TIA/EIA Standard on this subject. TIA/EIA Interim Standards must be cancelled by the Committee and removed from the TIA/EIA Standards Catalog before the end of their third year of existence.

Publication of this TIA/EIA Interim Standard for trial use and comment has been approved by the Telecommunications Industry Association. Distribution of this TIA/EIA Interim Standard for comment shall not continue beyond 36 months from the date of publication. It is expected that following this 36 month period, this TIA/EIA Interim Standard, revised as necessary, will be submitted to the American National Standards Institute for approval as an American National Standard. Suggestions for revision should be directed to: Standards & Technology Department, Telecommunications Industry Association, 2500 Wilson Boulevard, Arlington, VA 22201.

(From Project No. 4223, formulated under the cognizance of the TIA TR-8.4 Subcommittee on Vocoders.)

Published by

©TELECOMMUNICATIONS INDUSTRY ASSOCIATION 2000
Standards & Technology Department
2500 Wilson Boulevard
Arlington, VA 22201

PRICE: Please refer to current Catalog of
EIA ELECTRONIC INDUSTRIES ALLIANCE STANDARDS and ENGINEERING PUBLICATIONS or call Global Engineering Documents, USA and Canada (1-800-854-7179) International (303-397-7956)

PLEASE!

DON'T VIOLATE
THE
LAW!

Foreword

(This foreword is not part of this standard)

This Enhanced Digital Access Communications System (EDACS™) IMBE Vocoder description describes the vocoder for land mobile radios meeting EDACS requirements.

As a group, the family of Enhanced Digital Access Communications Systems documents describe the system, inclusive of the equipment requirements which allow both compatibility and interoperability between various systems and elements. The family of documents will be backward compatible and interoperable with existing installed Enhanced Digital Access Communications Systems as further defined within this family of documents.

This document has been developed with inputs from the Vocoders subcommittee (TR-8.4), TIA Industry Members, and the International EDACS User's Group, under the sponsorship of TIA.

For information on specific implementations, as they are developed, the reader is referred to the EDACS System and Shell Standard, originally published as TSB69 for; An EDACS Overview, a Glossary, and a Statement of Requirements.

The reader's attention is called to the possibility that compliance with this Standard may require the use of one or more inventions covered by patent rights.

By publication of this Interim Standard, no position is taken with respect to the validity of those claims or any patent rights in connection therewith. The patent holders so far identified have, however, filed statements of willingness to grant licenses under those rights on reasonable and nondiscriminatory terms and conditions to applicants desiring to obtain such licenses. Details may be obtained from the publisher.

Jim Holthaus
Chairman TR-8.4

(This page intentionally left blank)

Enhanced Digital Access Communications System
IMBE™ Implementation

Digital Voice Systems Inc. (DVSI) claims certain rights, including patent rights, in the Improved Multi-Band Excitation (IMBE) voice coding algorithm described in this document and elsewhere. Any use of this technology requires written license from DVSI. DVSI is willing to grant a royalty-bearing license to use the IMBE voice coding algorithm for Enhanced Digital Access Communications Systems under a set of standard terms and conditions. Details may be obtained by contacting DVSI as indicated below.

Digital Voice Systems, Inc.
One Van deGraff Drive
Burlington, MA 01803
Phone: 781-270-1030
Fax: 781-270-0166

DVSI acknowledges the Massachusetts Institute of Technology where the Multi-Band Excitation speech model was developed. In addition DVSI acknowledges the Rome Air Development Center of the United States Air Force which supported the early development of the Multi-Band Excitation speech model.

September 8, 1998

(This page intentionally left blank)

CONTENTS

Figures

Tables

1 Scope

This document specifies a voice coding method for the Enhanced Digital Access Communication System. It describes the functional requirements for the transmission and reception of voice information using digital communication media described in the standard. This document is specifically intended to define the conversion of voice from an analog representation to a digital representation that consists of a net bit rate of 4.4 kbps for voice information, and a gross bit rate of 7.1 kbps after error control coding.

The voice coder (or vocoder) presented in this document is intended to be used through-out a system in any equipment that requires an analog-to-digital or digital-to-analog voice interface. Specifically, mobile and portable radios as well as console equipment and gateways to voice networks may contain the vocoder described in this document.

2 Introduction

This document provides a functional description of the Improved Multi-Band Excitation (IMBE) voice coding algorithm adopted for Enhanced Digital Access Communications Systems. This document describes the essential operations that are necessary and sufficient to implement this voice coding algorithm. However, it is highly recommended that the references be studied prior to the implementation of this algorithm. It is also recommended that implementations begin with a high-level language simulation of the algorithm, and then proceed to a real-time implementation using a digital signal processor. High performance real-time implementations have been demonstrated using both floating-point and fixed-point processors. The reader is cautioned that this document does not attempt to describe the most efficient means of implementing the IMBE vocoder. The reader should consult one or more references on efficient real-time programming for more information on this subject. Additionally this document does not address vocoder testing and verification. These subjects will be addressed in separate documents that may be released at a later time.

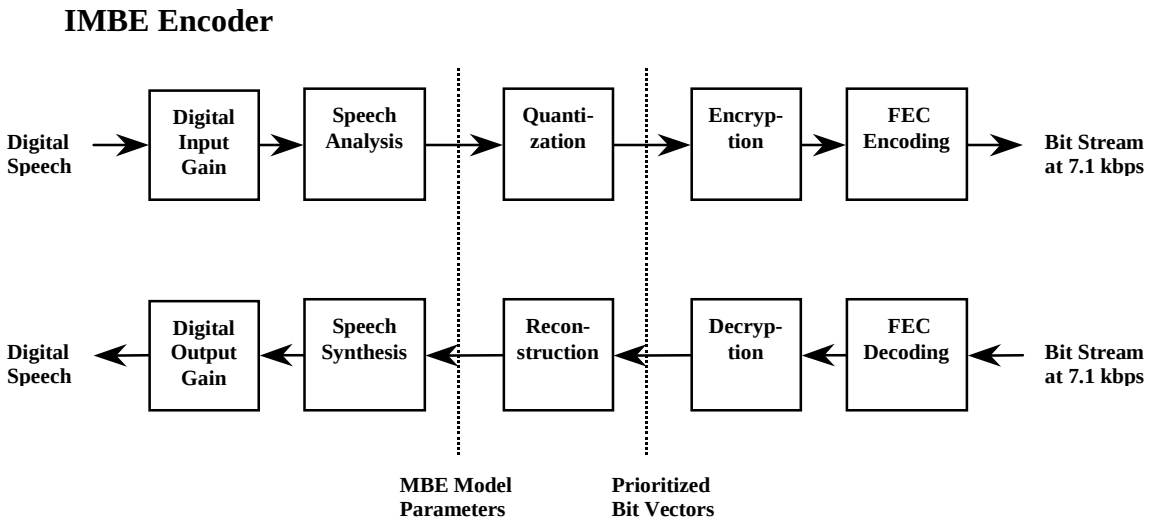

Figure 1: Improved Multi-Band Excitation Speech Coder

The IMBE speech coder is based on a robust speech model which is referred to as the Multi-Band Excitation (MBE) speech model [3]. The basic methodology of the coder is to divide a digital speech input signal into overlapping speech segments (or frames) using a window such as a Kaiser window. Each speech frame is then compared with the underlying speech model, and a set of model parameters are estimated for that particular frame. The encoder quantizes these model parameters and transmits a bit stream at 7.1 kbps. The decoder receives this bit stream, reconstructs the model parameters, and uses these model parameters to generate a synthetic speech signal. This synthesized speech signal is the output of the IMBE speech coder as shown in Figure 1. One should note that the IMBE speech coder shown in this figure and defined by this document is a digital-to-digital function.

The IMBE speech coder is a model-based speech coder, or vocoder, which does not try to reproduce the input speech signal on a sample by sample basis. Instead the IMBE speech coder constructs a synthetic speech signal which contains the same perceptual information as the original speech signal. Many previous vocoders (such as LPC vocoders, homomorphic vocoders, and channel vocoders) have not been successful in producing high quality synthetic speech. The IMBE speech coder has two primary advantages over these vocoders. First, the IMBE speech coder is based on the MBE speech model which is a more robust model than the traditional speech models used in previous vocoders. Second, the IMBE speech coder uses more sophisticated algorithms to estimate the speech model parameters, and to synthesize the speech signal from these model parameters.

This document is organized as follows. In Section 3 the MBE speech model is briefly reviewed. This section presents background material which is useful in understanding operation of the IMBE speech coder.

Section 4 describes the basic speech input/output requirements. Section 5 examines the methods used to estimate the speech model parameters, and Section 6 examines the quantization and reconstruction of the MBE model parameters. The error correction and the format of the 7.1 kbps bit stream is discussed in Section 7. This is followed by Section 8 which describes the enhancement of the spectral amplitudes, and Section 9 which describes the adaptive smoothing method used to reduce the effect of uncorrectable bit errors. Section 10 then demonstrates the encoding of a typical set of model parameters. Section 11 discusses the synthesis of speech from the MBE model parameters. A few additional comments on the algorithm and this document are provided in Section 12. Other information such as bit allocation tables, quantization levels and initialization vectors are contained in the attached appendices. In addition, Appendix K contains a set of flow charts describing certain elements of this vocoder. Note that these flow charts have been designed to help clarify the various algorithmic steps and do not necessarily describe the best or most efficient method of implementing the vocoder.

3 Multi-Band Excitation Speech Model

Let $s(n)$ denote a discrete speech signal obtained by sampling an analog speech signal. In order to focus attention on a short segment of speech over which the model parameters are assumed to be constant, a window $w(n)$ is applied to the speech signal $s(n)$. The windowed speech signal $s_w(n)$ is defined by

$$s_w(n) = s(n)w(n) \tag{1}$$

The sequence $s_w(n)$ is referred to as a speech segment or a speech frame. The IMBE analysis algorithm actually uses two different windows, $w_R(n)$ and $w_I(n)$, each of which is applied separately to the speech signal via Equation (1). This will be explained in more detail in Section 5 of this document. The speech signal $s(n)$ is shifted in time to select any desired segment. For notational convenience $s_w(n)$ refers to the current speech frame. The next speech frame is obtained by shifting $s(n)$ by 20 ms.

A speech segment $s_w(n)$ is modelled as the response of a linear filter $h_w(n)$ to some excitation signal $e_w(n)$. Therefore, $S_w(\omega)$, the Fourier Transform of $s_w(n)$, can be expressed as

$$S_w(\omega) = H_w(\omega)E_w(\omega) \tag{2}$$

where $H_w(\omega)$ and $E_w(\omega)$ are the Fourier Transforms of $h_w(n)$ and $e_w(n)$, respectively.

In traditional speech models, speech is divided into two classes depending upon the nature of excitation signal. For voiced speech the excitation signal is a periodic impulse sequence, where the distance between impulses is the pitch period P_0. For unvoiced speech the excitation signal is a white noise sequence. One of the primary distinctions between traditional vocoders is the method in which they model the linear filter $h_w(n)$. The frequency response of this filter is generally referred to as the spectral envelope of the speech signal. In a LPC vocoder, for example, the spectral envelope is modeled with a low order all-pole model. Similarly, in a homomorphic vocoder, the spectral envelope is modeled with a small number of cepstral coefficients.

A primary difference between traditional speech models and the MBE speech model is the excitation signal. In conventional speech models a single voiced/unvoiced (V/UV) decision is used for each speech segment. In contrast the MBE speech model divides the excitation spectrum into a number of non-overlapping frequency bands and makes a V/UV decision for each frequency band. This allows the excitation signal for a particular speech segment to be a mixture of periodic (voiced) energy and noise-like (unvoiced) energy. This added degree of freedom in the modelling of the excitation allows the MBE speech model to generate higher quality speech than conventional speech models. In addition it allows the MBE speech model to be robust to the presence of background noise.

In the MBE speech model the excitation spectrum is obtained from the pitch period (or the fundamental frequency) and the V/UV decisions. A periodic spectrum is used in the frequency bands declared voiced, while a random noise spectrum is used in the frequency bands declared unvoiced. The periodic spectrum is generated from a windowed periodic impulse train which is completely determined by the window and the pitch period. The random noise spectrum is generated from a windowed random noise sequence.

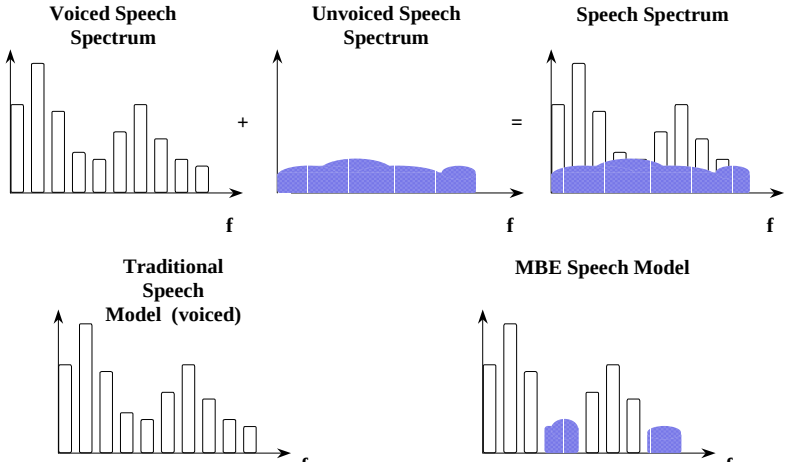

Figure 2: Comparison of Traditional and MBE Speech Models

A comparison of a traditional speech model and the MBE speech model is shown in Figure 2. In this example the traditional model has classified the speech segment as voiced, and consequently the

traditional speech model is composed completely of periodic energy. The MBE model has divided the spectrum into 10 frequency bands in this example. The fourth, fifth, ninth and tenth bands have been declared unvoiced while the remaining bands have been declared voiced. The excitation in the MBE model is comprised of periodic energy only in the frequency bands declared voiced, while the remaining bands are comprised of noise-like energy. This example shows an important feature of the MBE speech model. Namely, the V/UV determination is performed such that frequency bands where the ratio of periodic energy to noise-like energy is high are declared voiced, while frequency bands where this ratio is low are declared unvoiced. The details of this procedure are discussed in Section 5.2.

4 Speech Input/Output Requirements

This section presents a number of performance recommendations for the analog front end of a voice codec, including the gain, filtering, and conversion elements as depicted in Figure 3. The objective is to establish a set of input/output requirements that will ensure that the voice codec operates at its maximum capability. The reader should note that Figure 3 shows four reference points (analog input, analog output, digital input and digital output) which are used in this document and will be used in future documents describing the test and verification procedure used with this vocoder.

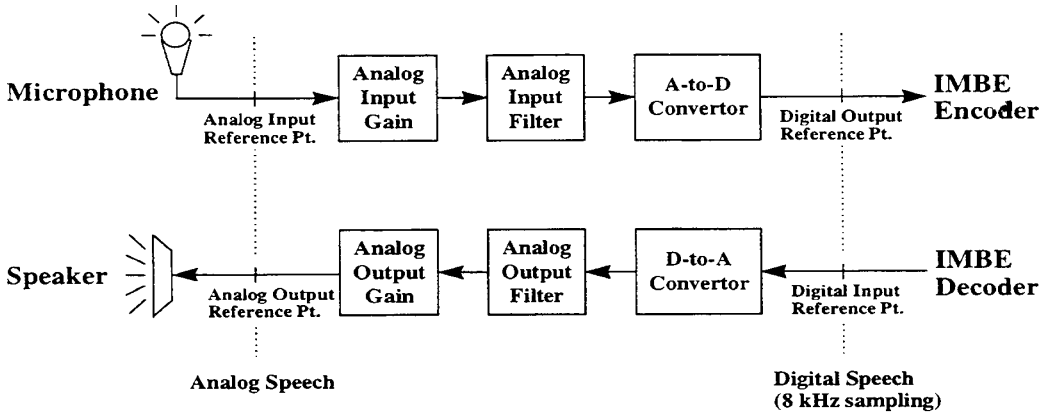

Fig. 3: Analog Front End

The voice encoder and decoder defined in the remainder of this document operates with unity (i.e. 0 dB) gain. Consequently the analog input and output gain elements shown in Figure 3 are only used to match the sensitivity of the microphone and speaker with the A-to-D converters and D-to-A converters, respectively. It is recommended that the analog input be set such that the RMS speech level under nominal input conditions is 25 dB below the saturation point of the A-to-D converter. This level (-22 dBm0) is designed to provide sufficient margin to prevent the peaks of the speech waveform from being clipped by the A-to-D converter.

The voice coder defined in this document requires the A-to-D and D-to-A converters to operate at an 8 kHz sampling rate (i.e. a sampling period of 125 microseconds) at the digital input/output reference points. This requirement necessitates the use of analog filters at both the input and output to eliminate any frequency components above the Nyquist frequency (4 kHz). The recommended input and output filter masks are shown in Figure 4. For proper operation, the frequency response of the analog filters should be bounded by the shaded zone depicted in this figure.

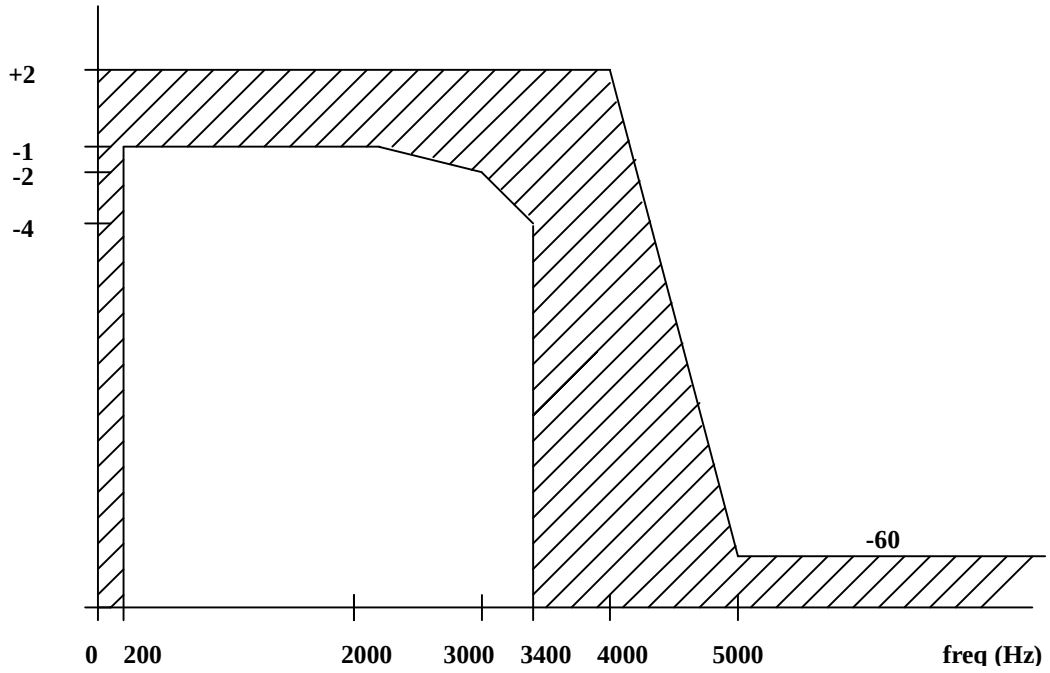

Fig. 4: Analog Input/Output Filter Mask

This vocoder description assumes that the A-to-D converter produces digital speech which is confined to the range [-32768, 32767], and similarly that the D-to-A converter accepts digital speech within this same range. If a converter is used which does not meet these assumptions then the digital gain elements shown in Figure 1 should be adjusted appropriately. Note that these assumptions are automatically satisfied if 16 bit linear A-to-D and D-to A converters are used, in which case the digital gain elements should be set to unity gain. Also note that the vocoder requires that any companding which is applied by the A-to-D converter (i.e. alaw or ulaw) should be removed prior to speech encoding. Similarly any companding used by the D-to-A converter must be applied after speech decoding.

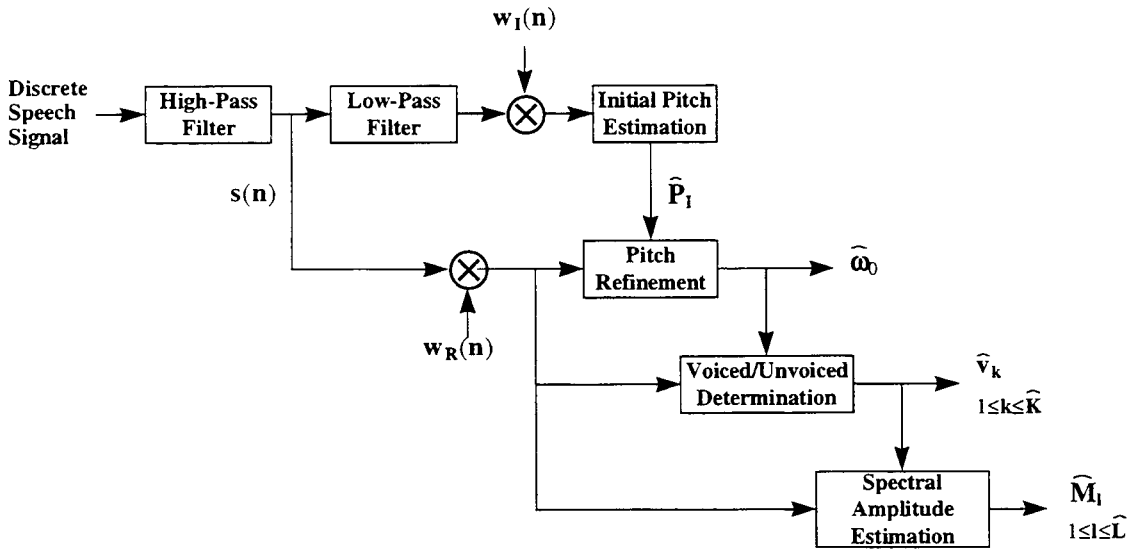

Fig. 5: IMBE Speech Analysis Algorithm

5 Speech Analysis

This section presents the methods used to estimate the MBE speech model parameters. To develop a high quality vocoder it is essential that robust and accurate algorithms are used to estimate the model parameters. The approach which is presented here differs from conventional approaches in a fundamental way. Typically algorithms for the estimation of the excitation parameters and algorithms for the estimation of the spectral envelope parameters operate independently. These parameters are usually estimated based on some reasonable but heuristic criterion without explicit consideration of how close the synthesized speech will be to the original speech. This can result in a synthetic spectrum quite different from the original spectrum. In the approach used in the IMBE speech coder the excitation and spectral envelope parameters are estimated simultaneously, so that the synthesized spectrum is closest in a least squares sense to the original speech spectrum. This approach can be viewed as an "analysis-by-synthesis" method. The theoretical derivation and justification of this approach is presented in references [3, 4, 6].

A block diagram of the analysis algorithm is shown in Figure 5. The MBE speech model parameters which must be estimated for each speech frame are the pitch period (or equivalently the fundamental frequency), the V/UV decisions, and the spectral amplitudes which characterize the spectral envelope. The organization of this section is as follows. First, the pitch estimation method is presented in Section 5.1. The V/UV determination is discussed in Section 5.2, and finally Section 5.3 discusses the estimation of the spectral amplitudes.

The input to the speech analyzer, and, consequently, the encoder, is a discrete speech signal generated using an A-to-D converter as described in Section 4. This speech signal must first be digitally

filtered to remove any residual energy at D.C. This is accomplished by passing the input signal through a discrete high-pass filter with the following transfer function:

$$H(z) = \frac{1 - z^{-1}}{1 - .99z^{-1}} \tag{3}$$

The resulting high-pass filtered signal is denoted by $s(n)$ throughout the remainder of this section. Figure 6 shows the frequency response of the filter specified in equation (3) using the convention that the Nyquist frequency (4 kHz) is mapped to a discrete frequency of π radians. For more information on this frequency convention, which is used throughout this document, the reader is referred to reference [11].

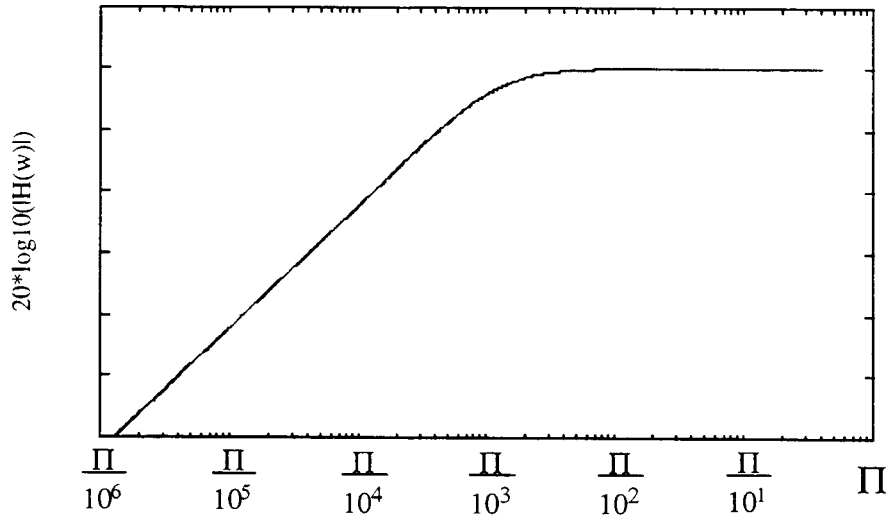

Fig. 6: High Pass Filter Frequency Response at 8 kHz Sampling Rate

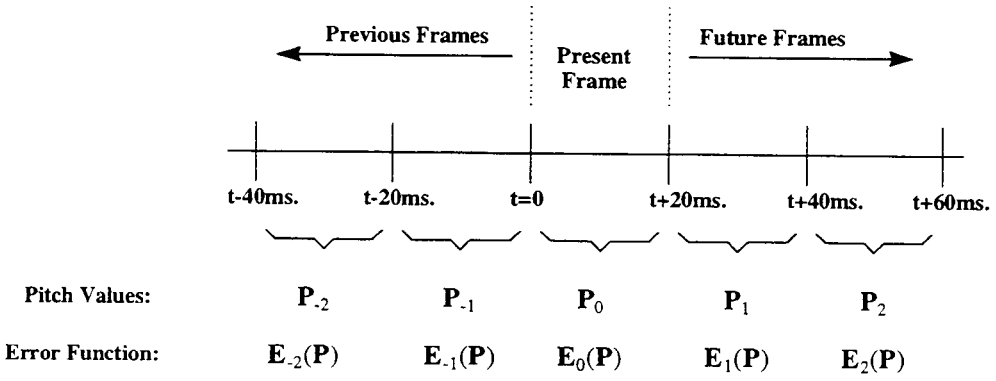

Fig. 7: Relationship between Speech Frames

5.1 Pitch Estimation

The objective in pitch estimation is to determine the pitch P_0 corresponding to the "current" speech frame $s_w(n)$. P_0 is related to the fundamental frequency ω_0 by

$$P_0 = \frac{2\pi}{\omega_0} \tag{4}$$

where P_0 is measured in samples (at 8 kHz) and ω_0 is measured in radians.

The pitch estimation algorithm attempts to preserve some continuity of the pitch between neighboring speech frames. A pitch tracking algorithm considers the pitch from previous and future frames, when determining the pitch of the current frame. Previous and future speech frames are obtained by shifting the speech signal in 160 sample (20 ms) time increments prior to the application of the window in Equation (1). The pitches corresponding to the two future speech frames are denoted by P_1 and P_2. Similarly, the pitch of the two previous speech frames are denoted by P_{-1} and P_{-2}. These relationships are shown in Figure 7.

The pitch is estimated using a two-step procedure. First an initial pitch estimate, denoted by $\hat{P}_I$, is obtained. The initial pitch estimate is restricted to be a member of the set {21, 21.5, … 121.5, 122}. It is then refined to obtain the final estimate of the fundamental frequency $\hat{\omega}_0$, which has one-quarter-sample accuracy. This two-part procedure is used in part to reduce the computational complexity, and in part to improve the robustness of the pitch estimate.

One important feature of the pitch estimation algorithm is that the initial pitch estimation algorithm uses a different window than the pitch refinement algorithm. The window used for initial pitch estimation, $w_I(n)$, is 301 samples long and is given in Annex B. The window used for pitch refinement (and also for spectral amplitude estimation and V/UV determination), $w_R(n)$, is 221 samples long and is given in Annex C. Throughout this document the window functions are assumed to be equal to zero outside the range given in the Annexes. The center point of the two windows must coincide, therefore the first non-zero point of $w_R(n)$ must begin 40 samples after the first non-zero point of $w_I(n)$. This constraint is typically met by adopting the convention that $w_R(n) = w_R(-n)$ and $w_I(n) = w_I(-n)$, as shown in Figure 8.

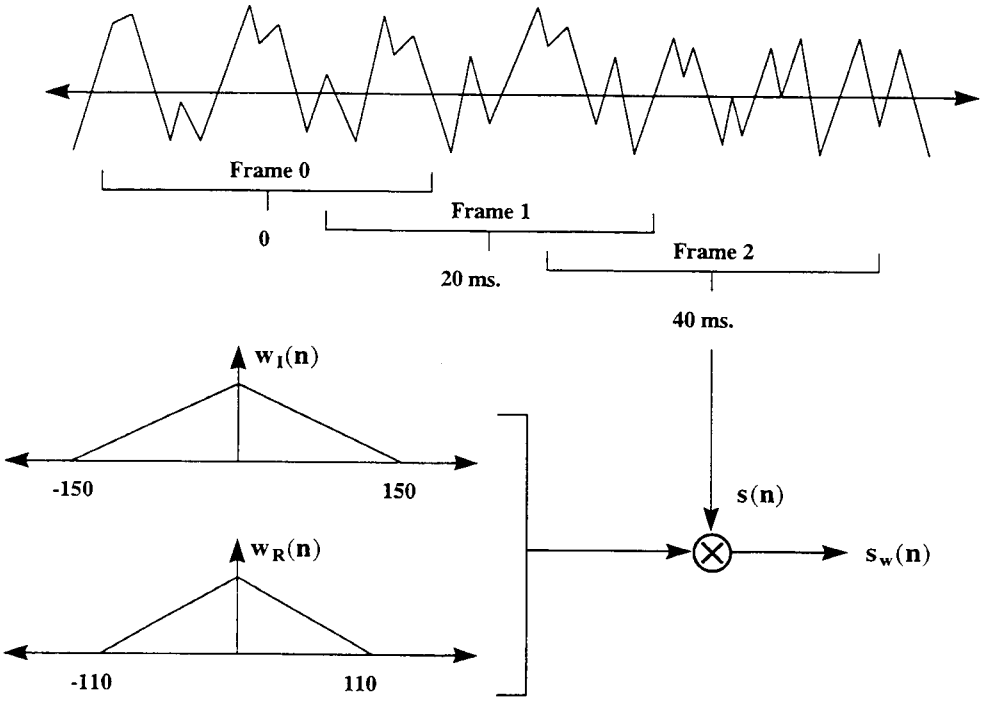

Fig. 8: Window Alignment

The amount of overlap between neighboring speech segments is a function of the window length. Specifically the overlap is equal to the window length minus the distance between frames (160 samples). Therefore the overlap when using $w_R(n)$ is equal to 61 samples and the overlap when using $w_I(n)$ is equal to 141 samples.

5.1.1 Determination of E(P)

To obtain the initial pitch estimate an error function, E(P), is evaluated for every P in the set {21, 21.5, … 121.5, 122}. Pitch tracking is then used to compare the evaluations of E(P), and the best candidate from this set is chosen as $\hat{P}_I$. This procedure is shown in Figure 9. The function E(P) is defined by

$$E(P) = \frac{\sum_{j=-150}^{150} s_{LPF}^2(j) w_I^2(j) - P \cdot \sum_{n=-\lfloor \frac{150}{P} \rfloor}^{\lfloor \frac{150}{P} \rfloor} r(n \cdot P)}{[\sum_{j=-150}^{150} s_{LPF}^2(j) w_I^2(j)][1 - P \cdot \sum_{j=-150}^{150} w_I^4(j)]} \quad (5)$$

where $w_I(n)$ is normalized to meet the constraint

$$\sum_{j=-150}^{150} w_I^2(j) = 1.0 \quad (6)$$

This constraint is satisfied for $w_I(n)$ listed in Annex B. The function $r(t)$ is defined for integer values of t by

$$r(t) = \sum_{j=-150}^{150} s_{LPF}(j)w_I^2(j)s_{LPF}(j+t)w_I^2(j+t) \quad (7)$$

The function $r(t)$ is evaluated at non-integer values of t through linear interpolation:

$$r(t) = (1 + \lfloor t \rfloor - t) \cdot r(\lfloor t \rfloor) + (t - \lfloor t \rfloor) \cdot r(\lfloor t \rfloor + 1) \quad (8)$$

where $[x]$ is equal to the largest integer less than or equal to x (i.e. truncating values of x). The low-pass filtered speech signal is given by

$$s_{LPF}(n) = \sum_{j=-10}^{10} s(n-j)h_{LPF}(j) \quad (9)$$

where $h_{LPF}(n)$ is the 21 point FIR filter given in Annex D.

The theoretical justification for the error function E(P) is presented in [3, 6]. The initial pitch estimate $\hat{P}_I$ is chosen such that $E(\hat{P}_I)$ is small; however, $\hat{P}_I$ is not chosen simply to minimize E(P). Instead pitch tracking must be used to account for pitch continuity between neighboring speech frames.

5.1.2 Pitch Tracking

Pitch tracking is used to improve the pitch estimate by attempting to limit the pitch deviation between consecutive frames. If the pitch estimate is chosen to strictly minimize E(P), then the pitch estimate may change abruptly between succeeding frames. This abrupt change in the pitch can cause degradation in the synthesized speech. In addition, pitch typically changes slowly; therefore, the pitch estimates from neighboring frames can aid in estimating the pitch of the current frames.

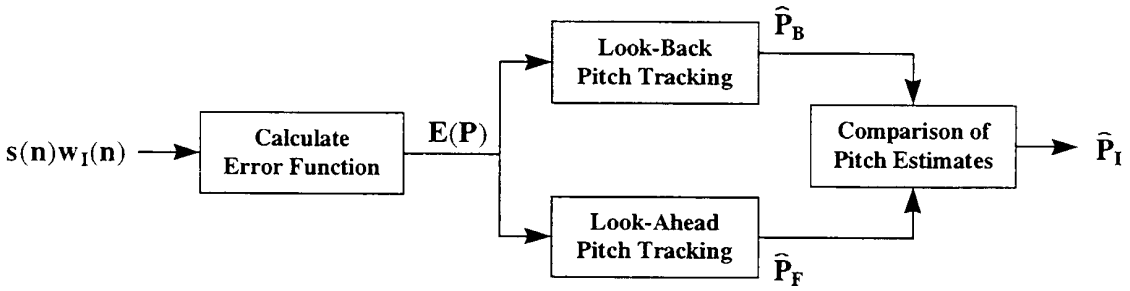

Fig. 9: Initial Pitch Estimation

For each speech frame two different pitch estimates are computed. The first, $\hat{P}_B$, is a backward estimate which maintains pitch continuity with previous speech frames. The second, $\hat{P}_F$, is a forward estimate which maintains pitch continuity with future speech frames. The backward pitch estimate is

calculated with the look-back pitch tracking algorithm, while the forward pitch estimate is calculated with the look-ahead pitch tracking algorithm. These two estimates are compared with a set of decision rules defined below, and either the backward or forward estimate is chosen as the initial pitch estimate, $\hat{P}_I$.

5.1.3 Look-Back Pitch Tracking

Let $\hat{P}_{-1}$ and $\hat{P}_{-2}$ denote the initial pitch estimates which are calculated during the analysis of the previous two speech frames. Let $E_{-1}(P)$ and $E_{-2}(P)$ denote the error functions of Equation (5) obtained from the analysis of these previous two frames as shown in Figure 7. Then $E_{-1}(\hat{P}_{-1})$ and $E_{-2}(\hat{P}_{-2})$ will have some specific values. Upon initialization the error functions $E_{-1}(P)$ and $E_{-2}(P)$ are assumed to be equal to zero, and $\hat{P}_{-1}$ and $\hat{P}_{-2}$ are assumed to be equal to 100.

Since pitch continuity with previous frames is desired, the pitch for the current speech frame is considered in a range near $\hat{P}_{-1}$. First, the error function E(P) is evaluated at each value of *P* which satisfies constraints (10) and (11).

$$.8\hat{P}_{-1} \leq P \leq 1.2\hat{P}_{-1} \tag{10}$$

$$P \in \{21, 21.5, ...121.5, 122\} \tag{11}$$

These values of E(P) are compared and $\hat{P}_B$ is defined as the value of *P* which satisfies these constraints and which minimizes E(P). The backward cumulative error $CE_B(\hat{P}_B)$ is then computed using the following formula:

$$CE_B(\hat{P}_B) = E(\hat{P}_B) + E_{-1}(\hat{P}_{-1}) + E_{-2}(\hat{P}_{-2}) \tag{12}$$

The backward cumulative error provides a confidence measure for the backward pitch estimate. It is compared against the forward cumulative error using a set of heuristics defined in Section 5.1.4. This comparison determines whether the forward pitch estimate or the backward pitch estimate is selected as the initial pitch estimate for the current frame.

5.1.4 Look-Ahead Pitch Tracking

Look-ahead tracking attempts to preserve pitch continuity between future speech frames. Let $E_1(P)$ and $E_2(P)$ denote the error functions of Equation (5) obtained from the two future speech frames as shown in Figure 7. Since the pitch has not been determined for these future frames, the look-ahead pitch tracking algorithm must select the pitch of these future frames. This is done in the following manner. First, P_0 is assumed to be fixed. Then the P_1 and P_2 are found which jointly minimize $E_1(P_1) + E_2(P_2)$, subject to constraints (13) through (16).

$$P_1 \in \{21, 21.5, ...121.5, 122\} \tag{13}$$

$$.8 \cdot P_0 \leq P_1 \leq 1.2 \cdot P_0 \tag{14}$$

$$P_2 \in \{21, 21.5, ...121.5, 122\} \tag{15}$$

$$.8 \cdot P_1 \leq P_2 \leq 1.2 \cdot P_1 \tag{16}$$

The values of P_1 and P_2 which jointly minimize $E_1(P_1)+E_2(P_2)$ subject to these constraints are denoted by $\hat{P}_1$ and $\hat{P}_2$, respectively. Once $\hat{P}_1$ and $\hat{P}_2$ have been computed the forward cumulative error function $CE_F(P_0)$ is computed according to:

$$CE_F(P_0) = E(P_0) + E_1(\hat{P}_1) + E_2(\hat{P}_2) \tag{17}$$

This process is repeated for each P_0 in the set {21, 21.5, … 121.5, 122}. The corresponding values of $CE_F(P_0)$ are compared and $\hat{P}_0$ is defined as the value of P_0 in this set which results in the minimum value of $CE_F(P_0)$. Note that references [3, 6] should be consulted for more information on the theory and implementation of the look-ahead pitch tracking algorithm.

Once $\hat{P}_0$ has been found, the integer sub-multiples of $\hat{P}_0$ (i.e. $\frac{\hat{P}_0}{2}, \frac{\hat{P}_0}{3}, \ldots \frac{\hat{P}_0}{n}$) must be considered. Every sub-multiple which is greater than or equal to 21 is computed and replaced with the closest member of the set {21, 21.5, … 121.5, 122} (where closeness is measured with mean-square error). Sub-multiples which are less than 21 are disregarded.

The smallest of these sub-multiples is checked against constraints (18), (19) and (20). If this sub-multiple satisfies any of these constraints then it is selected as the forward pitch estimate, $\hat{P}_F$. Otherwise the next largest sub-multiple is checked against these constraints, and it is selected as the forward pitch estimate if it satisfies any of these constraints. This process continues until all pitch sub-multiples have been tested against these constraints. If no pitch sub-multiple satisfies any of these constraints then $\hat{P}_F = \hat{P}_0$. Note that this procedure will always select the smallest sub-multiple which satisfies any of these constraints as the forward pitch estimate.

$$CE_F(\frac{\hat{P}_0}{n}) \leq .85 \qquad \text{and} \qquad \frac{CE_F(\frac{\hat{P}_0}{n})}{CE_F(\hat{P}_0)} \leq 1.7 \tag{18}$$

$$CE_F(\frac{\hat{P}_0}{n}) \leq .4 \qquad \text{and} \qquad \frac{CE_F(\frac{\hat{P}_0}{n})}{CE_F(\hat{P}_0)} \leq 3.5 \tag{19}$$

$$CE_F(\frac{\hat{P}_0}{n}) \leq .05 \tag{20}$$

Once the forward pitch estimate and the backward pitch estimate have both been computed the forward cumulative error and the backward cumulative error are compared. Depending on the result of this comparison either $\hat{P}_F$ or $\hat{P}_B$ will be selected as the initial pitch estimate $\hat{P}_I$. The following set of decision rules is used to select the initial pitch estimate from among these two candidates:

If

$$CE_B(\hat{P}_B) \leq .48, \text{ then } \hat{P}_I = \hat{P}_B \tag{21}$$

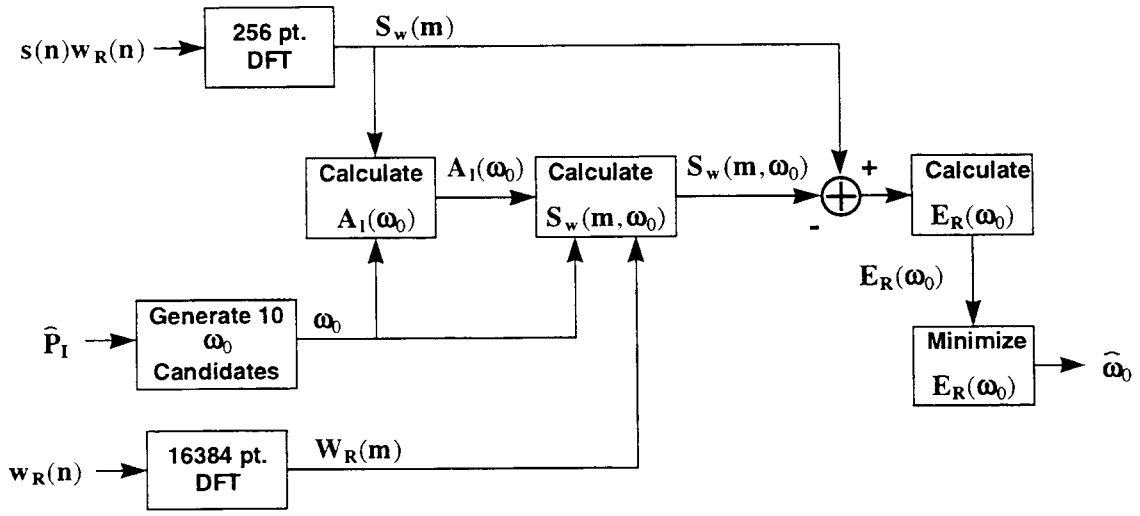

Fig. 10: Pitch Refinement

Else if

$$CE_B(\hat{P}_B) \leq CE_F(\hat{P}_F), \text{ then } \hat{P}_I = \hat{P}_B \tag{22}$$

Then

$$\hat{P}_I = \hat{P}_F \tag{23}$$

The flow charts in Annex K should be examined for more information on initial pitch estimation. Note that the initial pitch estimate, $\hat{P}_I$, is a member of the set {21, 21.5, … 121.5, 122}, and therefore it has half-sample accuracy.

5.1.5 Pitch Refinement

The pitch refinement algorithm improves the resolution of the pitch estimate from one half sample to one quarter sample. Ten candidate pitches are formed from the initial pitch estimate. These are $\hat{P}_I - \frac{9}{8}, \hat{P}_I - \frac{7}{8}, \ldots, \hat{P}_I + \frac{7}{8}$, and $\hat{P}_I + \frac{9}{8}$. These candidates are converted to their equivalent fundamental frequency using Equation (4). The error function $E_R(\omega_0)$, defined in Equation (24), is evaluated for each candidate fundamental frequency ω_0. The candidate fundamental frequency which results in the minimum value of $E_R(\omega_0)$ is selected as the refined fundamental frequency $\hat{\omega}_0$. A block diagram of this process is shown in Figure 10.

$$E_R(\omega_0) = \sum_{m=50}^{\lfloor \lfloor \frac{.9254\pi}{\omega_0} - .5 \rfloor \frac{256}{2\pi}\omega_0 \rfloor} |S_w(m) - S_w(m, \omega_0)|^2 \tag{24}$$

The synthetic spectrum $S_w(m, \omega_0)$ is given by,

$$S_w(m, \omega_0) = \begin{cases} A_0(\omega_0) W_R(64m) & \text{for } \lceil a_0 \rceil \le m < \lceil b_0 \rceil \\ A_1(\omega_0) W_R(\lfloor 64m - \frac{16384}{2\pi}\omega_0 + .5 \rfloor) & \text{for } \lceil a_1 \rceil \le m < \lceil b_1 \rceil \\ \quad . & \\ \quad . & \\ A_l(\omega_0) W_R(\lfloor 64m - \frac{16384}{2\pi} l\omega_0 + .5 \rfloor) & \text{for } \lceil a_l \rceil \le m < \lceil b_l \rceil \\ \quad . & \end{cases} \tag{25}$$

where a_l, b_l and A_l are defined in equations (26) through (28), respectively. The notation $\lceil x \rceil$ denotes the smallest integer greater than or equal to *x*.

$$a_l = \frac{256}{2\pi}(l - .5)\omega_0 \tag{26}$$

$$b_l = \frac{256}{2\pi}(l + .5)\omega_0 \tag{27}$$

$$A_l(\omega_0) = \frac{\sum_{m=\lceil a_l \rceil}^{\lceil b_l \rceil - 1} S_w(m) W_R^*(\lfloor 64m - \frac{16384}{2\pi} l\omega_0 + .5 \rfloor)}{\sum_{m=\lceil a_l \rceil}^{\lceil b_l \rceil - 1} |W_R(\lfloor 64m - \frac{16384}{2\pi} l\omega_0 + .5 \rfloor)|^2} \tag{28}$$

The function $S_w(m)$ refers to the 256 point Discrete Fourier Transform of $s(n) \cdot w_R(n)$, and $W_R(m)$ refers to the 16384 point Discrete Fourier Transform of $w_R(n)$. These relationships are expressed below. Reference [11] should be consulted for more information on the DFT.

$$S_w(m) = \sum_{n=-110}^{110} s(n) w_R(n) e^{-j\frac{2\pi mn}{256}} \qquad \text{for } -127 \leq m \leq 128 \tag{29}$$

$$W_R(m) = \sum_{n=-110}^{110} w_R(n) e^{-j\frac{2\pi mn}{16384}} \qquad \text{for } -8191 \leq m \leq 8192 \tag{30}$$

The notation $W_R^*(m)$ refers to the complex conjugate of $W_R(m)$. However, since $w_R(n)$ is a real symmetric sequence, $W_R^*(m) = W_R(m)$.

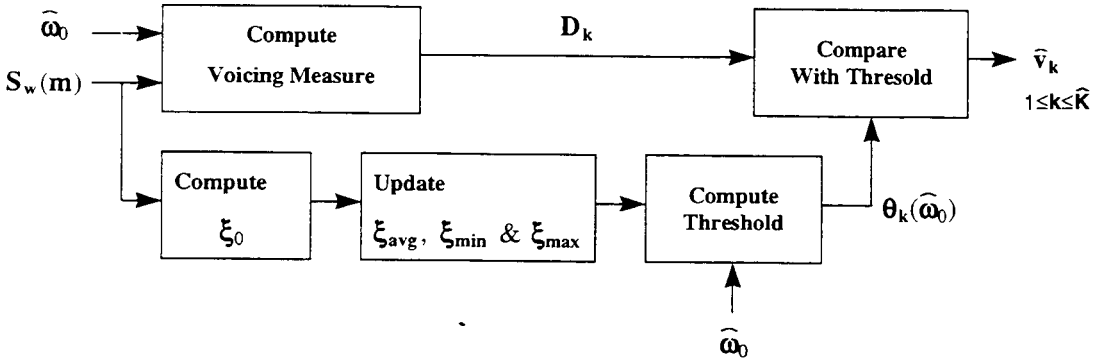

Fig. 11: IMBE Voiced/Unvoiced Determination

Once the refined fundamental frequency has been selected from among the ten candidates, it is used to compute the number of harmonics in the current segment, $\hat{L}$, according to the relationship:

$$\hat{L} = \lfloor .9254 * \lfloor \frac{\pi}{\hat{\omega}_0} + .25 \rfloor \rfloor \tag{31}$$

Due to the limits on $\hat{\omega}_0$, equation (37) confines $\hat{L}$ to the range $9 \leq \hat{L} \leq 56$. Once this equation has been computed, the parameters $\hat{a}_l$ and $\hat{b}_l$ for $1 \leq l \leq \hat{L}$ are computed from $\hat{\omega}_0$ according to equations (32) and (33), respectively.

$$\hat{a}_l = \frac{256}{2\pi}(l - .5)\hat{\omega}_0 \tag{32}$$

$$\hat{b}_l = \frac{256}{2\pi}(l + .5)\hat{\omega}_0 \tag{33}$$

5.2 Voiced/Unvoiced Determination

The voiced/unvoiced (V/UV) decisions, $\hat{v}_k$ for $1 \leq k \leq \hat{K}$, are found by dividing the spectrum into $\hat{K}$ frequency bands and evaluating a voicing measure, D_k, for each band. The number of frequency bands is a function of $\hat{L}$ and is given by:

$$\hat{K} = \begin{cases} \lfloor \frac{(\hat{L}+2)}{3} \rfloor & \text{if } \hat{L} \leq 36 \\ 12 & \text{otherwise} \end{cases} \tag{34}$$

The voicing measure for $1 \leq k \leq \hat{K}$- 1 is given by

$$D_k = \frac{\sum_{m=\lceil \hat{a}_{3k-2} \rceil}^{\lceil \hat{b}_{3k} \rceil - 1} |S_w(m) - S_w(m, \hat{\omega}_0)|^2}{\sum_{m=\lceil \hat{a}_{3k-2} \rceil}^{\lceil \hat{b}_{3k} \rceil - 1} |S_w(m)|^2} \tag{35}$$

where $\hat{\omega}_0$ is the refined fundamental frequency, and $\hat{a}_l$, $\hat{b}_l$, $S_w(m)$, and $S_w(m, \omega_0)$ are defined in section 5.1.5. Similarly, the voicing measure for the highest frequency band is given by

$$D_{\hat{K}} = \frac{\sum_{m=\lceil \hat{a}_{3\hat{K}-2} \rceil}^{\lceil \hat{b}_{\hat{L}} \rceil - 1} |S_w(m) - \hat{S}_w(m, \hat{\omega}_0)|^2}{\sum_{m=\lceil \hat{a}_{3\hat{K}-2} \rceil}^{\lceil \hat{b}_{\hat{L}} \rceil - 1} |S_w(\omega)|^2} \tag{36}$$

The parameters D_k for $1 \leq k \leq \hat{K}$ are compared with a threshold function $\Theta_\xi(k, \hat{\omega}_0)$ given by:

$$\Theta_\xi(k, \hat{\omega}_0) = \begin{cases} 0 & \text{if } E(\hat{P}_I) > .5 \text{ and } k \geq 2 \\ .5625\ [1.0 - .3096(k-1)\hat{\omega}_0] \cdot M(\xi) & \text{else if } \hat{v}_k(-1) = 1 \\ .45\ [1.0 - .3096(k-1)\hat{\omega}_0] \cdot M(\xi) & \text{otherwise} \end{cases} \tag{37}$$

where $M(\xi)$ is an energy dependent function which is computed from a set of local energy parameters and $\hat{v}_k(-1)$ is the value of the $k'th$ V/UV decision for the previous frame. Evaluation of this threshold function requires the parameters ξ_{LF}, ξ_{HF}, and ξ_0 to be computed for the current segment in the following manner, where the value $W_R(0)$ is the found by evaluating equation (30) at $m = 0$.

$$\xi_{LF} = \sum_{m=0}^{63} \frac{|S_w(m)|^2}{|W_R(0)|^2} \tag{38}$$

$$\xi_{HF} = \sum_{m=64}^{128} \frac{|S_w(m)|^2}{|W_R(0)|^2} \tag{39}$$

$$\xi_0 = \xi_{LF} + \xi_{HF} \tag{40}$$

These parameters are then used to update the parameter ξ_{max} according to the rules presented below. Throughout this section the notation ξ_{max} (0) or ξ_{max} is used to refer to the value of the parameter in the current frame, while the notation ξ_{max} (-1) is used to refer to the value of the parameter in the previous frame.

$$\xi_{max}(0) = \begin{cases} .5\,\xi_{max}(-1) + .5\,\xi_0 & \text{if } \xi_0 > \xi_{max}(-1) \\ .99\,\xi_{max}(-1) + .01\,\xi_0 & \text{else if } .99\,\xi_{max}(-1) + .01\,\xi_0 > 20000 \\ 20000 & \text{otherwise} \end{cases} \quad (41)$$

The completed set of energy parameters for the current frame is used to calculate the function $M(\xi)$ as shown below.

$$M(\xi) = \begin{cases} \left(\frac{.0025\,\xi_{max}+\xi 0}{.01\,\xi_{max}+\xi 0}\right) & \text{if } \xi_{LF} \geq 5\,\xi_{HF} \\ \left(\frac{.0025\,\xi_{max}+\xi 0}{.01\,\xi_{max}+\xi 0}\right)\left(\frac{\xi_{LF}}{5\,\xi_{HF}}\right)^{\frac{1}{2}} & \text{otherwise} \end{cases} \quad (42)$$

$\mathbf{L \leq 36,\ 3K\text{-}2 \leq L \leq 3K}$

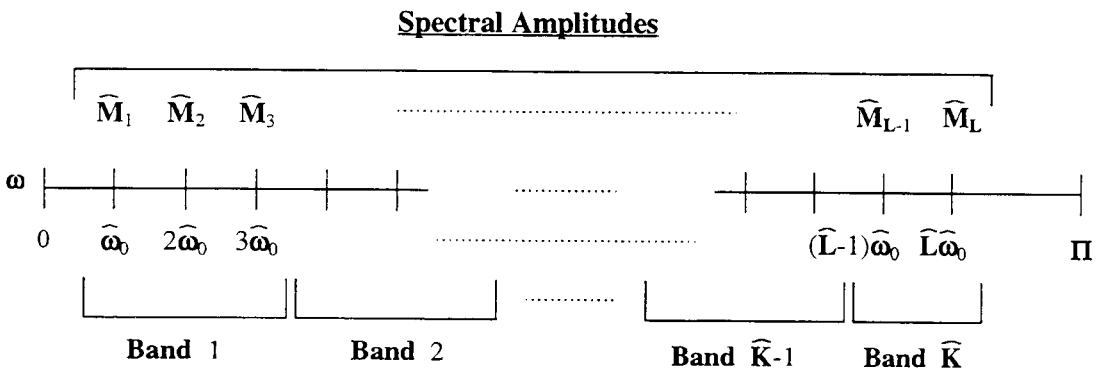

Fig. 12: IMBE Frequency Band Structure

This function is then used in Equation (37) to calculate the V/UV threshold function. If D_k is less than the threshold function then the frequency band $\hat{a}_{3k-2} \leq \omega < \hat{b}_{3k}$ is declared voiced; otherwise this frequency band is declared unvoiced. A block diagram of this procedure is shown in Figure 11. The adopted convention is that if the frequency band $\hat{a}_{3k-2} \leq \omega < \hat{b}_{3k}$ is declared voiced, then $\hat{v}_k = 1$. Alternatively, if the frequency band $\hat{a}_{3k-2} \leq \omega < \hat{b}_{3k}$ is declared unvoiced, then $\hat{v}_k = 0$.

With the exception of the highest frequency band, the width of each frequency band is equal to $3\hat{\omega}_0$. Therefore all but the highest frequency band contain three harmonics of the refined fundamental frequency. The highest frequency band (as defined by Equation (34)) may contain more or less than three harmonics of the fundamental frequency. If a particular frequency band is declared voiced, then all of the harmonics within that band are defined to be voiced harmonics. Similarly, if a particular frequency band is declared unvoiced, then all of the harmonics within that band are defined to be unvoiced harmonics.

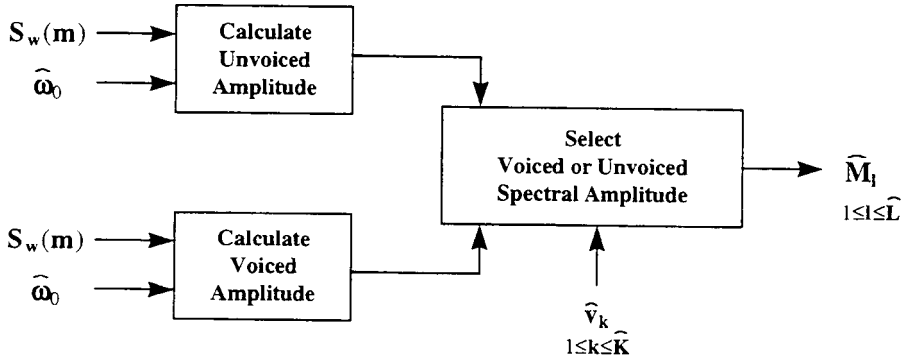

Fig. 13: IMBE Spectral Amplitude Estimation

5.3 Estimation of the Spectral Amplitudes

Once the V/UV decisions have been determined the spectral envelope can be estimated as shown in Figure 13. In the IMBE speech coder the spectral envelope in the frequency band $\hat{a}_{3k-2} \le \omega < \hat{b}_{3k}$ is specified by 3 spectral amplitudes, which are denoted by $\hat{M}_{3k-2}$, $\hat{M}_{3k-1}$, and $\hat{M}_{3k}$. The relationship between the frequency bands and the spectral amplitudes is shown in Figure 12. If the frequency band $\hat{a}_{3k-2} \le \omega < \hat{b}_{3k}$ is declared voiced, then $\hat{M}_{3k-2}$, $\hat{M}_{3k-1}$, and $\hat{M}_{3k}$ are estimated by,

$$\hat{M}_l = \left[\frac{\sum_{m=\lceil \hat{a}_l \rceil}^{\lceil \hat{b}_l \rceil - 1} |S_w(m)|^2}{\sum_{m=\lceil a_l \rceil}^{\lceil b_l \rceil - 1} |W_R(\lfloor 64m - \frac{16384}{2\pi} l\hat{\omega}_0 + .5 \rfloor)|^2} \right]^{\frac{1}{2}} \tag{43}$$

for l in the range $3k - 2 \le l \le 3k$. Alternatively, if the frequency band $\hat{a}_{3k-2} \le \omega < \hat{b}_{3k}$ is declared unvoiced, then $\hat{M}_{3k-2}$, $\hat{M}_{3k-1}$, and $\hat{M}_{3k}$ are estimated according to:

$$\hat{M}_l = \left[\frac{1}{\sum_{n=-110}^{110} w_R(n)} \right] \cdot \left[\frac{\sum_{m=\lceil \hat{a}_l \rceil}^{\lceil \hat{b}_l \rceil - 1} |S_w(m)|^2}{(\lceil \hat{b}_l \rceil - \lceil \hat{a}_l \rceil)} \right]^{\frac{1}{2}} \tag{44}$$

for l in the range $3k - 2 \le l \le 3k$.

This procedure must be modified slightly for the highest frequency band which covers the frequency interval $\hat{a}_{3\hat{K}-2} \leq \omega < \hat{b}_{\hat{L}}$. The spectral envelope in this frequency band is represented by $\hat{L} - 3\hat{K} + 3$ spectral amplitudes, denoted $\hat{M}_{3\hat{K}-2}$, $\hat{M}_{3\hat{K}-1}$, ..., $\hat{M}_{\hat{L}}$. If this frequency band is declared voiced then these spectral amplitudes are estimated using equation (43) for $3\hat{K} - 2 \leq l \leq \hat{L}$. Alternatively, if this frequency band is declared unvoiced then these spectral amplitudes are estimated using equation (44) for $3\hat{K} - 2 \leq l \leq \hat{L}$.

As described above, the spectral amplitudes $\hat{M}_l$ are estimated in the range $1 \leq l \leq \hat{L}$, where $\hat{L}$ is given in Equation (31). Note that the lowest frequency band, $a_1 \leq \omega < b_3$, is specified by $\hat{M}_1$, $\hat{M}_2$, and $\hat{M}_3$. The D.C. spectral amplitude, $\hat{M}_0$, is ignored in the IMBE speech coder and can be assumed to be zero.

Parameter	*Number of Bits*
Fundamental Frequency	8
Voiced/Unvoiced Decisions	$\hat{K}$
Spectral Amplitudes	$79 - \hat{K}$
Synchronization	1

Table 1: Bit Allocation Among Model Parameters

6 Parameter Encoding and Decoding

The analysis of each speech frame generates a set of model parameters consisting of the fundamental frequency, $\hat{\omega}_0$, the V/UV decisions, $\hat{v}_k$ for $1 \leq k \leq \hat{K}$, and the spectral amplitudes, $\hat{M}_l$ for $1 \leq l \leq \hat{L}$. Since the speech coder is designed to operate at 7.1 kbps with a 20 ms frame length, 142 bits per frame are available for encoding the model parameters. Of these 142 bits, 54 are reserved for error control as is discussed in Section 7 of this document, and the remaining 88 bits are divided among the model parameters as shown in Table 1. This section describes the manner in which these bits are used to quantize, encode, decode and reconstruct the model parameters. In Section 6.1 the encoding and decoding of the fundamental frequency is discussed, while Section 6.2 discusses the encoding and decoding of the V/UV decisions. Section 6.3 discusses the quantization and encoding of the spectral amplitudes, and Section 6.4 discusses the decoding and reconstruction of the spectral amplitudes. Reference [7] provides general information on many of the techniques used in this section.

6.1 Fundamental Frequency Encoding and Decoding

The fundamental frequency is estimated with one-quarter sample resolution in the interval $\frac{2\pi}{123.125} \leq \hat{\omega}_0 \leq \frac{2\pi}{19.875}$; however, it is only encoded at half-sample resolution. This is accomplished by finding the value of $\hat{b}_0$ which satisfies:

$$\hat{b}_0 = \lfloor \frac{4\pi}{\hat{\omega}_0} - 39 \rfloor \tag{45}$$

value	*bits*
0	0000 0000
1	0000 0001
2	0000 0010
.	.
.	.
.	.
255	1111 1111

Table 2: Eight Bit Binary Representation

The quantizer value $\hat{b}_0$ is represented with 8 bits using the unsigned binary representation shown in Table 2. This representation is used throughout the IMBE speech coder to convert quantized values into a specific bit pattern.

The fundamental frequency is decoded and reconstructed at the receiver by using Equation (46) to convert $\hat{b}_0$ to the received fundamental frequency $\tilde{\omega}_0$. In addition $\tilde{b}_0$ is used to calculate $\tilde{K}$ and $\tilde{L}$, the number of V/UV decisions and the number of spectral amplitudes, respectively. Theses relationships are given in Equations (47) and (48).

$$\tilde{\omega}_0 = \frac{4\pi}{\tilde{b}_0 + 39.5} \tag{46}$$

$$\tilde{L} = \lfloor .9254 \lfloor \frac{\pi}{\tilde{\omega}_0} + .25 \rfloor \rfloor \tag{47}$$

$$\tilde{K} = \begin{cases} \lfloor \frac{(\tilde{L}+2)}{3} \rfloor & \text{if } \tilde{L} \leq 36 \\ 12 & \text{otherwise} \end{cases} \tag{48}$$

Since $\tilde{K}$ and $\tilde{L}$ control subsequent bit allocation by the receiver, it is important that they equal $\hat{K}$ and $\hat{L}$, respectively. This occurs if there are no uncorrectable bit errors in the six most significant bits (MSB) of $\tilde{b}_0$. For this reason these six bits are well protected by the error correction scheme discussed in

Section 7. A block diagram of the fundamental frequency encoding and decoding process is shown in Figure 14.

Since the pitch estimation algorithm described in Section 5.1 restricts the range of $\hat{\omega}_0$ to $\frac{2\pi}{123.125} \leq \hat{\omega}_0 \leq \frac{2\pi}{19.875}$, the value of $\hat{b}_0$ computed according to Equation (45) is limited to the range $0 \leq \hat{b}_0 \leq 207$. The use of 8 bits to represent $\hat{b}_0$ leaves 48 values of $\hat{b}_0$ (i.e. $208 \leq \hat{b}_0 \leq 255$) which are outside the valid range of pitch values. These 48 values are reserved for future use.

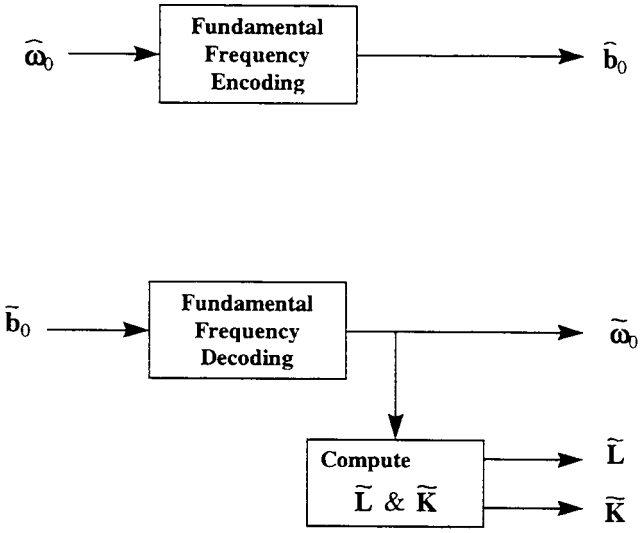

Fig. 14: Fundamental Frequency Encoding and Decoding

6.2 Voiced/Unvoiced Decision Encoding and Decoding

The V/UV decisions $\hat{v}_k$, for $1 \leq k \leq \hat{K}$, are binary values which classify each frequency band as either voiced or unvoiced. These values are encoded using the quantizer value $\hat{b}_1$ is represented with $\hat{K}$ bits using an unsigned binary representation which is analogous to that shown in Table 2.

$$\hat{b}_1 = \sum_{k=1}^{\hat{K}} \hat{v}_k \, 2^{\hat{K}-k} \tag{49}$$

At the receiver the $\tilde{K}$ bits corresponding to $\tilde{b}_1$ are decoded into the V/UV decisions $\tilde{v}_l$ for $1 \leq l \leq \tilde{L}$. Note that this is a departure from the V/UV convention used by the encoder, which used a single V/UV decision to represent an entire frequency band. Instead the decoder uses a separate V/UV decision for each spectral amplitude. The decoder performs this conversion by using $\tilde{b}_1$ to determine which frequency bands

are voiced or unvoiced. The state of $\tilde{v}_l$ is then set depending upon whether the frequency $\omega = l \cdot \tilde{\omega}_0$ is within a voiced or unvoiced frequency band. This can be expressed mathematically as shown in the following two equations.

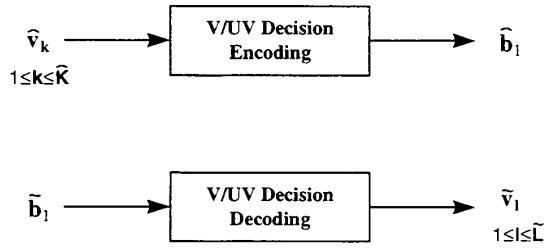

Fig. 15: V/UV Decision Encoding and Decoding

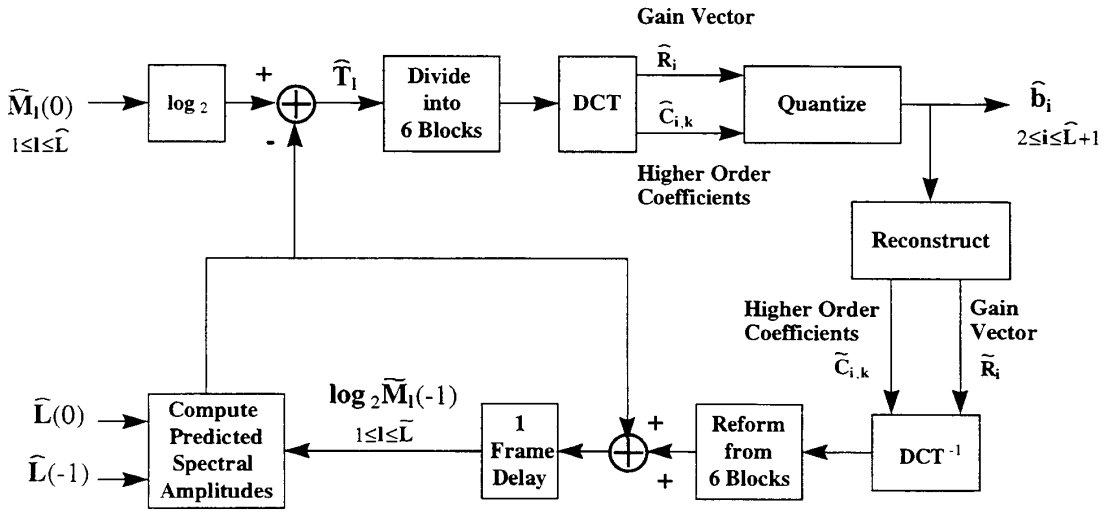

Fig. 16: Encoding of the Spectral Amplitudes

$$\kappa_l = \begin{cases} \lfloor \frac{(l+2)}{3} \rfloor & \text{if } l \le 36 \\ 12 & \text{otherwise} \end{cases} \tag{50}$$

$$\tilde{v}_l = \left\lfloor \frac{\tilde{b}_1}{2^{\tilde{K}-\kappa_l}} \right\rfloor - 2 \left\lfloor \frac{\tilde{b}_1}{2^{\tilde{K}+1-\kappa_l}} \right\rfloor \qquad \text{for } 1 \le l \le \tilde{L} \tag{51}$$

Figure 15 shows a block diagram of the V/UV decision encoding and decoding process.

6.3 Spectral Amplitudes Encoding

The spectral amplitudes $\hat{M}_l$, for $1 \le l \le \hat{L}$, are real values which must be quantized prior to encoding. This is accomplished as shown in Figure 16, by forming the spectral amplitude prediction residuals $\hat{T}_l$ for $1 \le l \le \hat{L}$, according to Equations (52) through (57). The reader is referred to [6] for more information on this topic.

For the purpose of this discussion $\hat{L}(0)$ or $\hat{L}$ refer to the number of harmonics in the current frame, while $\hat{L}(-1)$ refers to the number of harmonics in the previous frame. Similarly, $\hat{M}_l(0)$ for $1 \le l \le \hat{L}$ refers to the unquantized spectral amplitudes of the current frame, while $\tilde{M}_l(-1)$ for $1 \le l \le \hat{L}$ refers to the quantized spectral amplitudes of the previous frame.

$$\hat{k}_l = \frac{\hat{L}(-1)}{\hat{L}(0)} \cdot l \tag{52}$$

$$\hat{\delta}_l = \hat{k}_l - \lfloor \hat{k}_l \rfloor \tag{53}$$

$$\begin{aligned} \hat{T}_l = \log_2 \hat{M}_l(0) &- \rho\,(1-\hat{\delta}_l)\,\log_2 \tilde{M}_{\lfloor \hat{k}_l \rfloor}(-1) \\ &- \rho\,\hat{\delta}_l\,\log_2 \tilde{M}_{\lfloor \hat{k}_l \rfloor + 1}(-1) \\ &+ \frac{\rho}{\hat{L}(0)} \sum_{\lambda=1}^{\hat{L}(0)} [(1-\hat{\delta}_\lambda)\,\log_2 \tilde{M}_{\lfloor \hat{k}_\lambda \rfloor}(-1) + \hat{\delta}_\lambda\,\log_2 \tilde{M}_{\lfloor \hat{k}_\lambda \rfloor + 1}(-1)] \end{aligned} \tag{54}$$

The prediction coefficient, ρ, is adjusted each frame according to the following rule:

$$\rho = \begin{cases} .4 & \text{if } \hat{L}(0) \le 15 \\ .03\hat{L}(0) - .05 & \text{if } 15 < \hat{L}(0) \le 24 \\ .7 & \text{otherwise} \end{cases} \tag{55}$$

In order to form $\hat{T}_l$ using equations (52) through (55), the following assumptions are made:

$$\tilde{M}_0(-1) = 1.0 \tag{56}$$

$$\tilde{M}_l(-1) = \tilde{M}_{\tilde{L}(-1)}(-1) \qquad \text{for } l > \tilde{L}(-1) \tag{57}$$

Also upon initialization $\tilde{M}_l(-1)$ should be set equal to 1.0 for all l, and $\hat{L}(-1) = 30$.

The $\hat{L}$ prediction residuals are then divided into 6 blocks. The length of each block, denoted $\hat{J}_i$ for $1 \le i \le 6$, is adjusted such that the following constraints are satisfied:

$$\sum_{i=1}^{6} \hat{J}_i = \hat{L} \tag{58}$$

$$\lfloor \frac{\hat{L}}{6} \rfloor \le \hat{J}_i \le \hat{J}_{i+1} \le \lceil \frac{\hat{L}}{6} \rceil \qquad \text{for } 1 \le i \le 5 \tag{59}$$

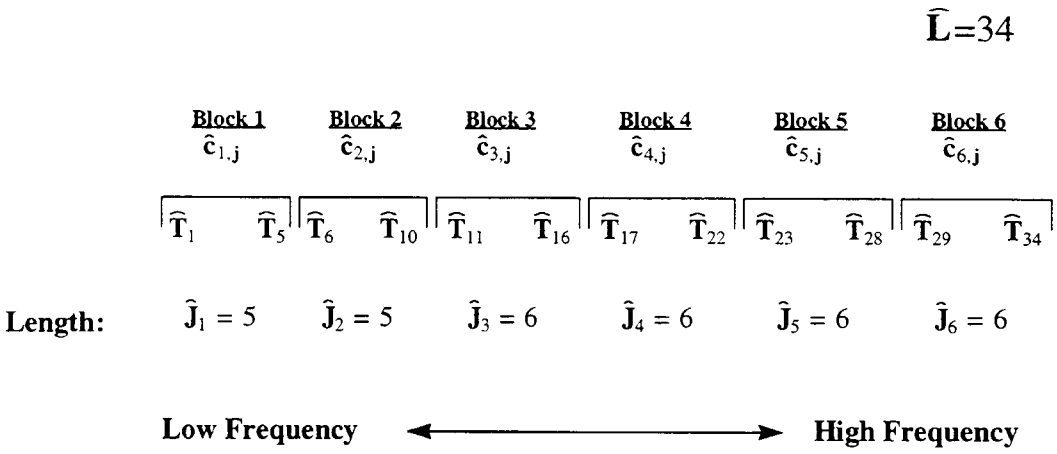

Fig. 17: Prediction Residual Blocks for $\hat{L} = 34$

The table shown in Annex J lists the six block lengths for all possible values of $\hat{L}$. The first or lowest frequency block is denoted by $\hat{c}_{1,j}$ for $1 \leq j \leq \hat{J}_1$, and it consists of the first $\hat{J}_1$ consecutive elements of $\hat{T}_l$ (i.e. $1 \leq l \leq \hat{J}_1$). The second block is denoted by $\hat{c}_{2,j}$ for $1 \leq j \leq \hat{J}_2$, and it consists of the next $\hat{J}_2$ consecutive elements of $\hat{T}_l$ (i.e. $\hat{J}_1+1 \leq l \leq \hat{J}_1+\hat{J}_2$). This continues through the sixth or highest frequency block, which is denoted by $\hat{c}_{6,j}$ for $1 \leq j \leq \hat{J}_6$. It consists of the last $\hat{J}_6$ consecutive elements of $\hat{T}_l$ (i.e. $\hat{L} + 1 - \hat{J}_6 \leq l \leq \hat{L}$). An example of this process is shown in Figure 17 for $\hat{L}$ = 34.

Each of the six blocks is transformed using a Discrete Cosine Transform (DCT), which is discussed in [7]. The length of the DCT for the i'th block is equal to $\hat{J}_i$. The DCT coefficients are denoted by $\hat{C}_{i,k}$, where $1 \leq i \leq 6$ refers to the block number, and $1 \leq k \leq \hat{J}_i$ refers to the particular coefficient within each block. The formula for the computation of these DCT coefficients is as follows:

$$\hat{C}_{i,k} = \frac{1}{\hat{J}_i} \sum_{j=1}^{\hat{J}_i} \hat{c}_{i,j} \cos\left[\frac{\pi(k-1)(j-\frac{1}{2})}{\hat{J}_i}\right] \qquad \text{for } 1 \leq k \leq \hat{J}_i \qquad (60)$$

The DCT coefficients from each of the six blocks are then divided into two groups. The first group consists of the first DCT coefficient from each of the six blocks. These coefficients are used to form a six element vector, $\hat{R}_i$ for $1 \leq i \leq 6$, where $\hat{R}_i = \hat{C}_{i,1}$. The vector $\hat{R}_i$ is referred to as the gain vector, and its construction is shown in Figure 18. The quantization of the gain vector is discussed in section 6.3.1.

The second group consists of the remaining higher order DCT coefficients. These coefficients correspond to $\hat{C}_{i,j}$, where $1 \leq i \leq 6$ and $2 \leq j \leq \hat{J}_i$. Note that if $\hat{J}_i = 1$, then there are no higher order DCT coefficients in the i'th block. The quantization of the higher order DCT coefficients is discussed in section 6.3.2.

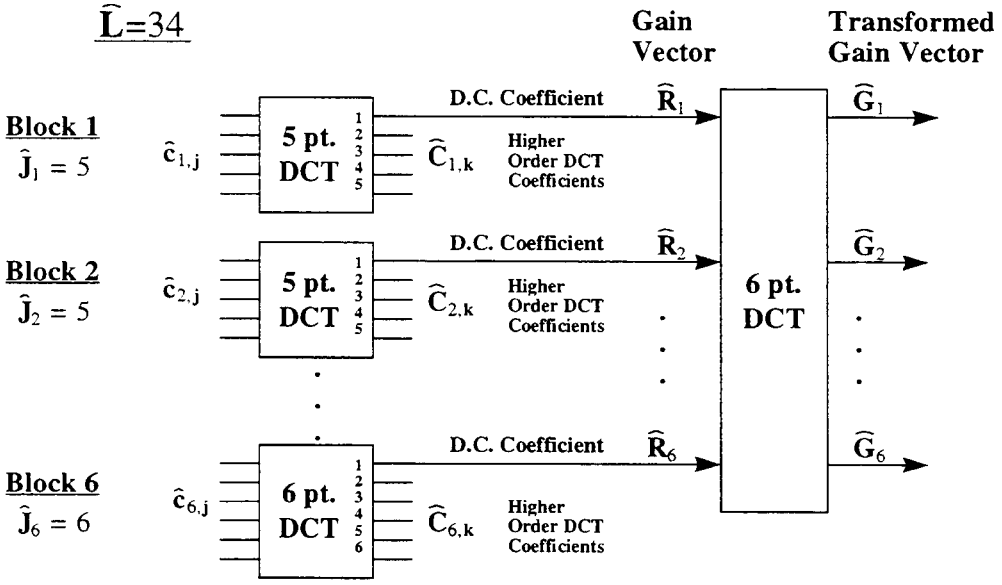

Fig. 18: Formation of Gain Vector

One important feature of the spectral amplitude encoding algorithm, is that the spectral amplitude information is transmitted differentially. Specifically, a prediction residual is transmitted which measures the change in the spectral envelope between the current frame and the previous frame. In order for a differential scheme of this type to work properly, the encoder must simulate the operation of the decoder and use the reconstructed spectral amplitudes from the previous frame to predict the spectral amplitudes of the current frame. The IMBE spectral amplitude encoder simulates the spectral amplitude decoder by setting $\tilde{L} = \hat{L}$ and then reconstructing the spectral amplitudes as discussed above. This is shown as the feedback path in Figure 16.

6.3.1 Encoding the Gain Vector

The gain vector can be viewed as a coarse representation of the spectral envelope of the current segment of speech. The quantization of the gain vector begins with a six point DCT of $\hat{R}_i$ for $1 \leq i \leq 6$ as shown in the following equation.

$$\hat{G}_m = \frac{1}{6}\sum_{i=1}^{6} \hat{R}_i \cos\left[\frac{\pi(m-1)(i-\frac{1}{2})}{6}\right] \qquad \text{for } 1 \leq m \leq 6 \qquad (61)$$

The resulting vector, denoted by $\hat{G}_m$ for $1 \leq m \leq 6$, is quantized in two parts. The first element, $\hat{G}_1$, can be viewed as representing the overall gain or level of the speech segment. This element is quantized using the 6 bit non-uniform quantizer given in Annex E. The 6 bit value $\hat{b}_2$ is defined as the index of the quantizer

value (as shown in Annex E) which is nearest to $\hat{G}_1$. The remaining five elements of $\hat{G}_m$ are quantized using uniform scalar quantizers where the five quantizer values $\hat{b}_3$ to $\hat{b}_7$ are computed from the vector elements as shown in Equation (62).

$$\hat{b}_m = \begin{cases} 0 & \text{if } \lfloor \frac{\hat{G}_{m-1}}{\hat{\Delta}_m} \rfloor < -2^{\hat{B}_m - 1} \\ 2^{\hat{B}_m} - 1 & \text{if } \lfloor \frac{\hat{G}_{m-1}}{\hat{\Delta}_m} \rfloor \geq 2^{\hat{B}_m - 1} \\ \lfloor \frac{\hat{G}_{m-1}}{\hat{\Delta}_m} \rfloor + 2^{\hat{B}_m - 1} & \text{otherwise} \end{cases} \qquad \text{for } 3 \leq m \leq 7 \qquad (62)$$

The parameters $\hat{B}_m$ and $\hat{\Delta}_m$ in Equation (62) are the number of bits and the step sizes used to quantize each element. These values are dependent upon $\hat{L}$, which is the number of harmonics in the current frame. This dependence is tabulated in Annex F. Since $\hat{L}$ is known by the encoder, the correct values $\hat{B}_m$ and $\hat{\Delta}_m$ are first obtained using Annex F and then the quantizer values $\hat{b}_m$ for $3 \leq m \leq 7$ are computed using Equation (62). The final step is to convert each quantizer value into an unsigned binary representation using the same method as shown in Table 2.

6.3.2 Encoding the Higher Order DCT Coefficients

Once the gain vector has been quantized, the remaining bits are used to encode the $\hat{L}$ - 6 higher order DCT coefficients which complete the representation of the spectral amplitudes. Annex G shows the bit allocation as a function of $\hat{L}$ for these coefficients. For each value of $\hat{L}$ the $\hat{L}$ - 6 entries, labeled $\hat{b}_8$ through $\hat{b}_{\hat{L}+1}$, provide the bit allocation for the higher order DCT coefficients. The adopted convention is that $[\hat{b}_8, \hat{b}_9, \ldots, \hat{b}_{\hat{L}+1}]$ correspond to $[\hat{C}_{1,2}, \hat{C}_{1,3}, \ldots, \hat{C}_{1,\hat{J}_1}, \ldots, \hat{C}_{6,2}, \hat{C}_{6,3}, \ldots, \hat{C}_{6,\hat{J}_6}]$, respectively.

Once the bit allocation for the higher order DCT coefficients has been obtained, these coefficients are quantized using uniform quantization. The step size used to quantize each coefficient must be computed from the bit allocation and the standard deviation of the DCT coefficient using Tables 3 and 4. For example, if 4 bits are allocated for a particular coefficient, then from Table 3 the step size, $\hat{\Delta}$, equals $.40\sigma$.

Number of Bits	*Step Size*
1	1.2σ
2	$.85\sigma$
3	$.65\sigma$
4	$.40\sigma$
5	$.28\sigma$
6	$.15\sigma$
7	$.08\sigma$
8	$.04\sigma$
9	$.02\sigma$
10	$.01\sigma$

Table 3: Uniform Quantizer Step Size for Higher Order DCT Coefficients

If this was the third DCT coefficient from any block (i.e. $\hat{C}_{i,3}$), then σ = .241 as shown in Table 4. Performing this multiplication gives a step size of .0964. Once the bit allocation and the step sizes for the higher order DCT coefficients have been determined, then the bit encodings $\hat{b}_m$ for $8 \leq m \leq \hat{L} + 1$ are computed according to Equation (63).

$$\hat{b}_m = \begin{cases} 0 & \text{if } \lfloor \frac{\hat{C}_{i,k}}{\hat{\Delta}_m} \rfloor < -2^{\hat{B}_m - 1} \\ 2^{\hat{B}_m} - 1 & \text{if } \lfloor \frac{\hat{C}_{i,k}}{\hat{\Delta}_m} \rfloor \geq 2^{\hat{B}_m - 1} \\ \lfloor \frac{\hat{C}_{i,k}}{\hat{\Delta}_m} \rfloor + 2^{\hat{B}_m - 1} & \text{otherwise} \end{cases} \qquad \text{for } 8 \leq m \leq \hat{L} + 1 \qquad (63)$$

The parameters $\hat{b}_m$, $\hat{B}_m$ and $\hat{\Delta}_m$ in equation (63) refer to the quantizer value, the number of bits and the step size which has been computed for $\hat{C}_{i,k}$, respectively. Note that the relationship between *m*, *i*, and *k* in Equation (63) is known and can be expressed as:

$$m = 6 + k + \sum_{n=1}^{i-1} \hat{J}_n \qquad (64)$$

Finally, each quantizer value is converted into the appropriate unsigned binary representation which is analogous to that shown in Table 2.

DCT Coefficient	σ
$C_{i,2}$	.307
$C_{i,3}$	.241
$C_{i,4}$	.207
$C_{i,5}$	.190
$C_{i,6}$	.179
$C_{i,7}$	.173
$C_{i,8}$	.165
$C_{i,9}$	.170
$C_{i,10}$	.170

Table 4: Standard Deviation of Higher Order DCT Coefficients

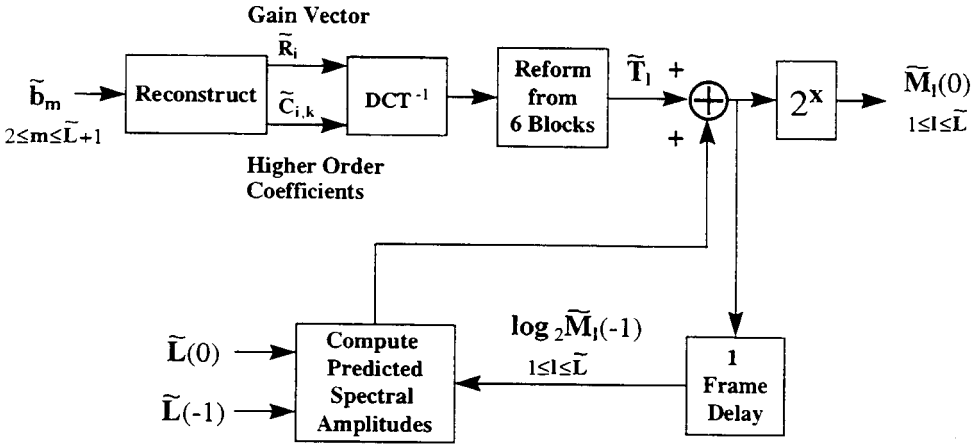

Fig. 19: Decoding of the Spectral Amplitudes

6.4 Spectral Amplitudes Decoding

In order for the decoder to reconstruct the spectral amplitudes, the parameter $\tilde{L}$ must first be computed from $\tilde{b}_0$ using Equations (46) and (47). Then the spectral amplitudes can be decoded and reconstructed by inverting the quantization and encoding procedure described above. A block diagram of the spectral amplitude decoder is shown in Figure 19.

The first step in the spectral amplitude reconstruction process is to divide the spectral amplitudes into six blocks. The length of each block, $\tilde{J}_i$ for $1 \le i \le 6$, is adjusted to meet the following constraints.

$$\sum_{i=1}^{6} \tilde{J}_i = \tilde{L} \tag{65}$$

$$\lfloor \frac{\tilde{L}}{6} \rfloor \leq \tilde{J}_i \leq \tilde{J}_{i+1} \leq \lceil \frac{\tilde{L}}{6} \rceil \qquad \text{for } 1 \leq i \leq 5 \tag{66}$$

The elements of these blocks are denoted by $\tilde{C}_{i,k}$, where $1 \leq i \leq 6$ denotes the block number and where $1 \leq k \leq \tilde{J}_i$ denotes the element within that block. The first element of each block is then set equal to the decoded gain vector, $\tilde{R}_i$, via equation (67). The formation of the decoded gain vector is discussed in Section 6.4.1.

$$\tilde{C}_{i,1} = \tilde{R}_i \qquad \text{for } 1 \leq i \leq 6 \tag{67}$$

The remaining elements of each block correspond to the decoded higher order DCT coefficients which are discussed in Section 6.4.2.

6.4.1 Decoding the Gain Vector

The gain is decoded in two parts. First the six bit value $\tilde{b}_2$ is used to decode the first element of the transformed gain vector, denoted by $\tilde{G}_1$. This is done by using the 6 bit value $\tilde{b}_2$ as an index into the quamtizer values listed in Annex E. Next the five quantizer values $\tilde{b}_2$ through $\tilde{b}_7$ are used to reconstruct the remaining five elements of the transformed gain vector, denoted by $\tilde{G}_2$ through $\tilde{G}_6$. This is done by using $\tilde{L}$, the number of harmonics in the current frame, in combination with the table in Annex F to establish the bit allocation and step size for each of these five elements. The relationship between the quantizer values and the transformed gain vector elements is expressed in Equation (68),

$$\tilde{G}_{m-1} = \begin{cases} 0 & \text{if } \tilde{B}_m = 0 \\ \tilde{\Delta}_m \, (\tilde{b}_m - 2^{\tilde{B}_m - 1} + .5) & \text{otherwise} \end{cases} \qquad \text{for } 3 \leq m \leq 7 \tag{68}$$

where $\tilde{\Delta}_m$ and $\tilde{B}_m$ are the step sizes and the number of bits found via Annex F. Once the transformed gain vector has been reconstructed in this manner, the gain vector $\tilde{R}_i$ for $1 \leq i \leq 6$ must be computed through an inverse DCT of $\tilde{G}_m$ as shown in the following equations.

$$\tilde{R}_i = \sum_{m=1}^{6} \alpha(m) \, \tilde{G}_m \cos[\frac{\pi(m-1)(i-\frac{1}{2})}{6}] \qquad \text{for } 1 \leq i \leq 6 \tag{69}$$

$$\alpha(m) = \begin{cases} 1 & \text{if } m = 1 \\ 2 & \text{otherwise} \end{cases} \tag{70}$$

6.4.2 Decoding the Higher Order DCT Coefficients

The higher order DCT coefficients, which are denoted by $\tilde{C}_{i,k}$ for $2 \le i \le 6$ and $1 \le k \le \tilde{J}_i$, are reconstructed from the quantizer values $\tilde{b}_8, \tilde{b}_9, \ldots, \tilde{b}_{\tilde{L}+1}$. First the bit allocation table listed in Annex G is used to determine the appropriate bit allocation. The adopted convention is that $[\tilde{b}_8, \tilde{b}_9, \ldots, \tilde{b}_{\tilde{L}+1}]$ correspond to $[\tilde{C}_{1,2}, \tilde{C}_{1,3}, \ldots, \tilde{C}_{1,\tilde{J}_1}, \quad \ldots, \quad \tilde{C}_{6,2}, \tilde{C}_{6,3}, \ldots, \tilde{C}_{6,\tilde{J}_6}]$, respectively. Once the bit allocation has been determined the step sizes for each $\tilde{C}_{i,k}$ are computed using Tables 3 and 4. The determination of the bit allocation and the step sizes proceeds in the same manner as is discussed in Section 6.3.2. Using the notation $\tilde{B}_m$ and $\tilde{\Delta}_m$ to denote the number of bits and the step size, respectively, then each higher order DCT coefficient can be reconstructed according to the following formula,

$$\tilde{C}_{i,k} = \begin{cases} 0 & \text{if } \tilde{B}_m = 0 \\ \tilde{\Delta}_m \, (\tilde{b}_m - 2^{\tilde{B}_m - 1} + .5) & \text{otherwise} \end{cases} \qquad \text{for } 8 \le m \le \tilde{L} + 1 \tag{71}$$

where as in Equation (64), the following equation can be used to relate *m*, *i*, and *k*.

$$m = 6 + k + \sum_{n=1}^{i-1} \tilde{J}_n \tag{72}$$

Once the DCT coefficients $\tilde{C}_{i,k}$ have been reconstructed, an inverse DCT is computed on each of the six blocks to form the vectors $\tilde{c}_{i,j}$. This is done using the following equations for $1 \le i \le 6$.

$$\tilde{c}_{i,j} = \sum_{k=1}^{\tilde{J}_i} \alpha(k) \tilde{C}_{i,k} \cos\left[\frac{\pi(k-1)(j-\frac{1}{2})}{\tilde{J}_i}\right] \qquad \text{for } 1 \le j \le \tilde{J}_i \tag{73}$$

$$\alpha(k) = \begin{cases} 1 & \text{if } k = 1 \\ 2 & \text{otherwise} \end{cases} \tag{74}$$

The six transformed blocks $\tilde{c}_{i,j}$ are then joined to form a single vector of length $\tilde{L}$, which is denoted $\tilde{T}_l$ for $1 \le l \le \tilde{L}$. The vector $\tilde{T}_l$ corresponds to the reconstructed spectral amplitude prediction residuals. The adopted convention is that the first $\tilde{J}_1$ elements of $\tilde{T}_l$ are equal to $\tilde{c}_{1,j}$ for $1 \le j \le \tilde{J}_1$. The next $\tilde{J}_2$ elements of $\tilde{T}_l$ are equal to $\tilde{c}_{2,j}$ for $1 \le j \le \tilde{J}_2$. This continues until the last $\tilde{J}_6$ elements of $\tilde{T}_l$ are equal to

$\tilde{c}_{6,j}$ for $1 \leq j \leq \tilde{J}_6$. Finally, the reconstructed $\log_2$ spectral amplitudes for the current frame are computed using the following equations.

$$\tilde{k}_l = \frac{\tilde{L}(-1)}{\tilde{L}(0)} \cdot l \tag{75}$$

$$\tilde{\delta}_l = \tilde{k}_l - \lfloor \tilde{k}_l \rfloor \tag{76}$$

$$\begin{aligned} \log_2 \tilde{M}_l(0) = \tilde{T}_l &+ \rho\,(1 - \tilde{\delta}_l)\ \log_2 \tilde{M}_{\lfloor \tilde{k}_l \rfloor}(-1) \\ &+ \rho\,\tilde{\delta}_l\ \log_2 \tilde{M}_{\lfloor \tilde{k}_l \rfloor + 1}(-1) \\ &- \frac{\rho}{\tilde{L}(0)} \sum_{\lambda=1}^{\tilde{L}(0)} [(1 - \tilde{\delta}_\lambda)\ \log_2 \tilde{M}_{\lfloor \tilde{k}_\lambda \rfloor}(-1) + \tilde{\delta}_\lambda\ \log_2 \tilde{M}_{\lfloor \tilde{k}_\lambda \rfloor + 1}(-1)] \end{aligned} \tag{77}$$

In order to reconstruct $\tilde{M}_l(0)$ using equations (75) through (77), the following assumptions are always made:

$$\tilde{M}_0(-1) = 1.0 \tag{78}$$

$$\tilde{M}_l(-1) = \tilde{M}_{\tilde{L}(-1)}(-1) \qquad \text{for } l > \tilde{L}(-1) \tag{79}$$

In addition it is assumed that upon initialization $\tilde{M}_l$(-1) = 1 for all *l*, and $\tilde{L}$(-1) = 30. Note that later sections of the IMBE decoder require the spectral amplitudes, $\tilde{M}_l$ for $1 \leq l \leq \tilde{L}$, which must be computed by applying the inverse $\log_2$ to each of the values computed with Equation (77).

One final note is that it should be clear that the IMBE speech coder uses adaptive bit allocation and quantization which is dependent upon the number of harmonics in each frame. At the encoder the value $\hat{L}$ is used to determine the bit allocation and quantizer step sizes, while at the decoder the value $\hat{L}$ is used to determine the bit allocation and quantizer step sizes. In order to ensure proper operation it is necessary that these two values be equal (i.e. $\hat{L} = \tilde{L}$). The encoder and decoder are designed to ensure this property except in the presence of a very large number of bit errors. In addition, the decoder is designed to detect frames where a large number of bit errors may prevent the generation of the correct bit allocation and quantizer step sizes. In this case the decoder discards the bits for the current frame and repeats the parameters from the previous frame. This is discussed in more detail in latter sections of this document.

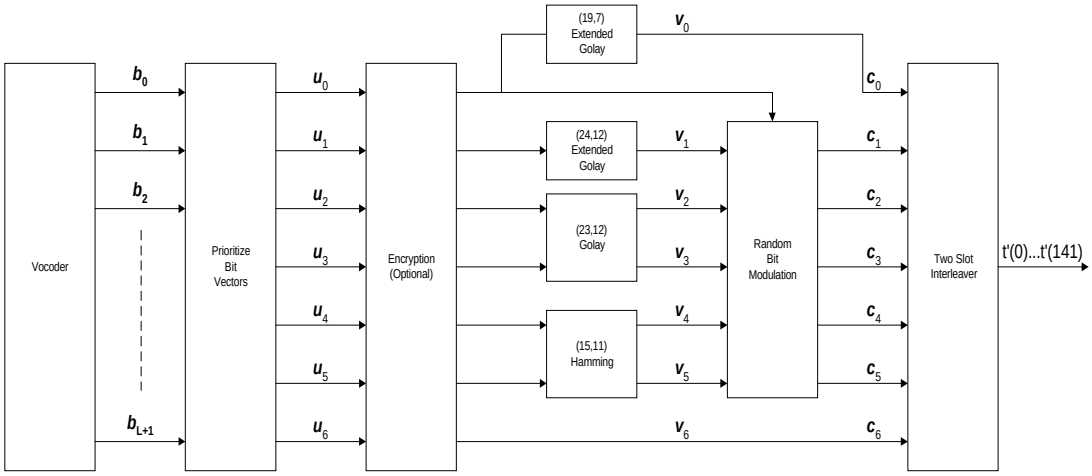

Fig 20: Encoder Bit Manipulations

7 Bit Manipulations

The IMBE coder uses a number of different manipulations in order to increase its robustness to channel degradations. The quantizer values, $\hat{b}_0, \ldots, \hat{b}_{\hat{L}+1}$, are first prioritized into a set of bit vectors denoted by $\hat{u}_0, \ldots, \hat{u}_6$. These vectors are optionally encrypted, and then they are protected with error control codes to produce a set of code vectors denoted by $\hat{v}_0, \ldots, \hat{v}_6$. These code vectors are then modulated to produce a set of modulated code vectors denoted by $\hat{c}_0, \ldots, \hat{c}_6$. Finally, intra-frame interleaving is used on the modulated code vectors in order to spread the effect of short burst errors. A block diagram of the bit manipulations performed by the encoder is shown in Figure 20.

The IMBE decoder reverses the bit manipulations performed by the encoder. First the decoder de-interleaves each frame to obtain the seven modulated code vectors, $\hat{c}_0, \ldots, \hat{c}_6$. The decoder then demodulates these vectors to produce the code vectors $\hat{v}_0, \ldots, \hat{v}_6$ and then error control decodes these code vectors to produce the bit vectors $\hat{u}_0, \ldots, \hat{u}_6$. Next the decoder must decrypt the bit vectors (if encryption is employed at the encoder), and then it must rearrange the bit vectors to reconstruct the quantizer values, denoted by $\hat{b}_0, \ldots, \hat{b}_{\hat{L}+1}$. These values are further decode use the techniques described in Section 6 and

finally used to synthesize the current frame of speech. A block diagram of the bit manipulations performed by the decoder is shown in Figure 21.

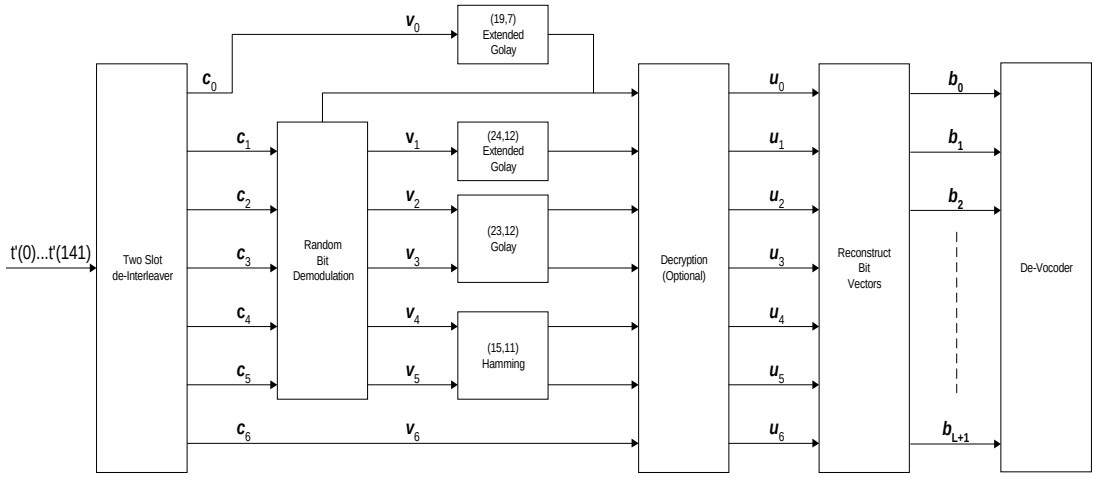

Fig 21: Decoder Bit Manipulations

7.1 Bit Prioritization

The first bit manipulation performed by the IMBE encode is a rearrangement of the quantizer values $\hat{b}_0$, …, $\hat{b}_{\hat{L}+1}$ into a set of seven prioritized bit vectors $\hat{u}_0$, …, $\hat{u}_6$. The bit vector $\hat{u}_0$ is 7 bits long. The bit vectors $\hat{u}_1$ through $\hat{u}_3$ are 12 bits long, $\hat{u}_4$ and $\hat{u}_5$ are 11 bits long, and $\hat{u}_6$ is 23 bits long. Throughout this section the convention has been adopted that the bit N-1, where N is the vector length, is the MSB and bit 0 is the LSB.

Prioritization of quantizer values into the set of bit vectors begins with $\hat{u}_0$. The most significant bit of $\hat{u}_0$ is set to 0. The six remaining bits of $\hat{u}_0$ (i.e. bits 6 through 1) are set equal to the six most significant bits (bits 7 through 2) of $\hat{b}_0$. The three most significant bits of $\hat{u}_1$ (bits 11 through 9) are set equal to the three most significant bits of $\hat{b}_2$. The quantizer values $\hat{b}_3$ through $\hat{b}_{\hat{L}+1}$ are scanned as described below and the 32 highest priority bits are copied to the remaining 9 bits of $\hat{u}_1$, the 12 bits of $\hat{u}_2$, and the 11 most significant bits (bits 11 through 1) of $\hat{u}_3$. Bit 0 of $\hat{u}_3$ is set equal to bit 2 of $\hat{b}_2$ and the most significant bit of $\hat{u}_4$ (bit 10) is set equal to bit 1 of $\hat{b}_2$. Next, all the bits of $\hat{b}_1$ are inserted into the

prioritized bit vectors beginning with bit 9 of $\hat{u}_4$. Scanning of the quantizer values $\hat{b}_3$, …, $\hat{b}_{\hat{L}+1}$ then continues and the remaining bits of $\hat{b}_3$, …, $\hat{b}_{\hat{L}+1}$ are inserted in the prioritized bit vectors. Scanning is complete when bit 2 of $\hat{u}_6$ is reached. Bit 0 of $\hat{b}_2$ is copied to bit 2 of $\hat{u}_6$ and bits 1 and 0 of $\hat{b}_0$ are copied to bits 1 and 0 of $\hat{u}_6$, respectively. Specifically, these quantizer values are arranged as shown in Figure 22. In this figure the shaded areas represent the number of bits which were allocated to each of these values assuming $\hat{L}$ = 16. Note that for other values of $\hat{L}$ this figure would change in accordance with the bit allocation information contained in Appendices Annex F and Annex G. The remaining three bits of $\hat{u}_0$ are then selected by beginning in the upper left hand corner of this figure (i.e. bit 10 of $\hat{b}_3$) and scanning left to right. When the end of any row is reached the scanning proceeds from left to right on the next lower row. Bit 8 of $\hat{u}_1$ is set equal to the bit corresponding to the first shaded block which is encountered using the prescribed scanning order. Similarly, bit 7 of $\hat{u}_1$ is set equal to the bit corresponding to the second shaded block which is encountered and bit 6 of $\hat{u}_0$ is set equal to the bit corresponding to the third shaded block which is encountered.

The scanning of the spectral amplitude quantizer values $\hat{b}_3$ through $\hat{b}_{\hat{L}+1}$ which is used to generate the last nine bits of $\hat{u}_1$ is continued for the bit vectors $\hat{u}_1$ through $\hat{u}_3$. Each successive bit in these vectors is set equal to the bit corresponding to the next shaded block. This process begins with bit 8 of $\hat{u}_1$, proceeds through bit 0 of $\hat{u}_1$ followed by bit 11 of $\hat{u}_2$, and continues in this manner until finally reaching bit 1 of $\hat{u}_3$. At this point the 43 highest priority bits have been assigned to the bit vectors $\hat{u}_0$ through $\hat{u}_3$ as shown in Figure 23.

The next bits to be inserted into the bit vectors are all of the bits of $\hat{b}_1$ (starting with the MSB), followed by bit 2 and then bit 1 of $\hat{b}_2$, and then continuing with the scanning of $\hat{b}_3$ through $\hat{b}_{\hat{L}+1}$ as described above. These bits are inserted into the bit vectors beginning with bit 10 of $\hat{u}_4$, proceeding through bit 0 of $\hat{u}_4$ followed by bit 10 of $\hat{u}_5$, and continuing in this manner until finally reaching bit 4 of $\hat{u}_6$. The final three bits of $\hat{u}_6$, beginning with bit 2 and ending with bit 0, are set equal to bit 0 of $\hat{b}_2$, bit 1 of $\hat{b}_0$, and bit 0 of $\hat{b}_0$, respectively. A block diagram of this procedure is shown in Figure 24 for $\hat{K}$ = 6.

$\widehat{L} = 16$

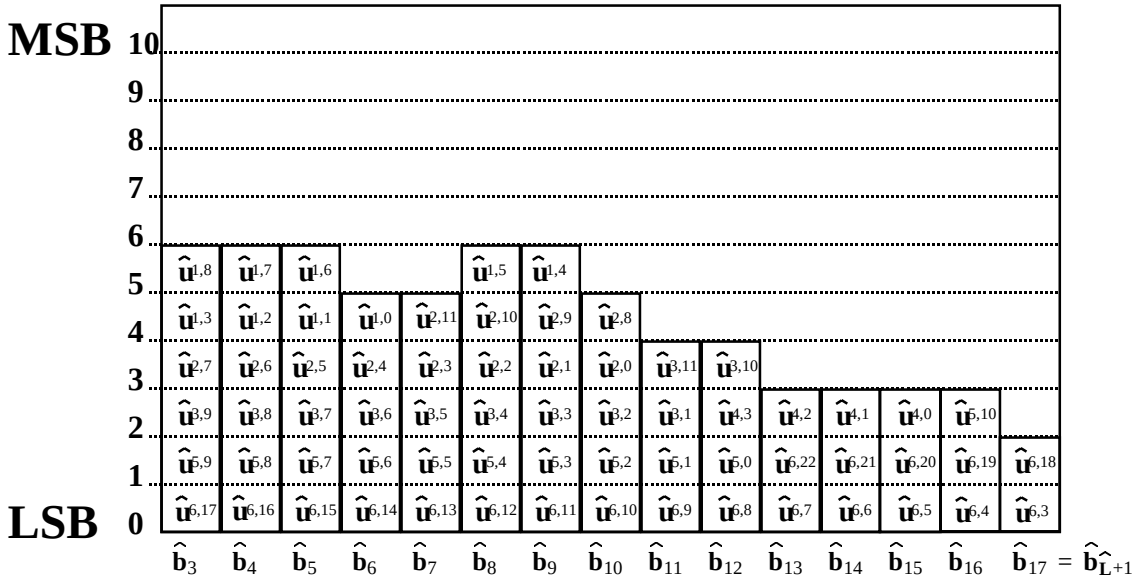

Figure 22: Priority Scanning of $\hat{b}_3$ through $\hat{b}_{\hat{L}+1}$

7.2 Encryption

This document treats optional encryption and decryption as transparent elements and does not attempt to define the actual encryption process. However, Figure 20 and 21 depict an encryption and decryption element, respectively, in order to illustrate the proper placement of these elements in the IMBE vocoder. During encryption the bit vectors $\hat{u}_0$, …, $\hat{u}_6$ are combined bit-by-bit with an encryption sequence. This same sequence must be used at the decoder to recover the bit vectors $\hat{u}_0$, …, $\hat{u}_6$. In order to be interoperable the encryption and decryption process must each use the same bit ordering. The standard ordering begins with the most significant bit (MSB) of $\hat{u}_0$ and continues in order of significance until the least significant bit (LSB) of $\hat{u}_0$ is reached. This is followed in order by the bit vectors $\hat{u}_0$, …, $\hat{u}_6$ respectively, where each bit vector proceeds from MSB to LSB.

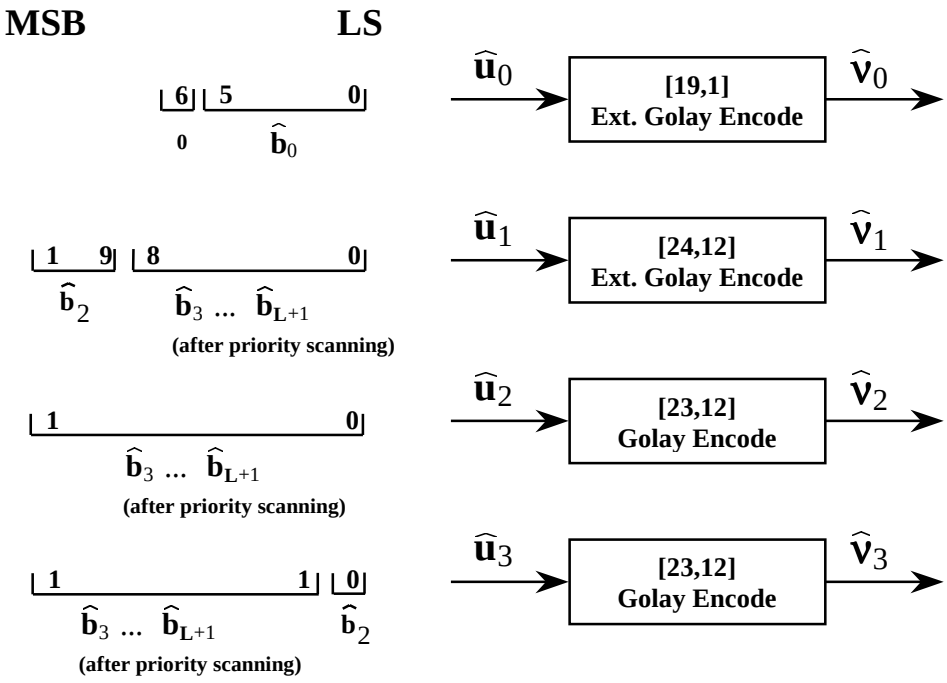

Figure 23: Formation of the Code Vectors $\hat{v}_0$ throught $\hat{v}_3$

7.3 Error Control Coding

Forward error correction (FEC) codes are used to transform the prioritized bit vectors $\hat{u}_0$ through $\hat{u}_6$ into the vectors $\hat{v}_0$ through $\hat{v}_6$ as shown in Figure 20. The 54 FEC bits are added to the 88 speech bits in $\hat{u}_0$ through $\hat{u}_6$ to produce $\hat{v}_0$ through $\hat{v}_6$. The 54 FEC bits are divided among one [19,7] extended Golay code, on [24,12] extended Golay code, two [23,12] Golay code, and two [15,11] Hamming codes. Generation of the v vectors is performed according to the following equations,

$$\hat{v}_0 = \hat{u}_0 \cdot g_{EG} \tag{80}$$

$$\hat{v}_1 = \hat{u}_1 \cdot g_{EG} \tag{81}$$

$$\hat{v}_2 = \hat{u}_2 \cdot g_G \tag{82}$$

$$\hat{v}_3 = \hat{u}_3 \cdot g_G \tag{83}$$

$$\hat{v}_4 = \hat{u}_4 \cdot g_H \tag{84}$$

$$\hat{v}_5 = \hat{u}_5 \cdot g_H \tag{85}$$

$$\hat{v}_6 = \hat{u}_6 \tag{86}$$

where g_{EG} is the generator matrix for the [24,12] extended Golay code, g_G is the generator matrix for the [23,12] Golay code, and g_H is the generator matrix for the [15,11] Hamming code. Elements of the matrices g_{EG}, g_G, and g_H are given below. Absent entries in the tables are equal to zero. Note that the matrix g_G is simply the first 23 columns of the matrix g_{EG}.

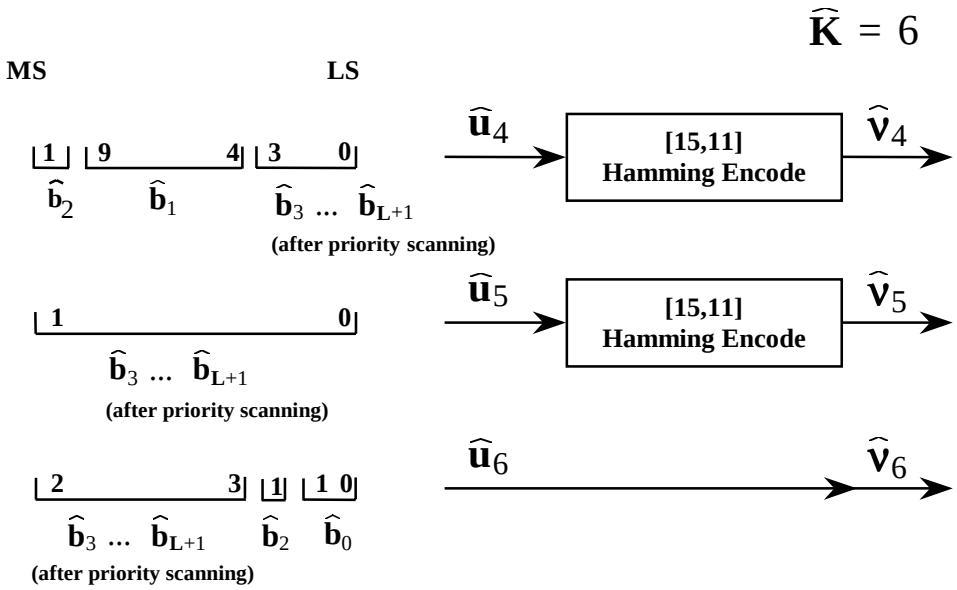

Figure 24: Formation of the Code Vectors $\hat{v}_4$ throught $\hat{v}_6$

$$g_{EG} = \begin{bmatrix}
1 & 0 & & & & & & & & & 1 & 1 & 0 & 0 & 0 & 1 & 1 & 1 & 0 & 1 & 0 & 1 \\
0 & 1 & 0 & & & & & & & & 0 & 1 & 1 & 0 & 0 & 0 & 1 & 1 & 1 & 0 & 1 & 1 \\
 & 0 & 1 & 0 & & & & & & & 1 & 1 & 1 & 1 & 0 & 1 & 1 & 0 & 1 & 0 & 0 & 0 \\
 & & 0 & 1 & 0 & & & & & & 0 & 1 & 1 & 1 & 1 & 0 & 1 & 1 & 0 & 1 & 0 & 0 \\
 & & & 0 & 1 & 0 & & & & & 0 & 0 & 1 & 1 & 1 & 1 & 0 & 1 & 1 & 0 & 1 & 0 \\
 & & & & 0 & 1 & 0 & & & & 1 & 1 & 0 & 1 & 1 & 0 & 0 & 1 & 1 & 0 & 0 & 1 \\
 & & & & & 0 & 1 & 0 & & & 0 & 1 & 1 & 0 & 1 & 1 & 0 & 0 & 1 & 1 & 0 & 1 \\
 & & & & & & 0 & 1 & 0 & & 0 & 0 & 1 & 1 & 0 & 1 & 1 & 0 & 0 & 1 & 1 & 1 \\
 & & & & & & & 0 & 1 & 0 & 1 & 1 & 0 & 1 & 1 & 1 & 0 & 0 & 0 & 1 & 1 & 0 \\
 & & & & & & & & 0 & 1 & 0 & 1 & 0 & 1 & 0 & 1 & 0 & 0 & 1 & 0 & 1 & 1 \\
 & & & & & & & & & 0 & 1 & 0 & 1 & 0 & 0 & 1 & 0 & 0 & 1 & 1 & 1 & 1 \\
 & & & & & & & & & & 0 & 1 & 1 & 0 & 0 & 0 & 1 & 1 & 1 & 0 & 1 & 0 & 1 & 1
\end{bmatrix}$$

$$g_{G} = \begin{bmatrix}
1 & 0 & & & & & & & & & 1 & 1 & 0 & 0 & 0 & 1 & 1 & 1 & 0 & 1 & 0 \\
0 & 1 & 0 & & & & & & & & 0 & 1 & 1 & 0 & 0 & 0 & 1 & 1 & 1 & 0 & 1 \\
 & 0 & 1 & 0 & & & & & & & 1 & 1 & 1 & 1 & 0 & 1 & 1 & 0 & 1 & 0 & 0 \\
 & & 0 & 1 & 0 & & & & & & 0 & 1 & 1 & 1 & 1 & 0 & 1 & 1 & 0 & 1 & 0 \\
 & & & 0 & 1 & 0 & & & & & 0 & 0 & 1 & 1 & 1 & 1 & 0 & 1 & 1 & 0 & 1 \\
 & & & & 0 & 1 & 0 & & & & 1 & 1 & 0 & 1 & 1 & 0 & 0 & 1 & 1 & 0 & 0 \\
 & & & & & 0 & 1 & 0 & & & 0 & 1 & 1 & 0 & 1 & 1 & 0 & 0 & 1 & 1 & 0 \\
 & & & & & & 0 & 1 & 0 & & 0 & 0 & 1 & 1 & 0 & 1 & 1 & 0 & 0 & 1 & 1 \\
 & & & & & & & 0 & 1 & 0 & 1 & 1 & 0 & 1 & 1 & 1 & 0 & 0 & 0 & 1 & 1 \\
 & & & & & & & & 0 & 1 & 0 & 1 & 0 & 1 & 0 & 1 & 0 & 0 & 1 & 0 & 1 & 1 \\
 & & & & & & & & & 0 & 1 & 0 & 1 & 0 & 0 & 1 & 0 & 0 & 1 & 1 & 1 & 1 \\
 & & & & & & & & & & 0 & 1 & 1 & 0 & 0 & 0 & 1 & 1 & 1 & 0 & 1 & 0 & 1
\end{bmatrix}$$

$$g_H = \begin{bmatrix}
1 & 0 & & & & & & & & & 1 & 0 & 0 & 1 \\
0 & 1 & 0 & & & & & & & & 1 & 1 & 0 & 1 \\
 & 0 & 1 & 0 & & & & & & & 1 & 1 & 1 & 1 \\
 & & 0 & 1 & 0 & & & & & & 1 & 1 & 1 & 0 \\
 & & & 0 & 1 & 0 & & & & & 0 & 1 & 1 & 1 \\
 & & & & 0 & 1 & 0 & & & & 1 & 0 & 1 & 0 \\
 & & & & & 0 & 1 & 0 & & & 0 & 1 & 0 & 1 \\
 & & & & & & 0 & 1 & 0 & & 1 & 0 & 1 & 1 \\
 & & & & & & & 0 & 1 & 0 & 1 & 1 & 0 & 0 \\
 & & & & & & & & 0 & 1 & 0 & 0 & 1 & 1 & 0 \\
 & & & & & & & & & 0 & 1 & 0 & 0 & 1 & 1
\end{bmatrix}$$

7.4 Bit Modulation

The IMBE speech code uses bit modulation keyed off the code vector $\hat{v}_0$ to provide a mechanism for detecting errors in $\hat{v}_0$ beyond the errors that the [19,7] extended Golay code can correct. Not that the term bit modulation in the context of this document refers to the presented method for multiplying (or modulating) each frame of code vectors by a data dependent pseudo-random sequence. The first step in this procedure is to generate a set of binary modulation vectors which are added (modulo 2) to the code vectors $\hat{v}_0$ through $\hat{v}_6$. The modulation vectors are generated from a pseudo-random sequence whose

$$p_r(0) = 16\hat{u}_0 \quad \textbf{(87)}$$

$$p_r(n) = 173p_r(n-1) + 13849 - 65536\left\lfloor \frac{173p_r(n-1) + 13849}{65536} \right\rfloor \quad \textbf{(88)}$$

seed is derived from $\hat{u}_0$. Specifically, the sequence define in the following equations is used, where the bit vector $\hat{u}_0$ is interpreted as an unsigned 7 bit number in the range (0, 127). Equation (88) is used to recursively compute the pseudi-random sequence, $p_r(n)$, over the range $1 \leq n \leq 100$. Each element of this sequence can be interpreted as a 16 bit random number which is uniformly distributed over the interval (0,

65535). Using this interpretation, a set of binary modulation vectors, denoted by $\hat{m}_0$ through $\hat{m}_6$, are generated from this sequence as shown below.

$$\hat{m}_0 = [0, 0, \ldots, 0] \quad (89)$$

$$\hat{m}_1 = \left[\left\lfloor \frac{p_r(1)}{32768} \right\rfloor, \left\lfloor \frac{p_r(2)}{32768} \right\rfloor, \ldots, \left\lfloor \frac{p_r(24)}{32768} \right\rfloor \right] \quad (90)$$

$$\hat{m}_2 = \left[\left\lfloor \frac{p_r(25)}{32768} \right\rfloor, \left\lfloor \frac{p_r(26)}{32768} \right\rfloor, \ldots, \left\lfloor \frac{p_r(47)}{32768} \right\rfloor \right] \quad (91)$$

$$\hat{m}_3 = \left[\left\lfloor \frac{p_r(48)}{32768} \right\rfloor, \left\lfloor \frac{p_r(49)}{32768} \right\rfloor, \ldots, \left\lfloor \frac{p_r(70)}{32768} \right\rfloor \right] \quad (92)$$

$$\hat{m}_4 = \left[\left\lfloor \frac{p_r(71)}{32768} \right\rfloor, \left\lfloor \frac{p_r(72)}{32768} \right\rfloor, \ldots, \left\lfloor \frac{p_r(85)}{32768} \right\rfloor \right] \quad (93)$$

$$\hat{m}_5 = \left[\left\lfloor \frac{p_r(86)}{32768} \right\rfloor, \left\lfloor \frac{p_r(87)}{32768} \right\rfloor, \ldots, \left\lfloor \frac{p_r(100)}{32768} \right\rfloor \right] \quad (94)$$

$$\hat{m}_6 = [0, 0, \ldots, 0] \quad (95)$$

Once these modulation vectors have been computed in this manner, the modulated code vectors, $\hat{\nu}_i$ for $0 \leq i \leq 6$, are computed by adding (modulo 2) the code vectors to the modulation vectors.

$$\hat{c}_i = \hat{\nu}_i + \hat{m}_i \qquad \text{for } 0 \leq i \leq 6 \quad (96)$$

One should note that the bit modulation performed by the IMBE encoder can be inverted by the decoder if $\tilde{c}_0$ does not contain any uncorrectable bit errors. In this case Golay decoding $\tilde{c}_0$, which always equals $\tilde{\nu}_0$ since $\tilde{m}_0 = 0$, will yield the correct value of $\tilde{u}_0$. The decoder can then use $\tilde{u}_0$ to reconstruct the pseudo-random sequence and the modulation vectors $\tilde{m}_1$ through $\tilde{m}_6$. Subtracting these vectors from $\tilde{c}_1$ though $\tilde{c}_6$ will then yield the code vectors $\tilde{\nu}_1$ though $\tilde{\nu}_6$. At this point the remaining error control decoding can be performed. In the other case, where $\tilde{c}_0$ contains uncorrectable bit errors, the modulation cannot generally be inverted by the decoder. In this case the likely result of Golay decoding $\tilde{c}_0$ will be some $\tilde{u}_0$ which does not equal $\hat{u}_0$. Consequently the decoder will initialize the pseudo-random sequence incorrectly, and the modulation vectors computed by the decoder will be uncorrelated with the modulation vectors used by the encoder. Using these incorrect modulation vectors to reconstruct the code vectors is essentially the same as passing $\tilde{\nu}_1, \ldots, \tilde{\nu}_6$ through a 50 percent bit error rate (BER) channel. The IMBE decoder exploits the fact that, statistically, a 50 percent BER causes the Golay and Hamming codes employed on $\tilde{\nu}_1$ through $\tilde{\nu}_6$ to

correct a number of errors which is near the maximum capability of the code. By counting the total number of errors which are corrected in all of these code vectors, the decoder is able to reliably detect frames in which $\tilde{c}_0$ is likely to contain uncorrectable bit errors. The decoder performs frame repeats during these frames in order to reduce the perceived degradation in the presence of bit errors. This is explained more fully in Sections 7.6 and 7.7.

7.5 Bit Interleaving

Intra-frame bit interleaving is used to spread short bursts of errors among several code words. The interleaving table for the 142 bits in each frame is tabulated in Annex H. This annex uses the notation scheme where bit N-1 (where N is the vector length) is the MSB and bit 0 is the LSB. The minimum separation between any two bits of the same error correction code is, in most cases, 6 bits.

7.6 Error Estimation

The IMBE speech decoder estimates the number of errors in each received data frame by computing the number of errors corrected by the [19,7] Extended Golay code, the [24,12] Extended Golay code, the [23,12] Golay codes, and the [15,11] Hamming codes. The number of errors for each code vector is denoted ϵ_i for $0 \leq i \leq 6$, where ϵ_i refers to the number of bit errors which were corrected during the error decoding of $\tilde{u}_i$. From these error values two other error parameters are computed as shown below.

$$\varepsilon_T = \sum_{i=0}^{5} \varepsilon_i \tag{97}$$

$$\varepsilon_R(0) = 0.95 * \varepsilon_R(-1) + 0.00042\varepsilon_T \tag{98}$$

The parameter $\epsilon_R(0)$ is the estimate of the error rate for the current frame, while $\epsilon_R(-1)$ is the estimate of the error rate for the previous frame. These error parameters are used to control the frame repeat process described below, and to control the parametric smoothing functions described in Section 9.

7.7 Frame Repeats

The IMBE decoder examines each received data frame in order to detect and discard frames which are highly corrupted. A number of different fault conditions are checked and if any of these conditions indicate the current frame is invalid, then a frame repeat is performed. The IMBE speech encoder uses values of $\hat{b}_0$

in the range $0 \leq \hat{b}_0 \leq 207$ to represent valid pitch estimates. The remaining values of $\hat{b}_0$ are reserved for future expansion and are currently considered invalid. A frame repeat is performed by the decoder if it receives an invalid value of $\tilde{b}_0$, or if both of the following two equations are true.

$$\epsilon_0 \geq 2 \tag{99}$$

$$\epsilon_T \geq 12 \tag{100}$$

These two equations are used to detect the incorrect bit demodulation which results if there are uncorrectable bit errors in $\tilde{c}_0$. The decoder performs a frame repeat by taking the following steps:

1) The current 142 bit received data frame is marked as invalid and subsequently ignored during future processing steps.
2) The IMBE model parameters for the current frame are set equal to the IMBE model parameters for the previous frame. Specifically, the following update expressions are computed.

$$\tilde{\omega}_0(0) = \tilde{\omega}_0(-1) \tag{101}$$

$$\tilde{L}_0(0) = \tilde{L}_0(-1) \tag{102}$$

$$\tilde{K}_0(0) = \tilde{K}_0(-1) \tag{103}$$

$$\tilde{v}_k(0) = \tilde{v}_k(-1) \qquad \text{for } 1 \leq k \leq \tilde{K} \tag{104}$$

$$\tilde{M}_l(0) = \tilde{M}_l(-1) \qquad \text{for } 1 \leq l \leq \tilde{L} \tag{105}$$

$$\overline{M}_l(0) = \overline{M}_l(-1) \qquad \text{for } 1 \leq l \leq \tilde{L} \tag{106}$$

3) The repeated model parameters are used in all future processing wherever the current model parameters are required. This includes the synthesis of the current segment of speech as is described in Section 11.

7.8 Frame Muting

The IMBE decoder is required to mute in severe bit error environments for which ϵ_R > .0875. This capability causes the decoder to squelch its output if reliable communication cannot be supported.

The recommended muting method is to first compute the update equations as listed in step (2) of the frame repeat process (see Section 7.7). The decoder should then bypass the speech synthesis algorithm described in Section 11 and, instead, set the synthetic speech signal, $\tilde{s}(n)$ to random noise which is uniformly distributed over the interval (-5, 5). This technique provides for a small amount of "comfort noise" as is typically done in telecommunication systems.

8 Spectral Amplitude Enhancement

The IMBE speech decoder attempts to improve the perceived quality of the synthesized speech by enhancing the spectral amplitudes. The unenhanced spectral amplitudes are required by future frames in the computation of Equation (77). However, the enhanced spectral amplitudes are used in speech synthesis. The spectral amplitude enhancement is accomplished by generating a set of spectral weights from the model parameters of the current frame. First R_{M0} and Rm_1 are calculated as shown below.

$$R_{M0} = \sum_{l=1}^{\tilde{L}} \tilde{M}_l^2 \tag{107}$$

$$R_{M1} = \sum_{l=1}^{\tilde{L}} \tilde{M}_l^2 \cos(\tilde{\omega}_0 \, l) \tag{108}$$

Next, the parameters R_{M0} and R_{M1} are used to calculate a set of weights, W_l, given by

$$W_l = \sqrt{\tilde{M}_l} \cdot \left[\frac{.96\pi \left(R_{M0}^2 + R_{M1}^2 - 2R_{M0}R_{M1}\cos(\tilde{\omega}_0 l) \right)}{\tilde{\omega}_0 R_{M0}(R_{M0}^2 - R_{M1}^2)} \right]^{\frac{1}{4}} \qquad \text{for } 1 \le l \le \tilde{L} \tag{109}$$

These weights are then used to enhance the spectral amplitudes for the current frame according to the relationship:

$$\bar{M}_l = \begin{cases} \tilde{M}_l & \text{if } 8\,l \le \tilde{L} \\ 1.2 \cdot \tilde{M}_l & \text{else if } W_l > 1.2 \\ .5 \cdot \tilde{M}_l & \text{else if } W_l < .5 \\ W_l \cdot \tilde{M}_l & \text{otherwise} \end{cases} \qquad \text{for } 1 \le l \le \tilde{L} \tag{110}$$

A final step is to scale the enhanced spectral amplitudes in order to remove any energy difference between the enhanced and unenhanced amplitudes. The correct scale factor, denoted by γ, is given below.

$$\gamma = \left[\frac{R_{M0}}{\sum_{l=1}^{\bar{L}} \left| \bar{M}_l \right|^2} \right]^{\frac{1}{2}} \tag{111}$$

This scale factor is applied to each of the enhanced spectral amplitudes as shown in Equation (112).

$$\tilde{M}_l = \gamma \cdot \bar{M}_l \qquad \text{for } 1 \le l \le \tilde{L} \tag{112}$$

For notational simplicity this equation refers to both the scaled and unscaled spectral amplitudes as $\tilde{M}_l$. This convention has been adopted since the unscaled amplitudes are discarded and only the scaled amplitudes are subsequently used by the decoder during parameter smoothing and speech synthesis.

The value of R_{M0} expressed in Equation (107) is a measure of the energy in the current frame. This value is used to update a local energy parameter in accordance with the following rule.

$$S_E(0) = \begin{cases} .95\,S_E(-1) + .05\,R_{M0} & \text{if } .95\,S_E(-1) + .05\,R_{M0} \ge 10000.0 \\ 10000.0 & \text{otherwise} \end{cases} \tag{113}$$

This equation generates the local energy parameter for the current frame, $S_E(0)$, from R_{M0} and the value of the local energy parameter from the previous frame $S_E(-1)$. The parameter $S_E(0)$ is used in the following section.

9 Adaptive Smoothing

As part of the error control process described in Section 7.6, the decoder estimates two error rate parameters, ϵ_T and ϵ_R, which measure the total number of errors and the local error rate for the current

Frame, respectively. These parameters are used by the decoder to adaptively smooth the decoded model parameters. The result is improved performance in high bit error environments.

The first parameters to be smoothed by the decoder are the V/UV decisions. First an adaptive threshold V_M is calculated using equation (114),

$$V_M = \begin{cases} \infty & \text{if } \epsilon_R(0) \leq .005 \text{ and } \epsilon_T \leq 4 \\ \frac{45.255\,(S_E(0))^{.375}}{\exp(277.26\epsilon_R(0))} & \text{else if } \epsilon_R(0) \leq .0125 \text{ and } \epsilon_4 = 0 \\ 1.414\,(S_E(0))^{.375} & \text{otherwise} \end{cases} \tag{114}$$

where the energy parameter $S_E(0)$ is defined in Equation (113) in Section 8. After the adaptive threshold is computed each enhanced spectral amplitude $\bar{M}_l$ for $1 \leq l \leq \tilde{L}$ is compared against V_M, and if $\bar{M}_l > V_M$ then the V/UV decision for that spectral amplitude is left unchanged. This process can be expressed mathematically as shown below.

$$\bar{v}_l = \begin{cases} 1 & \text{if } \bar{M}_l > V_M \\ \bar{v}_l & \text{otherwise} \end{cases} \qquad \text{for } 1 \leq l \leq \tilde{L} \tag{115}$$

Once the V/UV decisions have been smoothed, the decoder adaptively smoothes the spectral amplitudes $\bar{M}_l$ for $1 \leq l \leq \tilde{L}$. The spectral amplitude smoothing algorithm computes the following amplitude measure for the current segment.

$$A_M = \sum_{l=1}^{\tilde{L}} \bar{M}_l \tag{116}$$

Next an amplitude threshold is updated according to the following equation,

$$\tau_M(0) = \begin{cases} 20480 & \text{if } \epsilon_R(0) \leq .005 \text{ and } \epsilon_T(0) \leq 6 \\ 6000 - 300\epsilon_T + \tau_M(-1) & \text{otherwise} \end{cases} \tag{117}$$

where $\tau_M(0)$ and $\tau_M(-1)$ represent the value of the amplitude threshold for the current and previous frames respectively. The two parameters A_M and $\tau_M(0)$ are then used to compute a scale factor γ_M given below.

$$\gamma_M = \begin{cases} 1.0 & \text{if } \tau_M(0) > A_M \\ \frac{\tau_M(0)}{A_M} & \text{otherwise} \end{cases} \tag{118}$$

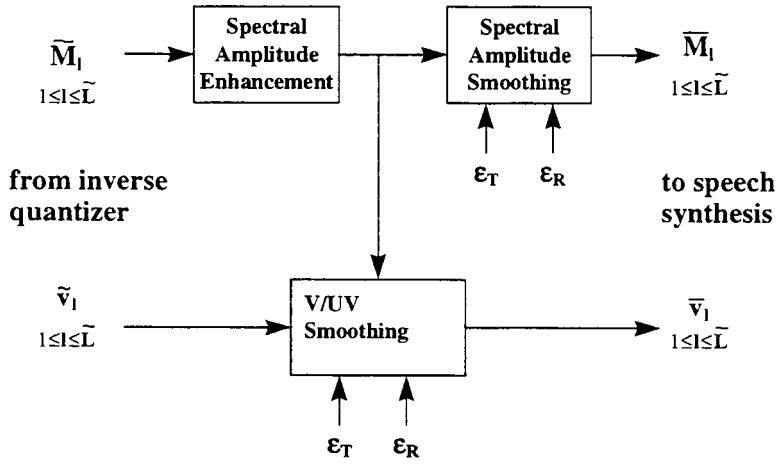

Fig. 25: Parameter Enhancement and Smoothing

This scale factor is multiplied by each of the spectral amplitudes $\tilde{M}_l$ for $1 \leq l \leq \tilde{L}$. Note that this step must be completed after spectral amplitude enhancement has been performed using the methods of Section 8 and after V_M has been computed according to Equation 112. The correct sequence is shown in Figure 25.

i	$\hat{J}_i$	$\hat{c}_{i,1} \ \ldots \ \hat{c}_{i,\hat{J}_i}$
1	2	$\hat{T}_1, \hat{T}_2$
2	2	$\hat{T}_3, \hat{T}_4$
3	3	$\hat{T}_5, \hat{T}_6, \hat{T}_7$
4	3	$\hat{T}_8, \hat{T}_9, \hat{T}_{10}$
5	3	$\hat{T}_{11}, \hat{T}_{12}, \hat{T}_{13}$
6	3	$\hat{T}_{14}, \hat{T}_{15}, \hat{T}_{16}$

Table 5: Division of Prediction Residuals into Blocks in Encoding Example

10 Parameter Encoding Example

This section provides an example of the quantization and bit manipulation for a typical parameter frame. In this example the fundamental frequency is assumed to be equal to $\hat{\omega}_0 = \frac{2\pi}{35.125}$. Since the values of $\hat{L}$ and $\hat{K}$ are related to $\hat{\omega}_0$ through equations (37) and (38), they are equal to $\hat{L}$ = 16 and $\hat{K}$ = 6. The remaining model parameters are left unspecified since they do not affect the numbers presented in this example.

The encoding of this example parameter frame proceeds as follows. First the fundamental frequency is encoded into the 8 bit value $\hat{b}_0$ using equation (45), and the 6 voiced/unvoiced decisions are encoded into the 6 bit value $\hat{b}_1$ using equation (49). The 16 spectral amplitude prediction residuals, $\hat{T}_l$ for $1 \leq l \leq 16$, are then formed using equations (52) through (55). Next, these prediction residuals are divided into six blocks where the lengths of each block, $\hat{J}_i$ for $1 \leq i \leq 6$, are shown in Table 5. The spectral amplitude prediction residuals are then divided into the six vectors $\hat{c}_{i,j}$ for $1 \leq i \leq 6$ and $1 \leq j \leq \hat{J}_i$. The first $\hat{J}_1$ elements of $\hat{T}_l$ form $\hat{c}_{1,j}$. The next $\hat{J}_2$ elements of $\hat{T}_l$ for $\hat{c}_{2,j}$, and so on. This is shown in Table 5. Each block $\hat{c}_{i,j}$ for $1 \leq i \leq 6$, is transformed with a $\hat{J}_i$ point DCT using equation (60) to produce the set DCT coefficients $\hat{C}_{i,k}$ for $1 \leq k \leq \hat{J}_i$. The first DCT coefficient from each of the six blocks is used to form the gain vector $\hat{R}_i$. The gain vector is then transformed into the vector $\hat{G}_m$ using the six point DCT shown in Equation (61). The first element of the transformed gain vector, denoted by $\hat{G}_1$, is then quantized using the non uniform quantizer tabulated in Annex E. The 6 bit value $\hat{b}_2$ is set equal to the index of the quantizer element which

m	$\hat{G}_m$	$\hat{B}_m$	$\hat{\Delta}_m$
2	$\hat{G}_2$	6	.04650
3	$\hat{G}_3$	6	.03015
4	$\hat{G}_4$	6	.02520
5	$\hat{G}_5$	5	.04060
6	$\hat{G}_6$	5	.03696

Table 6: Example Bit Allocation and Step Size for the Transformed Gain Vector

is closest to $\hat{G}_1$. The remaining five elements of the transformed gain vector are quantized using the uniform quantizers generated from Annex F with $\hat{L}$ = 16. The correct step sizes and bit allocation for G_2 through G_6 is shown in Table 6. Once the bit allocation and step sizes have been computed, the bit encodings $\hat{b}_3$ through $\hat{b}_7$ are generated using Equation (62).

After the gain vector has been quantized and encoded, the remaining bits are distributed among the ten higher order DCT coefficients, $\hat{C}_{i,k}$ for $1 \leq i \leq 6$ and $2 \leq k \leq \hat{J}_i$. This is done using Annex G and the

resulting bit allocation is shown in Table 7. Each DCT coefficient is then quantized using equation (63). The step sizes for these quantizers are computed using Tables 3 and 4, and the results are shown in Table 7.

Finally, the 18 bit encodings, $\hat{b}_0$ through $\hat{b}_{17}$ are then rearranged into the seven bit vectors $\hat{u}_0$ through $\hat{u}_6$. This is accomplished using the procedure described in Section 7, and the result is shown in Tables 8 through 10. The convention in these tables is that the appropriate bit from the vector listed in the first two columns is set equal to the appropriate bit from the bit encoding listed in the last two columns, where the least significant bit corresponds to bit 1. The bit vector $\hat{u}_0$ is encoded with a [19,7] Extended Golay code into the code vector $\hat{v}_0$. Bit vector $\hat{u}_1$ is encoded with a [24,12] Extended Golay code into the code vector $\hat{v}_1$. Bit vectors $\hat{u}_2$ and $\hat{u}_3$ are encoded with a [23,12] Golay code into the code vectors $\hat{v}_2$ and $\hat{v}_3$, respectively. Similarly, the two bit vectors $\hat{u}_4$ and $\hat{u}_5$ are each encoded with a [15,11] Hamming code into the code vectors $\hat{v}_4$ and $\hat{v}_5$. The vector $\hat{v}_6$ is set equal to $\hat{u}_6$. These code vectors are then modulated using Equation (96) to produce the modulated code vectors $\hat{c}_0$ through $\hat{c}_6$. The seven modulated code vectors are then interleaved as specified in Appendix H, and finally the frame bits are embedded in the Enhance Digital Access Communications System format in ascending order.

m	$\hat{C}_{i,k}$	$\hat{B}_m$	$\hat{\Delta}_m$
8	$\hat{C}_{1,2}$	6	.04605
9	$\hat{C}_{2,2}$	6	.04605
10	$\hat{C}_{3,2}$	5	.08596
11	$\hat{C}_{3,3}$	4	.09640
12	$\hat{C}_{4,2}$	4	.12280
13	$\hat{C}_{4,3}$	3	.15665
14	$\hat{C}_{5,2}$	3	.19955
15	$\hat{C}_{5,3}$	3	.15665
16	$\hat{C}_{6,2}$	3	.19955
17	$\hat{C}_{6,3}$	2	.20485

Table 7: Example Bit Allocation and Step Size for Higher Order DCT Coefficients

Vector	*Bit Number*	*Vector*	*Bit Number*
$\hat{u}_0$	7	n/a	$\hat{u}_{0,7} = 0$
$\hat{u}_0$	6	$\hat{b}_0$	8
$\hat{u}_0$	5	$\hat{b}_0$	7
$\hat{u}_0$	4	$\hat{b}_0$	6
$\hat{u}_0$	3	$\hat{b}_0$	5
$\hat{u}_0$	2	$\hat{b}_0$	4
$\hat{u}_0$	1	$\hat{b}_0$	3
$\hat{u}_1$	12	$\hat{b}_2$	6
$\hat{u}_1$	11	$\hat{b}_2$	5
$\hat{u}_1$	10	$\hat{b}_2$	4
$\hat{u}_1$	9	$\hat{b}_3$	6
$\hat{u}_1$	8	$\hat{b}_4$	6
$\hat{u}_1$	7	$\hat{b}_5$	6
$\hat{u}_1$	6	$\hat{b}_8$	6
$\hat{u}_1$	5	$\hat{b}_9$	6
$\hat{u}_1$	4	$\hat{b}_3$	5
$\hat{u}_1$	3	$\hat{b}_4$	5
$\hat{u}_1$	2	$\hat{b}_5$	5
$\hat{u}_1$	1	$\hat{b}_6$	5
$\hat{u}_2$	12	$\hat{b}_7$	5
$\hat{u}_2$	11	$\hat{b}_8$	5
$\hat{u}_2$	10	$\hat{b}_9$	5
$\hat{u}_2$	9	$\hat{b}_{10}$	5
$\hat{u}_2$	8	$\hat{b}_3$	4
$\hat{u}_2$	7	$\hat{b}_4$	4
$\hat{u}_2$	6	$\hat{b}_5$	4
$\hat{u}_2$	5	$\hat{b}_6$	4
$\hat{u}_2$	4	$\hat{b}_7$	4

Table 8: Construction of the $\hat{u}_i$ in Encoding Example (1 of 3)

Vector	*Bit Number*	*Vector*	*Bit Number*
$\hat{u}_2$	3	$\hat{b}_8$	4
$\hat{u}_2$	2	$\hat{b}_9$	4
$\hat{u}_2$	1	$\hat{b}_{10}$	4
$\hat{u}_3$	12	$\hat{b}_{11}$	4
$\hat{u}_3$	11	$\hat{b}_{12}$	4
$\hat{u}_3$	10	$\hat{b}_3$	3
$\hat{u}_3$	9	$\hat{b}_4$	3
$\hat{u}_3$	8	$\hat{b}_5$	3
$\hat{u}_3$	7	$\hat{b}_6$	3
$\hat{u}_3$	6	$\hat{b}_7$	3
$\hat{u}_3$	5	$\hat{b}_8$	3
$\hat{u}_3$	4	$\hat{b}_9$	3
$\hat{u}_3$	3	$\hat{b}_{10}$	3
$\hat{u}_3$	2	$\hat{b}_{11}$	3
$\hat{u}_3$	1	$\hat{b}_2$	3
$\hat{u}_4$	11	$\hat{b}_2$	2
$\hat{u}_4$	10	$\hat{b}_1$	6
$\hat{u}_4$	9	$\hat{b}_1$	5
$\hat{u}_4$	8	$\hat{b}_1$	4
$\hat{u}_4$	7	$\hat{b}_1$	3
$\hat{u}_4$	6	$\hat{b}_1$	1
$\hat{u}_4$	5	$\hat{b}_1$	1
$\hat{u}_4$	4	$\hat{b}_{12}$	3
$\hat{u}_4$	3	$\hat{b}_{13}$	3
$\hat{u}_4$	2	$\hat{b}_{14}$	3
$\hat{u}_4$	1	$\hat{b}_{15}$	3
$\hat{u}_5$	11	$\hat{b}_{16}$	3
$\hat{u}_5$	10	$\hat{b}_3$	2

Table 9: Construction of the $\hat{u}_i$ in Encoding Example (2 of 3)

Vector	*Bit Number*	*Vector*	*Bit Number*
$\hat{u}_5$	9	$\hat{b}_{10}$	2
$\hat{u}_5$	8	$\hat{b}_{11}$	2
$\hat{u}_5$	7	$\hat{b}_{12}$	2
$\hat{u}_5$	6	$\hat{b}_{13}$	2
$\hat{u}_5$	5	$\hat{b}_{14}$	2
$\hat{u}_5$	4	$\hat{b}_{15}$	2
$\hat{u}_5$	3	$\hat{b}_{16}$	2
$\hat{u}_5$	2	$\hat{b}_{17}$	2
$\hat{u}_5$	1	$\hat{b}_3$	2
$\hat{u}_6$	23	$\hat{b}_4$	2
$\hat{u}_6$	22	$\hat{b}_5$	2
$\hat{u}_6$	21	$\hat{b}_6$	2
$\hat{u}_6$	20	$\hat{b}_7$	2
$\hat{u}_6$	19	$\hat{b}_{17}$	2
$\hat{u}_6$	18	$\hat{b}_3$	1
$\hat{u}_6$	17	$\hat{b}_4$	1
$\hat{u}_6$	16	$\hat{b}_5$	1
$\hat{u}_6$	15	$\hat{b}_6$	1
$\hat{u}_6$	14	$\hat{b}_7$	1
$\hat{u}_6$	13	$\hat{b}_8$	1
$\hat{u}_6$	12	$\hat{b}_9$	1
$\hat{u}_6$	11	$\hat{b}_{10}$	1
$\hat{u}_6$	10	$\hat{b}_{11}$	1
$\hat{u}_6$	9	$\hat{b}_{12}$	1
$\hat{u}_6$	8	$\hat{b}_{13}$	1
$\hat{u}_6$	7	$\hat{b}_{14}$	1
$\hat{u}_6$	6	$\hat{b}_{15}$	1
$\hat{u}_6$	5	$\hat{b}_{16}$	1
$\hat{u}_6$	4	$\hat{b}_{17}$	1
$\hat{u}_6$	3	$\hat{b}_2$	1
$\hat{u}_6$	2	$\hat{b}_0$	2
$\hat{u}_6$	1	$\hat{b}_0$	1

Table 10: Construction of the $\hat{u}_i$ in Encoding Example (3 of 3)

11 Speech Synthesis

As was discussed in Section 5, the IMBE speech coder estimates a set of model parameters for each speech frame. These parameters consist of the fundamental frequency $\hat{\omega}_0$, the V/UV decisions for each frequency band $\hat{v}_k$, and the spectral amplitudes $\hat{M}_l$. After the transmitted bits are received and decoded, a reconstructed set of model parameters is available for synthesizing speech. These reconstructed model parameters (after parameter enhancement and smoothing) are denoted $\tilde{\omega}_0$, $\bar{v}_l$ and $\bar{M}_l$, and they correspond to the reconstructed fundamental frequency, V/UV decisions and spectral amplitudes, respectively. In addition the parameter $\tilde{L}$, defined as the number of spectral amplitudes in the current frame, is generated from $\tilde{\omega}_0$ according to Equation (47). Because of a number of factors (such as quantization and channel errors) the reconstructed model parameters are not the same as the estimated model parameters $\tilde{\omega}_0$, $\hat{v}_k$ and $\hat{M}_l$.

11.1 Speech Synthesis Notation

The IMBE speech synthesis algorithm uses the reconstructed model parameters to generate a speech signal which is perceptually similar to the original speech signal. For each new set of model parameters, the synthesis algorithm generates a 20 ms frame of speech, $\tilde{s}(n)$, which is interpolated between the previous set of model parameters and the newest or current set of model parameters. The notation $\tilde{L}(0)$, $\tilde{\omega}_0(0)$, $\bar{v}_l(0)$, and $\bar{M}_l(0)$ is used to denote the current set of reconstructed model parameters, while the notation $\tilde{L}(-1)$, $\tilde{\omega}_0(-1)$, $\bar{v}_l(-1)$ and $\bar{M}_l(-1)$ is used to denote the previous set of reconstructed model parameters. For each new set of model parameters, $\tilde{s}(n)$ is generated in the range $0 \leq n \leq N$, where N equals 160 samples (20 ms.). This synthetic speech signal is the output of the IMBE voice coder and is suitable for digital to analog conversion with a sixteen bit converter,

The synthetic speech signal is divided into a voiced component $\tilde{s}_v(n)$ and an unvoiced component $\tilde{s}_{uv}(n)$. These two components are synthesized separately, as shown in Figure 26, and then summed to form $\tilde{s}(n)$. The unvoiced speech synthesis algorithm is discussed in Section 11.2 and the voiced speech synthesis algorithm is discussed in Section 11.3.

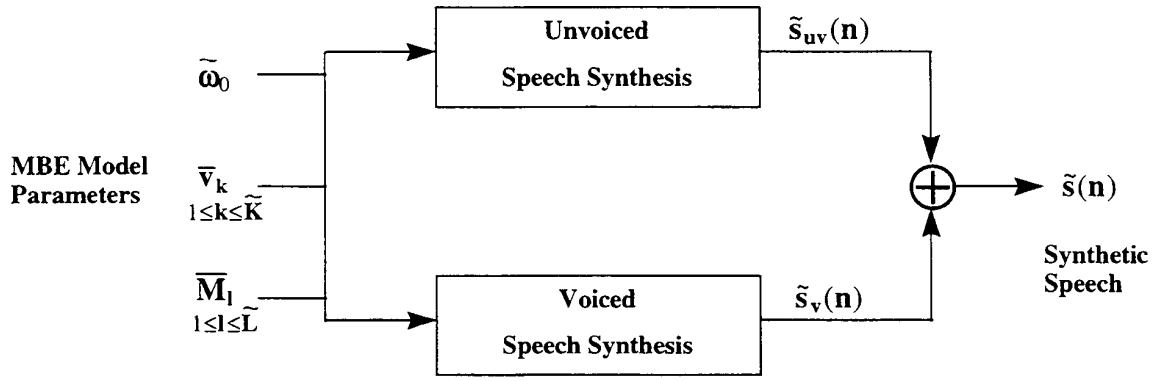

Fig. 26: IMBE Speech Synthesis

11.2 Unvoiced Speech Synthesis

The energy from unvoiced spectral amplitudes is synthesized with an unvoiced speech synthesis algorithm. First a white noise sequence, $u(n)$, is generated. This noise sequence can have an arbitrary mean. A recommended noise sequence (10) can be generated as shown below.

$$u(n+1) = 171u(n) + 11213 - 53125\left\lfloor \frac{171u(n) + 11213}{53125} \right\rfloor \qquad (119)$$

The noise sequence is initialized to $u(-105) = 3147$.

For each successive synthesis frame, $u(n)$ is shifted by 20 ms. (160 samples) and windowed with $w_S(n)$, which is given in Annex I. Since $w_S(n)$ has a non-zero length of 209 samples, there is a 49 sample overlap between the noise signal used in successive synthesis frames. Once the noise sequence has been shifted and windowed, the 256 point Discrete Fourier Transform $U_w(m)$ is computed according to:

$$U_w(m) = \sum_{n=-104}^{104} u(n) w_S(n) e^{-j\frac{2\pi mn}{256}} \qquad \text{for } -128 \le m \le 127 \qquad (120)$$

The function $U_w(m)$ is generated in a manner which is analogous to $S_w(m)$ defined in Equation (28) except that $u(n)$ and $w_S(n)$ are used in place of $s(n)$ and $w_R(n)$.

The function $U_w(m)$ is then modified to create $\tilde{U}_w(m)$. For each *l* in the range $1 \le l \le \tilde{L}(0)$, $\tilde{U}_w(m)$ is computed according to Equation (122) if the *l*'th spectral amplitude is unvoiced.

$$\tilde{U}_w(m) = 0 \qquad \text{for } \lceil \tilde{a}_l \rceil \le |m| < \lceil \tilde{b}_l \rceil \tag{121}$$

$$\tilde{U}_m(m) = \frac{\gamma_m \overline{M}_l(0) U_m(m)}{\left[\frac{\sum_{\eta=\lceil \tilde{a}_L \rceil}^{\lceil \tilde{b}_l \rceil - 1} |U_w(\eta)|^2}{(\lceil \tilde{b}_l \rceil - \lceil \tilde{a}_l \rceil)} \right]^{\frac{1}{2}}} \qquad \text{for } \lceil \tilde{a} \rceil \le |m| < \lceil \tilde{b} \rceil \tag{122}$$

The unvoiced scaling coefficient γ_w is a function of the synthesis window $w_S(n)$ and the pitch refinement window $w_R(n)$. It is computed according to the formula:

$$\gamma_w = \left[\sum_{n=-110}^{110} w_R(n) \right] \cdot \left[\frac{\sum_{n=-104}^{104} w_S^2(n)}{\sum_{n=-110}^{110} w_R^2(n)} \right]^{\frac{1}{2}} \tag{123}$$

The frequency bands edges $\tilde{a}_l$ and $\tilde{b}_l$ are computed from $\tilde{\omega}_0$ according to equations (124) and (125), respectively.

$$\tilde{a}_l = \frac{256}{2\pi}(l - .5) \cdot \tilde{\omega}_0 \tag{124}$$

$$\tilde{b}_l = \frac{256}{2\pi}(l + .5) \cdot \tilde{\omega}_0 \tag{125}$$

Finally, the very low frequency and very high frequency components of $\tilde{U}_w(m)$ are set equal to zero as shown in the following equation.

$$\tilde{U}_w(m) = \begin{cases} 0 & \text{for } |m| < \lceil \tilde{a}_1 \rceil \\ 0 & \text{for } \lceil \tilde{b}_{\tilde{L}} \rceil \le |m| \le 128 \end{cases} \tag{126}$$

The sequence $\tilde{u}_w(n)$, defined as the 256 point Inverse Discrete Fourier Transform of $\tilde{U}_w(m)$, is the unvoiced speech for the current frame. The sequence $\tilde{u}_w(n)$ is computed as shown in the following equation.

$$\tilde{u}_w(n) = \frac{1}{256} \sum_{m=128}^{127} \tilde{U}_w(m) e^{j\frac{2\pi mn}{256}} \qquad \text{for } -128 \le n \le 127 \tag{127}$$

In order to generate $\tilde{s}_{uv}(n)$, $\tilde{u}_w(n)$ must be combined with the unvoiced speech from the previous frame. This is accomplished using the Weighted Overlap Add algorithm described in (4). If $\tilde{u}_w(n,0)$ is used to denote the unvoiced speech for the previous frame, then $\tilde{s}_{uv}(n)$ is given by

$$\tilde{s}_{uv}(n) = \frac{w_S(n)\tilde{u}_w(n,-1) + w_S(n-N)\tilde{u}_w(n-N,0)}{w_S^2(n) + w_S^2(n-N)} \qquad \text{for } 0 \le n < N \qquad (128)$$

In this equation $w_S(n)$ is assumed to be zero outside the range -105 ≤ *n* ≤ 105, and $\tilde{u}_w(n,0)$ and $\tilde{u}_w(n,-1)$ are assumed to be zero outside the range -128 ≤ *n* ≤ 127.

11.3 Voiced Speech Synthesis

The voiced speech is synthesized by summing a voiced signal for each spectral amplitude according to the following equation.

$$\tilde{s}_v(n) = \sum_{l=1}^{\max\left[\tilde{L}(-1),\tilde{L}(0)\right]} 2 \cdot \tilde{s}_{v,l}(n) \qquad \text{for } 0 \le n \le N \qquad (129)$$

The reader is referred to references (1, 3) for background information on the algorithm described in this section. The voiced synthesis algorithm attempts to match the *l*'th spectral amplitude of the current frame with the *l*'th spectral amplitude of the previous frame. The algorithm assumes that all spectral amplitudes outside the allowed range are equal to zero as shown in Equations (130) and (131).

$$\bar{M}_l(0) = 0 \qquad \text{for } l > \tilde{L}(0) \qquad (130)$$

$$\bar{M}_l(-1) = 0 \qquad \text{for } l > \tilde{L}(-1) \qquad (131)$$

In addition it assumes that these spectral amplitudes are unvoiced. These assumptions are needed for the case where the number of spectral amplitudes in the current frame is not equal to the number of spectral amplitudes in the previous frame. (i.e. $\tilde{L}(0) \neq \tilde{L}(-1)$).

The signal $\tilde{s}_{v,l}(n)$ is computed differently for each spectral amplitude. If the *l*'th spectral amplitude is unvoiced for both the previous and current speech frame then $\tilde{s}_{v,l}(n)$ is set equal to zero as shown in the following equation. In this case the energy in this region of the spectrum is completely synthesized by the unvoiced synthesis algorithm described in the previous section.

$$\tilde{s}_{v,l}(n) = 0 \qquad \text{for } 0 \le n < N \qquad (132)$$

Alternatively, if the *l*'th spectral amplitude is unvoiced for the current frame and voiced for the previous frame, then $\tilde{s}_{v,l}(n)$ is given by the following equation. In this case the energy in this region of the spectrum transitions from the voiced synthesis algorithm to the unvoiced synthesis algorithm.

$$\tilde{s}_{v,l}(n) = w_S(n)\,\bar{M}_l(-1)\,\cos[\tilde{\omega}_0(-1)\,n\,l + \phi_l(-1)] \qquad \text{for } 0 \le n < N \qquad (133)$$

Similarly, if the *l*'th spectral amplitude is voiced for the current frame and unvoiced for the previous frame then $\tilde{s}_{v,l}(n)$ is given by the following equation. In this case the energy in this region of the spectrum

Transitions from the unvoiced synthesis algorithm to the voiced synthesis algorithm

.

$$\tilde{s}_{v,l}(n) = w_S(n-N)\,\bar{M}_l(0)\,\cos[\tilde{\omega}_0(0)(n-N)\,l + \phi_l(0)] \qquad \text{for } 0 \le n < N \qquad (134)$$

Otherwise, if the *l*'th spectral amplitude is voiced for both the current and the previous frame, and if either *l* >= 8 or $|\tilde{\omega}_0(0) - \tilde{\omega}_0(-1)| \ge .1\ \tilde{\omega}_0(0)$, then $\tilde{s}_{v,l}(n)$ is given by the following equation. In this case the energy in this region of the spectrum is completely synthesized by the voiced synthesis algorithm.

$$\begin{aligned}\tilde{s}_{v,l}(n) &= w_S(n)\,\bar{M}_l(-1)\,\cos[\tilde{\omega}_0(-1)\,n\,l + \phi_l(-1)] \\ &+ w_S(n-N)\,\bar{M}_l(0)\,\cos[\tilde{\omega}_0(0)(n-N)\,l + \phi_l(0)]\end{aligned} \qquad (135)$$

The variable *n* is restricted to the range $0 \le n < N$. The synthesis window $w_S(n)$ used in Equations (133), (134) and (135) is assumed to be equal to zero outside the range $-105 \le n \le 105$.

A final rule is used if the *l*'th spectral amplitude is voiced for both the current and the previous frame, and if both $l < 8$ and $|\tilde{\omega}_0(0) - \tilde{\omega}_0(-1)| < .1\ \tilde{\omega}_0(0)$. In this case $\tilde{s}_{v,l}(n)$ is given by the following equation, and the energy in this region of the spectrum is completely synthesized by the voiced synthesis algorithm.

$$\tilde{s}_{v,l}(n) = a_l(n)\,\cos[\theta_l(n)] \qquad \text{for } 0 \le n < N \qquad (136)$$

The amplitude function $a_l(n)$ is given by,

$$a_l(n) = \bar{M}_l(-1) + \frac{n}{N}[\bar{M}_l(0) - \bar{M}_l(-1)] \tag{137}$$

and the phase function $\theta_l(n)$ is given by Equations (138) through (140).

$$\theta_l(n) = \phi_l(-1) + [\tilde{\omega}_0(-1) \cdot l + \Delta\omega_l(0)]n + [\tilde{\omega}_0(0) - \tilde{\omega}_0(-1)] \cdot \frac{ln^2}{2N} \tag{138}$$

$$\Delta\phi_l(0) = \phi_l(0) - \phi_l(-1) - [\tilde{\omega}_0(-1) + \tilde{\omega}_0(0)] \cdot \frac{lN}{2} \tag{139}$$

$$\Delta\omega_l(0) = \frac{1}{N}\left[\Delta\phi_l(0) - 2\pi\left\lfloor\frac{\Delta\phi_l(0) + \pi}{2\pi}\right\rfloor\right] \tag{140}$$

The phase parameter ϕ_l which is used in the above equations must be updated for each frame using Equations (141) through (143). The notation $\phi_l(0)$ and $\psi_l(0)$ refers to the parameter values in the current frame, while $\phi_l(-1)$ and $\psi_l(-1)$ denotes their counterparts in the previous frame.

$$\psi_l(0) = \psi_l(-1) + [\tilde{\omega}_0(-1) + \tilde{\omega}_0(0)] \cdot \frac{lN}{2} \qquad \text{for } 1 \le l \le 56 \tag{141}$$

$$\phi_l(0) = \begin{cases} \psi_l(0) & \text{for } 1 \le l \le \lfloor\frac{\tilde{L}}{4}\rfloor \\ \psi_l(0) + \frac{\tilde{L}_{uv}(0) \cdot \rho_l(0)}{\tilde{L}(0)} & \text{for } \lfloor\frac{\tilde{L}}{4}\rfloor < l \le \max[\tilde{L}(-1), \tilde{L}(0)] \end{cases} \tag{142}$$

The parameter $\tilde{L}_{uv}(0)$ is equal to the number of unvoiced spectral amplitudes in the current frame, and the parameter $\rho_l(0)$ used in equation (142) is defined to be a random number which is uniformly distributed in the interval $[-\pi, \pi)$. This random number can be generated using the following equation,

$$\rho_l(0) = \frac{2\pi}{53125}u(l) - \pi \tag{143}$$

where *u*(*l*) refers to shifted noise sequence for the current frame, which is described in Section 11.2.

Note that $\psi_l(0)$ must be updated every frame using Equation (141) for $1 \le l \le 56$, regardless of the value of $\tilde{L}$ or the value of the V/UV decisions.

Once $\tilde{s}_{v,l}(n)$ is generated for each spectral amplitude the complete voiced component is generated according to equation (129). The synthetic speech signal is then computed by summing the voiced and unvoiced components as shown in equation (144).

$$\tilde{s}(n) = \tilde{s}_{uv}(n) + \tilde{s}_{v}(n) \qquad \text{for } 0 \leq n < N. \tag{144}$$

This completes the IMBE speech synthesis algorithm.

Algorithm	*Delay (ms.)*
Analysis	73.75
Quantization	0.0
FEC/Interleaving	0.0
Reconstruction	0.0
Synthesis	6.25

Table 11: Breakdown of Algorithmic Delay

12 Additional Notes

The total algorithmic delay is 80 ms. This does not include any processing delay or transmission delay. The break down of the delay is shown in Table 11. The analysis delay is due to the filtering, windowing and two frame look-ahead used in the initial pitch estimation algorithm. The synthesis delay is introduced by the manner in which the synthesis algorithm smoothly transitions between the parameters estimated for consecutive speech frames.

In a few of the figures and the flow charts, the variable $\bar{x}$ is equivalent to the variable $\bar{x}$. For example the variable $\tilde{v}$ in Figure 15 refers to the variable $\tilde{v}$ in the text. This notational discrepancy is a consequence of the graphical software used to produce this document.

Annex A: Variable Initialization

Variable	*Initial Value*
P_{-1}	100
P_{-2}	100
$E_{-1}(P)$	0 for all P
$E_{-2}(P)$	0 for all P
ξ_{max}	100000
$\tilde{\omega}_0(-1)$	$.02985\pi$
$\tilde{M}_l(-1)$	1 for all l
$\bar{M}_l(-1)$	0 for all l
$\tilde{L}(-1)$	30
$\tilde{K}(-1)$	10
$\tilde{v}_k(-1)$	0 for all k
$\bar{v}_k(-1)$	0 for all k
ϵ_R	0.0
S_E	75000
$u(n)$	$u(-105) = 3147$
$\tilde{u}_w(n,-1)$	0 for all n
$\phi_l(-1)$	0 for all l
$\psi_l(-1)$	0 for all l

Annex B: Initial Pitch Estimation Window

n	$w_I(n)$	n	$w_I(n)$	n	$w_I(n)$	n	$w_I(n)$
-150	0.00270174	-110	0.02113325	-70	0.05359430	-30	0.08371302
-149	0.00295485	-109	0.02181198	-69	0.05446897	-29	0.08424167
-148	0.00321783	-108	0.02250030	-68	0.05534209	-28	0.08475497
-147	0.00349080	-107	0.02319806	-67	0.05621329	-27	0.08525267
-146	0.00377385	-106	0.02390509	-66	0.05708219	-26	0.08573447
-145	0.00406710	-105	0.02462122	-65	0.05794842	-25	0.08620022
-144	0.00437064	-104	0.02534628	-64	0.05881159	-24	0.08664963
-143	0.00468457	-103	0.02608007	-63	0.05967136	-23	0.08708246
-142	0.00500898	-102	0.02682242	-62	0.06052732	-22	0.08749853
-141	0.00534396	-101	0.02757312	-61	0.06137912	-21	0.08789764
-140	0.00568957	-100	0.02833197	-60	0.06222639	-20	0.08827950
-139	0.00604590	-99	0.02909875	-59	0.06306869	-19	0.08864402
-138	0.00641300	-98	0.02987323	-58	0.06390573	-18	0.08899096
-137	0.00679095	-97	0.03065519	-57	0.06473708	-17	0.08932017
-136	0.00717979	-96	0.03144442	-56	0.06556234	-16	0.08963151
-135	0.00757957	-95	0.03224064	-55	0.06638119	-15	0.08992471
-134	0.00799034	-94	0.03304362	-54	0.06719328	-14	0.09019975
-133	0.00841213	-93	0.03385311	-53	0.06799815	-13	0.09045644
-132	0.00884496	-92	0.03466884	-52	0.06879549	-12	0.09069464
-131	0.00928887	-91	0.03549054	-51	0.06958490	-11	0.09091420
-130	0.00974387	-90	0.03631795	-50	0.07036604	-10	0.09111510
-129	0.01020996	-89	0.03715080	-49	0.07113854	-9	0.09129713
-128	0.01068715	-88	0.03798876	-48	0.07190202	-8	0.09146029
-127	0.01117544	-87	0.03883159	-47	0.07265611	-7	0.09160442
-126	0.01167480	-86	0.03967896	-46	0.07340052	-6	0.09172948
-125	0.01218523	-85	0.04053057	-45	0.07413481	-5	0.09183547
-124	0.01270669	-84	0.04138612	-44	0.07485873	-4	0.09192220
-123	0.01323915	-83	0.04224531	-43	0.07557184	-3	0.09198972
-122	0.01378257	-82	0.04310780	-42	0.07627381	-2	0.09203795
-121	0.01433691	-81	0.04397328	-41	0.07696434	-1	0.09206691
-120	0.01490209	-80	0.04484143	-40	0.07764313	0	0.09207659
-119	0.01547807	-79	0.04571191	-39	0.07830978	1	0.09206691
-118	0.01606477	-78	0.04658438	-38	0.07896401	2	0.09203795
-117	0.01666212	-77	0.04745849	-37	0.07960547	3	0.09198972
-116	0.01727001	-76	0.04833391	-36	0.08023385	4	0.09192220
-115	0.01788837	-75	0.04921030	-35	0.08084887	5	0.09183547
-114	0.01851709	-74	0.05008731	-34	0.08145022	6	0.09172948
-113	0.01915605	-73	0.05096456	-33	0.08203757	7	0.09160442
-112	0.01980515	-72	0.05184171	-32	0.08261070	8	0.09146029
-111	0.02046427	-71	0.05271840	-31	0.08316927	9	0.09129713

n	$w_I(n)$	n	$w_I(n)$	n	$w_I(n)$	n	$w_I(n)$
10	0.09111510	50	0.07036604	90	0.03631795	130	0.00974387
11	0.09091420	51	0.06958490	91	0.03549054	131	0.00928887
12	0.09069464	52	0.06879549	92	0.03466884	132	0.00884496
13	0.09045644	53	0.06799815	93	0.03385311	133	0.00841213
14	0.09019975	54	0.06719328	94	0.03304362	134	0.00799034
15	0.08992471	55	0.06638119	95	0.03224064	135	0.00757957
16	0.08963151	56	0.06556234	96	0.03144442	136	0.00717979
17	0.08932017	57	0.06473708	97	0.03065519	137	0.00679095
18	0.08899096	58	0.06390573	98	0.02987323	138	0.00641300
19	0.08864402	59	0.06306869	99	0.02909875	139	0.00604590
20	0.08827950	60	0.06222639	100	0.02833197	140	0.00568957
21	0.08789764	61	0.06137912	101	0.02757312	141	0.00534396
22	0.08749853	62	0.06052732	102	0.02682242	142	0.00500898
23	0.08708246	63	0.05967136	103	0.02608007	143	0.00468457
24	0.08664963	64	0.05881159	104	0.02534628	144	0.00437064
25	0.08620022	65	0.05794842	105	0.02462122	145	0.00406710
26	0.08573447	66	0.05708219	106	0.02390509	146	0.00377385
27	0.08525267	67	0.05621329	107	0.02319806	147	0.00349080
28	0.08475497	68	0.05534209	108	0.02250030	148	0.00321783
29	0.08424167	69	0.05446897	109	0.02181198	149	0.00295485
30	0.08371302	70	0.05359430	110	0.02113325	150	0.00270174
31	0.08316927	71	0.05271840	111	0.02046427		
32	0.08261070	72	0.05184171	112	0.01980515		
33	0.08203757	73	0.05096456	113	0.01915605		
34	0.08145022	74	0.05008731	114	0.01851709		
35	0.08084887	75	0.04921030	115	0.01788837		
36	0.08023385	76	0.04833391	116	0.01727001		
37	0.07960547	77	0.04745849	117	0.01666212		
38	0.07896401	78	0.04658438	118	0.01606477		
39	0.07830978	79	0.04571191	119	0.01547807		
40	0.07764313	80	0.04484143	120	0.01490209		
41	0.07696434	81	0.04397328	121	0.01433691		
42	0.07627381	82	0.04310780	122	0.01378257		
43	0.07557184	83	0.04224531	123	0.01323915		
44	0.07485873	84	0.04138612	124	0.01270669		
45	0.07413481	85	0.04053057	125	0.01218523		
46	0.07340052	86	0.03967896	126	0.01167480		
47	0.07265611	87	0.03883159	127	0.01117544		
48	0.07190202	88	0.03798876	128	0.01068715		
49	0.07113854	89	0.03715080	129	0.01020996		

Annex C: Pitch Refinement Window

n	$w_R(n)$	n	$w_R(n)$	n	$w_R(n)$	n	$w_R(n)$	n	$w_R(n)$
-110	0.014873	-78	0.205355	-46	0.607067	-14	0.956477	18	0.928916
-109	0.017397	-77	0.215294	-45	0.620807	-13	0.962377	19	0.921074
-108	0.020102	-76	0.225466	-44	0.634490	-12	0.967866	20	0.912868
-107	0.022995	-75	0.235869	-43	0.648105	-11	0.972940	21	0.904307
-106	0.026081	-74	0.246497	-42	0.661638	-10	0.977592	22	0.895400
-105	0.029365	-73	0.257347	-41	0.675076	-9	0.981817	23	0.886157
-104	0.032852	-72	0.268413	-40	0.688406	-8	0.985610	24	0.876589
-103	0.036546	-71	0.279689	-39	0.701616	-7	0.988967	25	0.866705
-102	0.040451	-70	0.291171	-38	0.714692	-6	0.991884	26	0.856516
-101	0.044573	-69	0.302851	-37	0.727620	-5	0.994358	27	0.846033
-100	0.048915	-68	0.314724	-36	0.740390	-4	0.996386	28	0.835267
-99	0.053482	-67	0.326782	-35	0.752986	-3	0.997966	29	0.824231
-98	0.058277	-66	0.339018	-34	0.765397	-2	0.999095	30	0.812935
-97	0.063303	-65	0.351425	-33	0.777610	-1	0.999774	31	0.801391
-96	0.068563	-64	0.363994	-32	0.789612	0	1.000000	32	0.789612
-95	0.074062	-63	0.376718	-31	0.801391	1	0.999774	33	0.777610
-94	0.079801	-62	0.389588	-30	0.812935	2	0.999095	34	0.765397
-93	0.085782	-61	0.402594	-29	0.824231	3	0.997966	35	0.752986
-92	0.092009	-60	0.415727	-28	0.835267	4	0.996386	36	0.740390
-91	0.098483	-59	0.428978	-27	0.846033	5	0.994358	37	0.727620
-90	0.105205	-58	0.442337	-26	0.856516	6	0.991884	38	0.714692
-89	0.112176	-57	0.455793	-25	0.866705	7	0.988967	39	0.701616
-88	0.119398	-56	0.469336	-24	0.876589	8	0.985610	40	0.688406
-87	0.126872	-55	0.482955	-23	0.886157	9	0.981817	41	0.675076
-86	0.134596	-54	0.496640	-22	0.895400	10	0.977592	42	0.661638
-85	0.142572	-53	0.510379	-21	0.904307	11	0.972940	43	0.648105
-84	0.150799	-52	0.524160	-20	0.912868	12	0.967866	44	0.634490
-83	0.159276	-51	0.537971	-19	0.921074	13	0.962377	45	0.620807
-82	0.168001	-50	0.551802	-18	0.928916	14	0.956477	46	0.607067
-81	0.176974	-49	0.565639	-17	0.936386	15	0.950174	47	0.593284
-80	0.186192	-48	0.579470	-16	0.943474	16	0.943474	48	0.579470
-79	0.195653	-47	0.593284	-15	0.950174	17	0.936386	49	0.565639

n	$w_R(n)$	n	$w_R(n)$
50	0.551802	82	0.168001
51	0.537971	83	0.159276
52	0.524160	84	0.150799
53	0.510379	85	0.142572
54	0.496640	86	0.134596
55	0.482955	87	0.126872
56	0.469336	88	0.119398
57	0.455793	89	0.112176
58	0.442337	90	0.105205
59	0.428978	91	0.098483
60	0.415727	92	0.092009
61	0.402594	93	0.085782
62	0.389588	94	0.079801
63	0.376718	95	0.074062
64	0.363994	96	0.068563
65	0.351425	97	0.063303
66	0.339018	98	0.058277
67	0.326782	99	0.053482
68	0.314724	100	0.048915
69	0.302851	101	0.044573
70	0.291171	102	0.040451
71	0.279689	103	0.036546
72	0.268413	104	0.032852
73	0.257347	105	0.029365
74	0.246497	106	0.026081
75	0.235869	107	0.022995
76	0.225466	108	0.020102
77	0.215294	109	0.017397
78	0.205355	110	0.014873
79	0.195653		
80	0.186192		
81	0.176974		

Annex D: FIR Low Pass Filter

n	$h_{LPF}(n)$
-10	-.002898
-9	-.002831
-8	.005666
-7	.016601
-6	.008800
-5	-.026955
-4	-.055990
-3	-.015116
-2	.118754
1	.278990
0	.351338
1	.278990
2	.118754
3	-.015116
4	-.055990
5	-.026955
6	.008800
7	.016601
8	.005666
9	-.002831
10	-.002898

Annex E: Gain Quantizer Levels

$\hat{b}_2$	*Quantizer Level*	$\hat{b}_2$	*Quantizer Level*
0	-2.842205	32	2.653909
1	-2.694235	33	2.780654
2	-2.558260	34	2.925355
3	-2.382850	35	3.076390
4	-2.221042	36	3.220825
5	-2.095574	37	3.402869
6	-1.980845	38	3.585096
7	-1.836058	39	3.784606
8	-1.645556	40	3.955521
9	-1.417658	41	4.155636
10	-1.261301	42	4.314009
11	-1.125631	43	4.444150
12	-0.958207	44	4.577542
13	-0.781591	45	4.735552
14	-0.555837	46	4.909493
15	-0.346976	47	5.085264
16	-0.147249	48	5.254767
17	0.027755	49	5.411894
18	0.211495	50	5.568094
19	0.388380	51	5.738523
20	0.552873	52	5.919215
21	0.737223	53	6.087701
22	0.932197	54	6.280685
23	1.139032	55	6.464201
24	1.320955	56	6.647736
25	1.483433	57	6.834672
26	1.648297	58	7.022583
27	1.801447	59	7.211777
28	1.942731	60	7.471016
29	2.118613	61	7.738948
30	2.321486	62	8.124863
31	2.504443	63	8.695827

Annex F: Bit Allocation and Step Size for Transformed Gain Vector

$\hat{L}$	$\hat{G}_{m-1}$	$\hat{b}_m$	$\hat{B}_m$	$\hat{\Delta}_m$	$\hat{L}$	$\hat{G}_{m-1}$	$\hat{b}_m$	$\hat{B}_m$	$\hat{\Delta}_m$
9	$\hat{G}_2$	$\hat{b}_3$	10	0.003100	15	$\hat{G}_2$	$\hat{b}_3$	7	0.024800
9	$\hat{G}_3$	$\hat{b}_4$	9	0.004020	15	$\hat{G}_3$	$\hat{b}_4$	6	0.030150
9	$\hat{G}_4$	$\hat{b}_5$	9	0.003360	15	$\hat{G}_4$	$\hat{b}_5$	6	0.025200
9	$\hat{G}_5$	$\hat{b}_6$	9	0.002900	15	$\hat{G}_5$	$\hat{b}_6$	6	0.021750
9	$\hat{G}_6$	$\hat{b}_7$	9	0.002640	15	$\hat{G}_6$	$\hat{b}_7$	5	0.036960
10	$\hat{G}_2$	$\hat{b}_3$	9	0.006200	16	$\hat{G}_2$	$\hat{b}_3$	6	0.046500
10	$\hat{G}_3$	$\hat{b}_4$	9	0.004020	16	$\hat{G}_3$	$\hat{b}_4$	6	0.030150
10	$\hat{G}_4$	$\hat{b}_5$	8	0.006720	16	$\hat{G}_4$	$\hat{b}_5$	6	0.025200
10	$\hat{G}_5$	$\hat{b}_6$	8	0.005800	16	$\hat{G}_5$	$\hat{b}_6$	5	0.040600
10	$\hat{G}_6$	$\hat{b}_7$	8	0.005280	16	$\hat{G}_6$	$\hat{b}_7$	5	0.036960
11	$\hat{G}_2$	$\hat{b}_3$	8	0.012400	17	$\hat{G}_2$	$\hat{b}_3$	6	0.046500
11	$\hat{G}_3$	$\hat{b}_4$	8	0.008040	17	$\hat{G}_3$	$\hat{b}_4$	6	0.030150
11	$\hat{G}_4$	$\hat{b}_5$	8	0.006720	17	$\hat{G}_4$	$\hat{b}_5$	5	0.047040
11	$\hat{G}_5$	$\hat{b}_6$	7	0.011600	17	$\hat{G}_5$	$\hat{b}_6$	5	0.040600
11	$\hat{G}_6$	$\hat{b}_7$	7	0.010560	17	$\hat{G}_6$	$\hat{b}_7$	5	0.036960
12	$\hat{G}_2$	$\hat{b}_3$	8	0.012400	18	$\hat{G}_2$	$\hat{b}_3$	6	0.046500
12	$\hat{G}_3$	$\hat{b}_4$	7	0.016080	18	$\hat{G}_3$	$\hat{b}_4$	5	0.056280
12	$\hat{G}_4$	$\hat{b}_5$	7	0.013440	18	$\hat{G}_4$	$\hat{b}_5$	5	0.047040
12	$\hat{G}_5$	$\hat{b}_6$	7	0.011600	18	$\hat{G}_5$	$\hat{b}_6$	5	0.040600
12	$\hat{G}_6$	$\hat{b}_7$	7	0.010560	18	$\hat{G}_6$	$\hat{b}_7$	5	0.036960
13	$\hat{G}_2$	$\hat{b}_3$	7	0.024800	19	$\hat{G}_2$	$\hat{b}_3$	6	0.046500
13	$\hat{G}_3$	$\hat{b}_4$	7	0.016080	19	$\hat{G}_3$	$\hat{b}_4$	5	0.056280
13	$\hat{G}_4$	$\hat{b}_5$	7	0.013440	19	$\hat{G}_4$	$\hat{b}_5$	5	0.047040
13	$\hat{G}_5$	$\hat{b}_6$	6	0.021750	19	$\hat{G}_5$	$\hat{b}_6$	4	0.058000
13	$\hat{G}_6$	$\hat{b}_7$	6	0.019800	19	$\hat{G}_6$	$\hat{b}_7$	4	0.052800
14	$\hat{G}_2$	$\hat{b}_3$	7	0.024800	20	$\hat{G}_2$	$\hat{b}_3$	6	0.046500
14	$\hat{G}_3$	$\hat{b}_4$	6	0.030150	20	$\hat{G}_3$	$\hat{b}_4$	5	0.056280
14	$\hat{G}_4$	$\hat{b}_5$	6	0.025200	20	$\hat{G}_4$	$\hat{b}_5$	5	0.047040
14	$\hat{G}_5$	$\hat{b}_6$	6	0.021750	20	$\hat{G}_5$	$\hat{b}_6$	4	0.058000
14	$\hat{G}_6$	$\hat{b}_7$	6	0.019800	20	$\hat{G}_6$	$\hat{b}_7$	4	0.052800

$\hat{L}$	$\hat{G}_{m-1}$	$\hat{b}_m$	$\hat{B}_m$	$\hat{\Delta}_m$	$\hat{L}$	$\hat{G}_{m-1}$	$\hat{b}_m$	$\hat{B}_m$	$\hat{\Delta}_m$
21	$\hat{G}_2$	$\hat{b}_3$	5	0.086800	27	$\hat{G}_2$	$\hat{b}_3$	5	0.086800
21	$\hat{G}_3$	$\hat{b}_4$	5	0.056280	27	$\hat{G}_3$	$\hat{b}_4$	4	0.080400
21	$\hat{G}_4$	$\hat{b}_5$	5	0.047040	27	$\hat{G}_4$	$\hat{b}_5$	4	0.067200
21	$\hat{G}_5$	$\hat{b}_6$	4	0.058000	27	$\hat{G}_5$	$\hat{b}_6$	3	0.094250
21	$\hat{G}_6$	$\hat{b}_7$	4	0.052800	27	$\hat{G}_6$	$\hat{b}_7$	3	0.085800
22	$\hat{G}_2$	$\hat{b}_3$	5	0.086800	28	$\hat{G}_2$	$\hat{b}_3$	4	0.124000
22	$\hat{G}_3$	$\hat{b}_4$	5	0.056280	28	$\hat{G}_3$	$\hat{b}_4$	4	0.080400
22	$\hat{G}_4$	$\hat{b}_5$	4	0.067200	28	$\hat{G}_4$	$\hat{b}_5$	4	0.067200
22	$\hat{G}_5$	$\hat{b}_6$	4	0.058000	28	$\hat{G}_5$	$\hat{b}_6$	3	0.094250
22	$\hat{G}_6$	$\hat{b}_7$	4	0.052800	28	$\hat{G}_6$	$\hat{b}_7$	3	0.085800
23	$\hat{G}_2$	$\hat{b}_3$	5	0.086800	29	$\hat{G}_2$	$\hat{b}_3$	4	0.124000
23	$\hat{G}_3$	$\hat{b}_4$	4	0.080400	29	$\hat{G}_3$	$\hat{b}_4$	4	0.080400
23	$\hat{G}_4$	$\hat{b}_5$	4	0.067200	29	$\hat{G}_4$	$\hat{b}_5$	4	0.067200
23	$\hat{G}_5$	$\hat{b}_6$	4	0.058000	29	$\hat{G}_5$	$\hat{b}_6$	3	0.094250
23	$\hat{G}_6$	$\hat{b}_7$	4	0.052800	29	$\hat{G}_6$	$\hat{b}_7$	3	0.085800
24	$\hat{G}_2$	$\hat{b}_3$	5	0.086800	30	$\hat{G}_2$	$\hat{b}_3$	4	0.124000
24	$\hat{G}_3$	$\hat{b}_4$	4	0.080400	30	$\hat{G}_3$	$\hat{b}_4$	4	0.080400
24	$\hat{G}_4$	$\hat{b}_5$	4	0.067200	30	$\hat{G}_4$	$\hat{b}_5$	4	0.067200
24	$\hat{G}_5$	$\hat{b}_6$	4	0.058000	30	$\hat{G}_5$	$\hat{b}_6$	3	0.094250
24	$\hat{G}_6$	$\hat{b}_7$	4	0.052800	30	$\hat{G}_6$	$\hat{b}_7$	3	0.085800
25	$\hat{G}_2$	$\hat{b}_3$	5	0.086800	31	$\hat{G}_2$	$\hat{b}_3$	4	0.124000
25	$\hat{G}_3$	$\hat{b}_4$	4	0.080400	31	$\hat{G}_3$	$\hat{b}_4$	4	0.080400
25	$\hat{G}_4$	$\hat{b}_5$	4	0.067200	31	$\hat{G}_4$	$\hat{b}_5$	3	0.109200
25	$\hat{G}_5$	$\hat{b}_6$	4	0.058000	31	$\hat{G}_5$	$\hat{b}_6$	3	0.094250
25	$\hat{G}_6$	$\hat{b}_7$	3	0.085800	31	$\hat{G}_6$	$\hat{b}_7$	3	0.085800
26	$\hat{G}_2$	$\hat{b}_3$	5	0.086800	32	$\hat{G}_2$	$\hat{b}_3$	4	0.124000
26	$\hat{G}_3$	$\hat{b}_4$	4	0.080400	32	$\hat{G}_3$	$\hat{b}_4$	4	0.080400
26	$\hat{G}_4$	$\hat{b}_5$	4	0.067200	32	$\hat{G}_4$	$\hat{b}_5$	3	0.109200
26	$\hat{G}_5$	$\hat{b}_6$	3	0.094250	32	$\hat{G}_5$	$\hat{b}_6$	3	0.094250
26	$\hat{G}_6$	$\hat{b}_7$	3	0.085800	32	$\hat{G}_6$	$\hat{b}_7$	3	0.085800

$\hat{L}$	$\hat{G}_{m-1}$	$\hat{b}_m$	$\hat{B}_m$	$\hat{\Delta}_m$	$\hat{L}$	$\hat{G}_{m-1}$	$\hat{b}_m$	$\hat{B}_m$	$\hat{\Delta}_m$
33	$\hat{G}_2$	$\hat{b}_3$	4	0.124000	39	$\hat{G}_2$	$\hat{b}_3$	4	0.124000
33	$\hat{G}_3$	$\hat{b}_4$	3	0.130650	39	$\hat{G}_3$	$\hat{b}_4$	3	0.130650
33	$\hat{G}_4$	$\hat{b}_5$	3	0.109200	39	$\hat{G}_4$	$\hat{b}_5$	3	0.109200
33	$\hat{G}_5$	$\hat{b}_6$	3	0.094250	39	$\hat{G}_5$	$\hat{b}_6$	3	0.094250
33	$\hat{G}_6$	$\hat{b}_7$	3	0.085800	39	$\hat{G}_6$	$\hat{b}_7$	2	0.112200
34	$\hat{G}_2$	$\hat{b}_3$	4	0.124000	40	$\hat{G}_2$	$\hat{b}_3$	4	0.124000
34	$\hat{G}_3$	$\hat{b}_4$	3	0.130650	40	$\hat{G}_3$	$\hat{b}_4$	3	0.130650
34	$\hat{G}_4$	$\hat{b}_5$	3	0.109200	40	$\hat{G}_4$	$\hat{b}_5$	3	0.109200
34	$\hat{G}_5$	$\hat{b}_6$	3	0.094250	40	$\hat{G}_5$	$\hat{b}_6$	3	0.094250
34	$\hat{G}_6$	$\hat{b}_7$	3	0.085800	40	$\hat{G}_6$	$\hat{b}_7$	2	0.112200
35	$\hat{G}_2$	$\hat{b}_3$	4	0.124000	41	$\hat{G}_2$	$\hat{b}_3$	4	0.124000
35	$\hat{G}_3$	$\hat{b}_4$	3	0.130650	41	$\hat{G}_3$	$\hat{b}_4$	3	0.130650
35	$\hat{G}_4$	$\hat{b}_5$	3	0.109200	41	$\hat{G}_4$	$\hat{b}_5$	3	0.109200
35	$\hat{G}_5$	$\hat{b}_6$	3	0.094250	41	$\hat{G}_5$	$\hat{b}_6$	2	0.123250
35	$\hat{G}_6$	$\hat{b}_7$	3	0.085800	41	$\hat{G}_6$	$\hat{b}_7$	2	0.112200
36	$\hat{G}_2$	$\hat{b}_3$	4	0.124000	42	$\hat{G}_2$	$\hat{b}_3$	4	0.124000
36	$\hat{G}_3$	$\hat{b}_4$	3	0.130650	42	$\hat{G}_3$	$\hat{b}_4$	3	0.130650
36	$\hat{G}_4$	$\hat{b}_5$	3	0.109200	42	$\hat{G}_4$	$\hat{b}_5$	3	0.109200
36	$\hat{G}_5$	$\hat{b}_6$	3	0.094250	42	$\hat{G}_5$	$\hat{b}_6$	2	0.123250
36	$\hat{G}_6$	$\hat{b}_7$	3	0.085800	42	$\hat{G}_6$	$\hat{b}_7$	2	0.112200
37	$\hat{G}_2$	$\hat{b}_3$	4	0.124000	43	$\hat{G}_2$	$\hat{b}_3$	4	0.124000
37	$\hat{G}_3$	$\hat{b}_4$	3	0.130650	43	$\hat{G}_3$	$\hat{b}_4$	3	0.130650
37	$\hat{G}_4$	$\hat{b}_5$	3	0.109200	43	$\hat{G}_4$	$\hat{b}_5$	3	0.109200
37	$\hat{G}_5$	$\hat{b}_6$	3	0.094250	43	$\hat{G}_5$	$\hat{b}_6$	2	0.123250
37	$\hat{G}_6$	$\hat{b}_7$	2	0.112200	43	$\hat{G}_6$	$\hat{b}_7$	2	0.112200
38	$\hat{G}_2$	$\hat{b}_3$	4	0.124000	44	$\hat{G}_2$	$\hat{b}_3$	4	0.124000
38	$\hat{G}_3$	$\hat{b}_4$	3	0.130650	44	$\hat{G}_3$	$\hat{b}_4$	3	0.130650
38	$\hat{G}_4$	$\hat{b}_5$	3	0.109200	44	$\hat{G}_4$	$\hat{b}_5$	3	0.109200
38	$\hat{G}_5$	$\hat{b}_6$	3	0.094250	44	$\hat{G}_5$	$\hat{b}_6$	2	0.123250
38	$\hat{G}_6$	$\hat{b}_7$	2	0.112200	44	$\hat{G}_6$	$\hat{b}_7$	2	0.112200

$\hat{L}$	$\hat{G}_{m-1}$	$\hat{b}_m$	$\hat{B}_m$	$\hat{\Delta}_m$	$\hat{L}$	$\hat{G}_{m-1}$	$\hat{b}_m$	$\hat{B}_m$	$\hat{\Delta}_m$
45	$\hat{G}_2$	$\hat{b}_3$	4	0.124000	51	$\hat{G}_2$	$\hat{b}_3$	3	0.201500
45	$\hat{G}_3$	$\hat{b}_4$	3	0.130650	51	$\hat{G}_3$	$\hat{b}_4$	3	0.130650
45	$\hat{G}_4$	$\hat{b}_5$	3	0.109200	51	$\hat{G}_4$	$\hat{b}_5$	3	0.109200
45	$\hat{G}_5$	$\hat{b}_6$	2	0.123250	51	$\hat{G}_5$	$\hat{b}_6$	2	0.123250
45	$\hat{G}_6$	$\hat{b}_7$	2	0.112200	51	$\hat{G}_6$	$\hat{b}_7$	2	0.112200
46	$\hat{G}_2$	$\hat{b}_3$	3	0.201500	52	$\hat{G}_2$	$\hat{b}_3$	3	0.201500
46	$\hat{G}_3$	$\hat{b}_4$	3	0.130650	52	$\hat{G}_3$	$\hat{b}_4$	3	0.130650
46	$\hat{G}_4$	$\hat{b}_5$	3	0.109200	52	$\hat{G}_4$	$\hat{b}_5$	2	0.142800
46	$\hat{G}_5$	$\hat{b}_6$	2	0.123250	52	$\hat{G}_5$	$\hat{b}_6$	2	0.123250
46	$\hat{G}_6$	$\hat{b}_7$	2	0.112200	52	$\hat{G}_6$	$\hat{b}_7$	2	0.112200
47	$\hat{G}_2$	$\hat{b}_3$	3	0.201500	53	$\hat{G}_2$	$\hat{b}_3$	3	0.201500
47	$\hat{G}_3$	$\hat{b}_4$	3	0.130650	53	$\hat{G}_3$	$\hat{b}_4$	3	0.130650
47	$\hat{G}_4$	$\hat{b}_5$	3	0.109200	53	$\hat{G}_4$	$\hat{b}_5$	2	0.142800
47	$\hat{G}_5$	$\hat{b}_6$	2	0.123250	53	$\hat{G}_5$	$\hat{b}_6$	2	0.123250
47	$\hat{G}_6$	$\hat{b}_7$	2	0.112200	53	$\hat{G}_6$	$\hat{b}_7$	2	0.112200
48	$\hat{G}_2$	$\hat{b}_3$	3	0.201500	54	$\hat{G}_2$	$\hat{b}_3$	3	0.201500
48	$\hat{G}_3$	$\hat{b}_4$	3	0.130650	54	$\hat{G}_3$	$\hat{b}_4$	3	0.130650
48	$\hat{G}_4$	$\hat{b}_5$	3	0.109200	54	$\hat{G}_4$	$\hat{b}_5$	2	0.142800
48	$\hat{G}_5$	$\hat{b}_6$	2	0.123250	54	$\hat{G}_5$	$\hat{b}_6$	2	0.123250
48	$\hat{G}_6$	$\hat{b}_7$	2	0.112200	54	$\hat{G}_6$	$\hat{b}_7$	2	0.112200
49	$\hat{G}_2$	$\hat{b}_3$	3	0.201500	55	$\hat{G}_2$	$\hat{b}_3$	3	0.201500
49	$\hat{G}_3$	$\hat{b}_4$	3	0.130650	55	$\hat{G}_3$	$\hat{b}_4$	3	0.130650
49	$\hat{G}_4$	$\hat{b}_5$	3	0.109200	55	$\hat{G}_4$	$\hat{b}_5$	2	0.142800
49	$\hat{G}_5$	$\hat{b}_6$	2	0.123250	55	$\hat{G}_5$	$\hat{b}_6$	2	0.123250
49	$\hat{G}_6$	$\hat{b}_7$	2	0.112200	55	$\hat{G}_6$	$\hat{b}_7$	2	0.112200
50	$\hat{G}_2$	$\hat{b}_3$	3	0.201500	56	$\hat{G}_2$	$\hat{b}_3$	3	0.201500
50	$\hat{G}_3$	$\hat{b}_4$	3	0.130650	56	$\hat{G}_3$	$\hat{b}_4$	3	0.130650
50	$\hat{G}_4$	$\hat{b}_5$	3	0.109200	56	$\hat{G}_4$	$\hat{b}_5$	2	0.142800
50	$\hat{G}_5$	$\hat{b}_6$	2	0.123250	56	$\hat{G}_5$	$\hat{b}_6$	2	0.123250
50	$\hat{G}_6$	$\hat{b}_7$	2	0.112200	56	$\hat{G}_6$	$\hat{b}_7$	2	0.112200

Annex G: Bit Allocation for Higher Order DCT Coefficients

$\hat{L}$	$\hat{C}_{i,k}$	$\hat{b}_m$	$\hat{B}_m$	$\hat{L}$	$\hat{C}_{i,k}$	$\hat{b}_m$	$\hat{B}_m$
9	$\hat{C}_{4,2}$	$\hat{b}_8$	9	14	$\hat{C}_{6,2}$	$\hat{b}_{14}$	4
9	$\hat{C}_{5,2}$	$\hat{b}_9$	8	14	$\hat{C}_{6,3}$	$\hat{b}_{15}$	3
9	$\hat{C}_{6,2}$	$\hat{b}_{10}$	7				
				15	$\hat{C}_{1,2}$	$\hat{b}_8$	6
10	$\hat{C}_{3,2}$	$\hat{b}_8$	9	15	$\hat{C}_{2,2}$	$\hat{b}_9$	7
10	$\hat{C}_{4,2}$	$\hat{b}_9$	7	15	$\hat{C}_{3,2}$	$\hat{b}_{10}$	5
10	$\hat{C}_{5,2}$	$\hat{b}_{10}$	6	15	$\hat{C}_{4,2}$	$\hat{b}_{11}$	4
10	$\hat{C}_{6,2}$	$\hat{b}_{11}$	5	15	$\hat{C}_{4,3}$	$\hat{b}_{12}$	4
				15	$\hat{C}_{5,2}$	$\hat{b}_{13}$	3
11	$\hat{C}_{2,2}$	$\hat{b}_8$	9	15	$\hat{C}_{5,3}$	$\hat{b}_{14}$	3
11	$\hat{C}_{3,2}$	$\hat{b}_9$	7	15	$\hat{C}_{6,2}$	$\hat{b}_{15}$	3
11	$\hat{C}_{4,2}$	$\hat{b}_{10}$	6	15	$\hat{C}_{6,3}$	$\hat{b}_{16}$	3
11	$\hat{C}_{5,2}$	$\hat{b}_{11}$	5				
11	$\hat{C}_{6,2}$	$\hat{b}_{12}$	4	16	$\hat{C}_{1,2}$	$\hat{b}_8$	6
				16	$\hat{C}_{2,2}$	$\hat{b}_9$	6
12	$\hat{C}_{1,2}$	$\hat{b}_8$	8	16	$\hat{C}_{3,2}$	$\hat{b}_{10}$	5
12	$\hat{C}_{2,2}$	$\hat{b}_9$	7	16	$\hat{C}_{3,3}$	$\hat{b}_{11}$	4
12	$\hat{C}_{3,2}$	$\hat{b}_{10}$	6	16	$\hat{C}_{4,2}$	$\hat{b}_{12}$	4
12	$\hat{C}_{4,2}$	$\hat{b}_{11}$	5	16	$\hat{C}_{4,3}$	$\hat{b}_{13}$	3
12	$\hat{C}_{5,2}$	$\hat{b}_{12}$	4	16	$\hat{C}_{5,2}$	$\hat{b}_{14}$	3
12	$\hat{C}_{6,2}$	$\hat{b}_{13}$	3	16	$\hat{C}_{5,3}$	$\hat{b}_{15}$	3
				16	$\hat{C}_{6,2}$	$\hat{b}_{16}$	3
13	$\hat{C}_{1,2}$	$\hat{b}_8$	7	16	$\hat{C}_{6,3}$	$\hat{b}_{17}$	2
13	$\hat{C}_{2,2}$	$\hat{b}_9$	7				
13	$\hat{C}_{3,2}$	$\hat{b}_{10}$	6	17	$\hat{C}_{1,2}$	$\hat{b}_8$	5
13	$\hat{C}_{4,2}$	$\hat{b}_{11}$	5	17	$\hat{C}_{2,2}$	$\hat{b}_9$	5
13	$\hat{C}_{5,2}$	$\hat{b}_{12}$	4	17	$\hat{C}_{2,3}$	$\hat{b}_{10}$	5
13	$\hat{C}_{6,2}$	$\hat{b}_{13}$	3	17	$\hat{C}_{3,2}$	$\hat{b}_{11}$	4
13	$\hat{C}_{6,3}$	$\hat{b}_{14}$	3	17	$\hat{C}_{3,3}$	$\hat{b}_{12}$	4
				17	$\hat{C}_{4,2}$	$\hat{b}_{13}$	4
14	$\hat{C}_{1,2}$	$\hat{b}_8$	7	17	$\hat{C}_{4,3}$	$\hat{b}_{14}$	3
14	$\hat{C}_{2,2}$	$\hat{b}_9$	7	17	$\hat{C}_{5,2}$	$\hat{b}_{15}$	3
14	$\hat{C}_{3,2}$	$\hat{b}_{10}$	5	17	$\hat{C}_{5,3}$	$\hat{b}_{16}$	2
14	$\hat{C}_{4,2}$	$\hat{b}_{11}$	4	17	$\hat{C}_{6,2}$	$\hat{b}_{17}$	3
14	$\hat{C}_{5,2}$	$\hat{b}_{12}$	4	17	$\hat{C}_{6,3}$	$\hat{b}_{18}$	2
14	$\hat{C}_{5,3}$	$\hat{b}_{13}$	3				

$\hat{L}$	$\hat{C}_{i,k}$	$\hat{b}_m$	$\hat{B}_m$	$\hat{L}$	$\hat{C}_{i,k}$	$\hat{b}_m$	$\hat{B}_m$
18	$\hat{C}_{1,2}$	$\hat{b}_8$	5	20	$\hat{C}_{5,3}$	$\hat{b}_{17}$	2
18	$\hat{C}_{1,3}$	$\hat{b}_9$	4	20	$\hat{C}_{5,4}$	$\hat{b}_{18}$	1
18	$\hat{C}_{2,2}$	$\hat{b}_{10}$	5	20	$\hat{C}_{6,2}$	$\hat{b}_{19}$	3
18	$\hat{C}_{2,3}$	$\hat{b}_{11}$	5	20	$\hat{C}_{6,3}$	$\hat{b}_{20}$	2
18	$\hat{C}_{3,2}$	$\hat{b}_{12}$	4	20	$\hat{C}_{6,4}$	$\hat{b}_{21}$	1
18	$\hat{C}_{3,3}$	$\hat{b}_{13}$	3				
18	$\hat{C}_{4,2}$	$\hat{b}_{14}$	3	21	$\hat{C}_{1,2}$	$\hat{b}_8$	4
18	$\hat{C}_{4,3}$	$\hat{b}_{15}$	3	21	$\hat{C}_{1,3}$	$\hat{b}_9$	4
18	$\hat{C}_{5,2}$	$\hat{b}_{16}$	3	21	$\hat{C}_{2,2}$	$\hat{b}_{10}$	5
18	$\hat{C}_{5,3}$	$\hat{b}_{17}$	2	21	$\hat{C}_{2,3}$	$\hat{b}_{11}$	4
18	$\hat{C}_{6,2}$	$\hat{b}_{18}$	2	21	$\hat{C}_{3,2}$	$\hat{b}_{12}$	4
18	$\hat{C}_{6,3}$	$\hat{b}_{19}$	2	21	$\hat{C}_{3,3}$	$\hat{b}_{13}$	3
				21	$\hat{C}_{4,2}$	$\hat{b}_{14}$	3
19	$\hat{C}_{1,2}$	$\hat{b}_8$	5	21	$\hat{C}_{4,3}$	$\hat{b}_{15}$	2
19	$\hat{C}_{1,3}$	$\hat{b}_9$	4	21	$\hat{C}_{4,4}$	$\hat{b}_{16}$	2
19	$\hat{C}_{2,2}$	$\hat{b}_{10}$	5	21	$\hat{C}_{5,2}$	$\hat{b}_{17}$	3
19	$\hat{C}_{2,3}$	$\hat{b}_{11}$	4	21	$\hat{C}_{5,3}$	$\hat{b}_{18}$	2
19	$\hat{C}_{3,2}$	$\hat{b}_{12}$	4	21	$\hat{C}_{5,4}$	$\hat{b}_{19}$	1
19	$\hat{C}_{3,3}$	$\hat{b}_{13}$	3	21	$\hat{C}_{6,2}$	$\hat{b}_{20}$	3
19	$\hat{C}_{4,2}$	$\hat{b}_{14}$	3	21	$\hat{C}_{6,3}$	$\hat{b}_{21}$	2
19	$\hat{C}_{4,3}$	$\hat{b}_{15}$	3	21	$\hat{C}_{6,4}$	$\hat{b}_{22}$	1
19	$\hat{C}_{5,2}$	$\hat{b}_{16}$	3				
19	$\hat{C}_{5,3}$	$\hat{b}_{17}$	2	22	$\hat{C}_{1,2}$	$\hat{b}_8$	4
19	$\hat{C}_{6,2}$	$\hat{b}_{18}$	3	22	$\hat{C}_{1,3}$	$\hat{b}_9$	4
19	$\hat{C}_{6,3}$	$\hat{b}_{19}$	2	22	$\hat{C}_{2,2}$	$\hat{b}_{10}$	4
19	$\hat{C}_{6,4}$	$\hat{b}_{20}$	1	22	$\hat{C}_{2,3}$	$\hat{b}_{11}$	4
				22	$\hat{C}_{3,2}$	$\hat{b}_{12}$	4
20	$\hat{C}_{1,2}$	$\hat{b}_8$	5	22	$\hat{C}_{3,3}$	$\hat{b}_{13}$	3
20	$\hat{C}_{1,3}$	$\hat{b}_9$	4	22	$\hat{C}_{3,4}$	$\hat{b}_{14}$	2
20	$\hat{C}_{2,2}$	$\hat{b}_{10}$	5	22	$\hat{C}_{4,2}$	$\hat{b}_{15}$	3
20	$\hat{C}_{2,3}$	$\hat{b}_{11}$	4	22	$\hat{C}_{4,3}$	$\hat{b}_{16}$	2
20	$\hat{C}_{3,2}$	$\hat{b}_{12}$	4	22	$\hat{C}_{4,4}$	$\hat{b}_{17}$	2
20	$\hat{C}_{3,3}$	$\hat{b}_{13}$	3	22	$\hat{C}_{5,2}$	$\hat{b}_{18}$	3
20	$\hat{C}_{4,2}$	$\hat{b}_{14}$	3	22	$\hat{C}_{5,3}$	$\hat{b}_{19}$	2
20	$\hat{C}_{4,3}$	$\hat{b}_{15}$	2	22	$\hat{C}_{5,4}$	$\hat{b}_{20}$	1
20	$\hat{C}_{5,2}$	$\hat{b}_{16}$	3	22	$\hat{C}_{6,2}$	$\hat{b}_{21}$	2

$\hat{L}$	$\hat{C}_{i,k}$	$\hat{b}_m$	$\hat{B}_m$	$\hat{L}$	$\hat{C}_{i,k}$	$\hat{b}_m$	$\hat{B}_m$
9	$\hat{C}_{4,2}$	$\hat{b}_8$	9	14	$\hat{C}_{6,2}$	$\hat{b}_{14}$	4
9	$\hat{C}_{5,2}$	$\hat{b}_9$	8	14	$\hat{C}_{6,3}$	$\hat{b}_{15}$	3
9	$\hat{C}_{6,2}$	$\hat{b}_{10}$	7				
				15	$\hat{C}_{1,2}$	$\hat{b}_8$	6
10	$\hat{C}_{3,2}$	$\hat{b}_8$	9	15	$\hat{C}_{2,2}$	$\hat{b}_9$	7
10	$\hat{C}_{4,2}$	$\hat{b}_9$	7	15	$\hat{C}_{3,2}$	$\hat{b}_{10}$	5
10	$\hat{C}_{5,2}$	$\hat{b}_{10}$	6	15	$\hat{C}_{4,2}$	$\hat{b}_{11}$	4
10	$\hat{C}_{6,2}$	$\hat{b}_{11}$	5	15	$\hat{C}_{4,3}$	$\hat{b}_{12}$	4
				15	$\hat{C}_{5,2}$	$\hat{b}_{13}$	3
11	$\hat{C}_{2,2}$	$\hat{b}_8$	9	15	$\hat{C}_{5,3}$	$\hat{b}_{14}$	3
11	$\hat{C}_{3,2}$	$\hat{b}_9$	7	15	$\hat{C}_{6,2}$	$\hat{b}_{15}$	3
11	$\hat{C}_{4,2}$	$\hat{b}_{10}$	6	15	$\hat{C}_{6,3}$	$\hat{b}_{16}$	3
11	$\hat{C}_{5,2}$	$\hat{b}_{11}$	5				
11	$\hat{C}_{6,2}$	$\hat{b}_{12}$	4	16	$\hat{C}_{1,2}$	$\hat{b}_8$	6
				16	$\hat{C}_{2,2}$	$\hat{b}_9$	6
12	$\hat{C}_{1,2}$	$\hat{b}_8$	8	16	$\hat{C}_{3,2}$	$\hat{b}_{10}$	5
12	$\hat{C}_{2,2}$	$\hat{b}_9$	7	16	$\hat{C}_{3,3}$	$\hat{b}_{11}$	4
12	$\hat{C}_{3,2}$	$\hat{b}_{10}$	6	16	$\hat{C}_{4,2}$	$\hat{b}_{12}$	4
12	$\hat{C}_{4,2}$	$\hat{b}_{11}$	5	16	$\hat{C}_{4,3}$	$\hat{b}_{13}$	3
12	$\hat{C}_{5,2}$	$\hat{b}_{12}$	4	16	$\hat{C}_{5,2}$	$\hat{b}_{14}$	3
12	$\hat{C}_{6,2}$	$\hat{b}_{13}$	3	16	$\hat{C}_{5,3}$	$\hat{b}_{15}$	3
				16	$\hat{C}_{6,2}$	$\hat{b}_{16}$	3
13	$\hat{C}_{1,2}$	$\hat{b}_8$	7	16	$\hat{C}_{6,3}$	$\hat{b}_{17}$	2
13	$\hat{C}_{2,2}$	$\hat{b}_9$	7				
13	$\hat{C}_{3,2}$	$\hat{b}_{10}$	6	17	$\hat{C}_{1,2}$	$\hat{b}_8$	5
13	$\hat{C}_{4,2}$	$\hat{b}_{11}$	5	17	$\hat{C}_{2,2}$	$\hat{b}_9$	5
13	$\hat{C}_{5,2}$	$\hat{b}_{12}$	4	17	$\hat{C}_{2,3}$	$\hat{b}_{10}$	5
13	$\hat{C}_{6,2}$	$\hat{b}_{13}$	3	17	$\hat{C}_{3,2}$	$\hat{b}_{11}$	4
13	$\hat{C}_{6,3}$	$\hat{b}_{14}$	3	17	$\hat{C}_{3,3}$	$\hat{b}_{12}$	4
				17	$\hat{C}_{4,2}$	$\hat{b}_{13}$	4
14	$\hat{C}_{1,2}$	$\hat{b}_8$	7	17	$\hat{C}_{4,3}$	$\hat{b}_{14}$	3
14	$\hat{C}_{2,2}$	$\hat{b}_9$	7	17	$\hat{C}_{5,2}$	$\hat{b}_{15}$	3
14	$\hat{C}_{3,2}$	$\hat{b}_{10}$	5	17	$\hat{C}_{5,3}$	$\hat{b}_{16}$	2
14	$\hat{C}_{4,2}$	$\hat{b}_{11}$	4	17	$\hat{C}_{6,2}$	$\hat{b}_{17}$	3
14	$\hat{C}_{5,2}$	$\hat{b}_{12}$	4	17	$\hat{C}_{6,3}$	$\hat{b}_{18}$	2
14	$\hat{C}_{5,3}$	$\hat{b}_{13}$	3				

$\hat{L}$	$\hat{C}_{i,k}$	$\hat{b}_m$	$\hat{B}_m$	$\hat{L}$	$\hat{C}_{i,k}$	$\hat{b}_m$	$\hat{B}_m$
18	$\hat{C}_{1,2}$	$\hat{b}_8$	5	20	$\hat{C}_{5,3}$	$\hat{b}_{17}$	2
18	$\hat{C}_{1,3}$	$\hat{b}_9$	4	20	$\hat{C}_{5,4}$	$\hat{b}_{18}$	1
18	$\hat{C}_{2,2}$	$\hat{b}_{10}$	5	20	$\hat{C}_{6,2}$	$\hat{b}_{19}$	3
18	$\hat{C}_{2,3}$	$\hat{b}_{11}$	5	20	$\hat{C}_{6,3}$	$\hat{b}_{20}$	2
18	$\hat{C}_{3,2}$	$\hat{b}_{12}$	4	20	$\hat{C}_{6,4}$	$\hat{b}_{21}$	1
18	$\hat{C}_{3,3}$	$\hat{b}_{13}$	3				
18	$\hat{C}_{4,2}$	$\hat{b}_{14}$	3	21	$\hat{C}_{1,2}$	$\hat{b}_8$	4
18	$\hat{C}_{4,3}$	$\hat{b}_{15}$	3	21	$\hat{C}_{1,3}$	$\hat{b}_9$	4
18	$\hat{C}_{5,2}$	$\hat{b}_{16}$	3	21	$\hat{C}_{2,2}$	$\hat{b}_{10}$	5
18	$\hat{C}_{5,3}$	$\hat{b}_{17}$	2	21	$\hat{C}_{2,3}$	$\hat{b}_{11}$	4
18	$\hat{C}_{6,2}$	$\hat{b}_{18}$	2	21	$\hat{C}_{3,2}$	$\hat{b}_{12}$	4
18	$\hat{C}_{6,3}$	$\hat{b}_{19}$	2	21	$\hat{C}_{3,3}$	$\hat{b}_{13}$	3
				21	$\hat{C}_{4,2}$	$\hat{b}_{14}$	3
19	$\hat{C}_{1,2}$	$\hat{b}_8$	5	21	$\hat{C}_{4,3}$	$\hat{b}_{15}$	2
19	$\hat{C}_{1,3}$	$\hat{b}_9$	4	21	$\hat{C}_{4,4}$	$\hat{b}_{16}$	2
19	$\hat{C}_{2,2}$	$\hat{b}_{10}$	5	21	$\hat{C}_{5,2}$	$\hat{b}_{17}$	3
19	$\hat{C}_{2,3}$	$\hat{b}_{11}$	4	21	$\hat{C}_{5,3}$	$\hat{b}_{18}$	2
19	$\hat{C}_{3,2}$	$\hat{b}_{12}$	4	21	$\hat{C}_{5,4}$	$\hat{b}_{19}$	1
19	$\hat{C}_{3,3}$	$\hat{b}_{13}$	3	21	$\hat{C}_{6,2}$	$\hat{b}_{20}$	3
19	$\hat{C}_{4,2}$	$\hat{b}_{14}$	3	21	$\hat{C}_{6,3}$	$\hat{b}_{21}$	2
19	$\hat{C}_{4,3}$	$\hat{b}_{15}$	3	21	$\hat{C}_{6,4}$	$\hat{b}_{22}$	1
19	$\hat{C}_{5,2}$	$\hat{b}_{16}$	3				
19	$\hat{C}_{5,3}$	$\hat{b}_{17}$	2	22	$\hat{C}_{1,2}$	$\hat{b}_8$	4
19	$\hat{C}_{6,2}$	$\hat{b}_{18}$	3	22	$\hat{C}_{1,3}$	$\hat{b}_9$	4
19	$\hat{C}_{6,3}$	$\hat{b}_{19}$	2	22	$\hat{C}_{2,2}$	$\hat{b}_{10}$	4
19	$\hat{C}_{6,4}$	$\hat{b}_{20}$	1	22	$\hat{C}_{2,3}$	$\hat{b}_{11}$	4
				22	$\hat{C}_{3,2}$	$\hat{b}_{12}$	4
20	$\hat{C}_{1,2}$	$\hat{b}_8$	5	22	$\hat{C}_{3,3}$	$\hat{b}_{13}$	3
20	$\hat{C}_{1,3}$	$\hat{b}_9$	4	22	$\hat{C}_{3,4}$	$\hat{b}_{14}$	2
20	$\hat{C}_{2,2}$	$\hat{b}_{10}$	5	22	$\hat{C}_{4,2}$	$\hat{b}_{15}$	3
20	$\hat{C}_{2,3}$	$\hat{b}_{11}$	4	22	$\hat{C}_{4,3}$	$\hat{b}_{16}$	2
20	$\hat{C}_{3,2}$	$\hat{b}_{12}$	4	22	$\hat{C}_{4,4}$	$\hat{b}_{17}$	2
20	$\hat{C}_{3,3}$	$\hat{b}_{13}$	3	22	$\hat{C}_{5,2}$	$\hat{b}_{18}$	3
20	$\hat{C}_{4,2}$	$\hat{b}_{14}$	3	22	$\hat{C}_{5,3}$	$\hat{b}_{19}$	2
20	$\hat{C}_{4,3}$	$\hat{b}_{15}$	2	22	$\hat{C}_{5,4}$	$\hat{b}_{20}$	1
20	$\hat{C}_{5,2}$	$\hat{b}_{16}$	3	22	$\hat{C}_{6,2}$	$\hat{b}_{21}$	2

$\hat{L}$	$\hat{C}_{i,k}$	$\hat{b}_m$	$\hat{B}_m$	$\hat{L}$	$\hat{C}_{i,k}$	$\hat{b}_m$	$\hat{B}_m$
22	$\hat{C}_{6,3}$	$\hat{b}_{22}$	2	24	$\hat{C}_{6,2}$	$\hat{b}_{23}$	2
22	$\hat{C}_{6,4}$	$\hat{b}_{23}$	1	24	$\hat{C}_{6,3}$	$\hat{b}_{24}$	2
				24	$\hat{C}_{6,4}$	$\hat{b}_{25}$	1
23	$\hat{C}_{1,2}$	$\hat{b}_8$	4				
23	$\hat{C}_{1,3}$	$\hat{b}_9$	3	25	$\hat{C}_{1,2}$	$\hat{b}_8$	4
23	$\hat{C}_{2,2}$	$\hat{b}_{10}$	4	25	$\hat{C}_{1,3}$	$\hat{b}_9$	3
23	$\hat{C}_{2,3}$	$\hat{b}_{11}$	4	25	$\hat{C}_{1,4}$	$\hat{b}_{10}$	3
23	$\hat{C}_{2,4}$	$\hat{b}_{12}$	3	25	$\hat{C}_{2,2}$	$\hat{b}_{11}$	4
23	$\hat{C}_{3,2}$	$\hat{b}_{13}$	4	25	$\hat{C}_{2,3}$	$\hat{b}_{12}$	3
23	$\hat{C}_{3,3}$	$\hat{b}_{14}$	3	25	$\hat{C}_{2,4}$	$\hat{b}_{13}$	3
23	$\hat{C}_{3,4}$	$\hat{b}_{15}$	2	25	$\hat{C}_{3,2}$	$\hat{b}_{14}$	3
23	$\hat{C}_{4,2}$	$\hat{b}_{16}$	3	25	$\hat{C}_{3,3}$	$\hat{b}_{15}$	3
23	$\hat{C}_{4,3}$	$\hat{b}_{17}$	2	25	$\hat{C}_{3,4}$	$\hat{b}_{16}$	2
23	$\hat{C}_{4,4}$	$\hat{b}_{18}$	2	25	$\hat{C}_{4,2}$	$\hat{b}_{17}$	3
23	$\hat{C}_{5,2}$	$\hat{b}_{19}$	2	25	$\hat{C}_{4,3}$	$\hat{b}_{18}$	2
23	$\hat{C}_{5,3}$	$\hat{b}_{20}$	2	25	$\hat{C}_{4,4}$	$\hat{b}_{19}$	1
23	$\hat{C}_{5,4}$	$\hat{b}_{21}$	1	25	$\hat{C}_{5,2}$	$\hat{b}_{20}$	2
23	$\hat{C}_{6,2}$	$\hat{b}_{22}$	2	25	$\hat{C}_{5,3}$	$\hat{b}_{21}$	2
23	$\hat{C}_{6,3}$	$\hat{b}_{23}$	2	25	$\hat{C}_{5,4}$	$\hat{b}_{22}$	1
23	$\hat{C}_{6,4}$	$\hat{b}_{24}$	1	25	$\hat{C}_{6,2}$	$\hat{b}_{23}$	2
				25	$\hat{C}_{6,3}$	$\hat{b}_{24}$	1
24	$\hat{C}_{1,2}$	$\hat{b}_8$	4	25	$\hat{C}_{6,4}$	$\hat{b}_{25}$	1
24	$\hat{C}_{1,3}$	$\hat{b}_9$	3	25	$\hat{C}_{6,5}$	$\hat{b}_{26}$	1
24	$\hat{C}_{1,4}$	$\hat{b}_{10}$	3				
24	$\hat{C}_{2,2}$	$\hat{b}_{11}$	4	26	$\hat{C}_{1,2}$	$\hat{b}_8$	4
24	$\hat{C}_{2,3}$	$\hat{b}_{12}$	3	26	$\hat{C}_{1,3}$	$\hat{b}_9$	3
24	$\hat{C}_{2,4}$	$\hat{b}_{13}$	3	26	$\hat{C}_{1,4}$	$\hat{b}_{10}$	3
24	$\hat{C}_{3,2}$	$\hat{b}_{14}$	3	26	$\hat{C}_{2,2}$	$\hat{b}_{11}$	4
24	$\hat{C}_{3,3}$	$\hat{b}_{15}$	3	26	$\hat{C}_{2,3}$	$\hat{b}_{12}$	3
24	$\hat{C}_{3,4}$	$\hat{b}_{16}$	2	26	$\hat{C}_{2,4}$	$\hat{b}_{13}$	3
24	$\hat{C}_{4,2}$	$\hat{b}_{17}$	3	26	$\hat{C}_{3,2}$	$\hat{b}_{14}$	3
24	$\hat{C}_{4,3}$	$\hat{b}_{18}$	2	26	$\hat{C}_{3,3}$	$\hat{b}_{15}$	2
24	$\hat{C}_{4,4}$	$\hat{b}_{19}$	1	26	$\hat{C}_{3,4}$	$\hat{b}_{16}$	2
24	$\hat{C}_{5,2}$	$\hat{b}_{20}$	2	26	$\hat{C}_{4,2}$	$\hat{b}_{17}$	3
24	$\hat{C}_{5,3}$	$\hat{b}_{21}$	2	26	$\hat{C}_{4,3}$	$\hat{b}_{18}$	2
24	$\hat{C}_{5,4}$	$\hat{b}_{22}$	1	26	$\hat{C}_{4,4}$	$\hat{b}_{19}$	1

$\hat{L}$	$\hat{C}_{i,k}$	$\hat{b}_m$	$\hat{B}_m$	$\hat{L}$	$\hat{C}_{i,k}$	$\hat{b}_m$	$\hat{B}_m$
26	$\hat{C}_{5,2}$	$\hat{b}_{20}$	2	28	$\hat{C}_{2,4}$	$\hat{b}_{13}$	2
26	$\hat{C}_{5,3}$	$\hat{b}_{21}$	2	28	$\hat{C}_{3,2}$	$\hat{b}_{14}$	3
26	$\hat{C}_{5,4}$	$\hat{b}_{22}$	1	28	$\hat{C}_{3,3}$	$\hat{b}_{15}$	2
26	$\hat{C}_{5,5}$	$\hat{b}_{23}$	1	28	$\hat{C}_{3,4}$	$\hat{b}_{16}$	2
26	$\hat{C}_{6,2}$	$\hat{b}_{24}$	2	28	$\hat{C}_{3,5}$	$\hat{b}_{17}$	2
26	$\hat{C}_{6,3}$	$\hat{b}_{25}$	2	28	$\hat{C}_{4,2}$	$\hat{b}_{18}$	3
26	$\hat{C}_{6,4}$	$\hat{b}_{26}$	1	28	$\hat{C}_{4,3}$	$\hat{b}_{19}$	2
26	$\hat{C}_{6,5}$	$\hat{b}_{27}$	1	28	$\hat{C}_{4,4}$	$\hat{b}_{20}$	1
				28	$\hat{C}_{4,5}$	$\hat{b}_{21}$	1
27	$\hat{C}_{1,2}$	$\hat{b}_8$	4	28	$\hat{C}_{5,2}$	$\hat{b}_{22}$	2
27	$\hat{C}_{1,3}$	$\hat{b}_9$	3	28	$\hat{C}_{5,3}$	$\hat{b}_{23}$	2
27	$\hat{C}_{1,4}$	$\hat{b}_{10}$	2	28	$\hat{C}_{5,4}$	$\hat{b}_{24}$	1
27	$\hat{C}_{2,2}$	$\hat{b}_{11}$	4	28	$\hat{C}_{5,5}$	$\hat{b}_{25}$	1
27	$\hat{C}_{2,3}$	$\hat{b}_{12}$	3	28	$\hat{C}_{6,2}$	$\hat{b}_{26}$	2
27	$\hat{C}_{2,4}$	$\hat{b}_{13}$	2	28	$\hat{C}_{6,3}$	$\hat{b}_{27}$	1
27	$\hat{C}_{3,2}$	$\hat{b}_{14}$	3	28	$\hat{C}_{6,4}$	$\hat{b}_{28}$	1
27	$\hat{C}_{3,3}$	$\hat{b}_{15}$	2	28	$\hat{C}_{6,5}$	$\hat{b}_{29}$	1
27	$\hat{C}_{3,4}$	$\hat{b}_{16}$	2				
27	$\hat{C}_{4,2}$	$\hat{b}_{17}$	3	29	$\hat{C}_{1,2}$	$\hat{b}_8$	3
27	$\hat{C}_{4,3}$	$\hat{b}_{18}$	2	29	$\hat{C}_{1,3}$	$\hat{b}_9$	3
27	$\hat{C}_{4,4}$	$\hat{b}_{19}$	2	29	$\hat{C}_{1,4}$	$\hat{b}_{10}$	2
27	$\hat{C}_{4,5}$	$\hat{b}_{20}$	1	29	$\hat{C}_{2,2}$	$\hat{b}_{11}$	4
27	$\hat{C}_{5,2}$	$\hat{b}_{21}$	2	29	$\hat{C}_{2,3}$	$\hat{b}_{12}$	3
27	$\hat{C}_{5,3}$	$\hat{b}_{22}$	2	29	$\hat{C}_{2,4}$	$\hat{b}_{13}$	2
27	$\hat{C}_{5,4}$	$\hat{b}_{23}$	1	29	$\hat{C}_{2,5}$	$\hat{b}_{14}$	2
27	$\hat{C}_{5,5}$	$\hat{b}_{24}$	1	29	$\hat{C}_{3,2}$	$\hat{b}_{15}$	3
27	$\hat{C}_{6,2}$	$\hat{b}_{25}$	2	29	$\hat{C}_{3,3}$	$\hat{b}_{16}$	2
27	$\hat{C}_{6,3}$	$\hat{b}_{26}$	2	29	$\hat{C}_{3,4}$	$\hat{b}_{17}$	2
27	$\hat{C}_{6,4}$	$\hat{b}_{27}$	1	29	$\hat{C}_{3,5}$	$\hat{b}_{18}$	2
27	$\hat{C}_{6,5}$	$\hat{b}_{28}$	1	29	$\hat{C}_{4,2}$	$\hat{b}_{19}$	3
				29	$\hat{C}_{4,3}$	$\hat{b}_{20}$	2
28	$\hat{C}_{1,2}$	$\hat{b}_8$	4	29	$\hat{C}_{4,4}$	$\hat{b}_{21}$	1
28	$\hat{C}_{1,3}$	$\hat{b}_9$	3	29	$\hat{C}_{4,5}$	$\hat{b}_{22}$	1
28	$\hat{C}_{1,4}$	$\hat{b}_{10}$	2	29	$\hat{C}_{5,2}$	$\hat{b}_{23}$	2
28	$\hat{C}_{2,2}$	$\hat{b}_{11}$	4	29	$\hat{C}_{5,3}$	$\hat{b}_{24}$	1
28	$\hat{C}_{2,3}$	$\hat{b}_{12}$	3	29	$\hat{C}_{5,4}$	$\hat{b}_{25}$	1

$\hat{L}$	$\hat{C}_{i,k}$	$\hat{b}_m$	$\hat{B}_m$	$\hat{L}$	$\hat{C}_{i,k}$	$\hat{b}_m$	$\hat{B}_m$
29	$\hat{C}_{5,5}$	$\hat{b}_{26}$	1	31	$\hat{C}_{2,3}$	$\hat{b}_{13}$	3
29	$\hat{C}_{6,2}$	$\hat{b}_{27}$	2	31	$\hat{C}_{2,4}$	$\hat{b}_{14}$	2
29	$\hat{C}_{6,3}$	$\hat{b}_{28}$	1	31	$\hat{C}_{2,5}$	$\hat{b}_{15}$	2
29	$\hat{C}_{6,4}$	$\hat{b}_{29}$	1	31	$\hat{C}_{3,2}$	$\hat{b}_{16}$	3
29	$\hat{C}_{6,5}$	$\hat{b}_{30}$	1	31	$\hat{C}_{3,3}$	$\hat{b}_{17}$	2
				31	$\hat{C}_{3,4}$	$\hat{b}_{18}$	2
30	$\hat{C}_{1,2}$	$\hat{b}_8$	3	31	$\hat{C}_{3,5}$	$\hat{b}_{19}$	1
30	$\hat{C}_{1,3}$	$\hat{b}_9$	3	31	$\hat{C}_{4,2}$	$\hat{b}_{20}$	2
30	$\hat{C}_{1,4}$	$\hat{b}_{10}$	2	31	$\hat{C}_{4,3}$	$\hat{b}_{21}$	2
30	$\hat{C}_{1,5}$	$\hat{b}_{11}$	2	31	$\hat{C}_{4,4}$	$\hat{b}_{22}$	1
30	$\hat{C}_{2,2}$	$\hat{b}_{12}$	3	31	$\hat{C}_{4,5}$	$\hat{b}_{23}$	1
30	$\hat{C}_{2,3}$	$\hat{b}_{13}$	3	31	$\hat{C}_{5,2}$	$\hat{b}_{24}$	2
30	$\hat{C}_{2,4}$	$\hat{b}_{14}$	2	31	$\hat{C}_{5,3}$	$\hat{b}_{25}$	1
30	$\hat{C}_{2,5}$	$\hat{b}_{15}$	2	31	$\hat{C}_{5,4}$	$\hat{b}_{26}$	1
30	$\hat{C}_{3,2}$	$\hat{b}_{16}$	3	31	$\hat{C}_{5,5}$	$\hat{b}_{27}$	1
30	$\hat{C}_{3,3}$	$\hat{b}_{17}$	2	31	$\hat{C}_{6,2}$	$\hat{b}_{28}$	2
30	$\hat{C}_{3,4}$	$\hat{b}_{18}$	2	31	$\hat{C}_{6,3}$	$\hat{b}_{29}$	1
30	$\hat{C}_{3,5}$	$\hat{b}_{19}$	1	31	$\hat{C}_{6,4}$	$\hat{b}_{30}$	1
30	$\hat{C}_{4,2}$	$\hat{b}_{20}$	3	31	$\hat{C}_{6,5}$	$\hat{b}_{31}$	1
30	$\hat{C}_{4,3}$	$\hat{b}_{21}$	2	31	$\hat{C}_{6,6}$	$\hat{b}_{32}$	1
30	$\hat{C}_{4,4}$	$\hat{b}_{22}$	1				
30	$\hat{C}_{4,5}$	$\hat{b}_{23}$	1	32	$\hat{C}_{1,2}$	$\hat{b}_8$	3
30	$\hat{C}_{5,2}$	$\hat{b}_{24}$	2	32	$\hat{C}_{1,3}$	$\hat{b}_9$	3
30	$\hat{C}_{5,3}$	$\hat{b}_{25}$	1	32	$\hat{C}_{1,4}$	$\hat{b}_{10}$	2
30	$\hat{C}_{5,4}$	$\hat{b}_{26}$	1	32	$\hat{C}_{1,5}$	$\hat{b}_{11}$	2
30	$\hat{C}_{5,5}$	$\hat{b}_{27}$	1	32	$\hat{C}_{2,2}$	$\hat{b}_{12}$	3
30	$\hat{C}_{6,2}$	$\hat{b}_{28}$	2	32	$\hat{C}_{2,3}$	$\hat{b}_{13}$	3
30	$\hat{C}_{6,3}$	$\hat{b}_{29}$	1	32	$\hat{C}_{2,4}$	$\hat{b}_{14}$	2
30	$\hat{C}_{6,4}$	$\hat{b}_{30}$	1	32	$\hat{C}_{2,5}$	$\hat{b}_{15}$	2
30	$\hat{C}_{6,5}$	$\hat{b}_{31}$	1	32	$\hat{C}_{3,2}$	$\hat{b}_{16}$	3
				32	$\hat{C}_{3,3}$	$\hat{b}_{17}$	2
31	$\hat{C}_{1,2}$	$\hat{b}_8$	3	32	$\hat{C}_{3,4}$	$\hat{b}_{18}$	2
31	$\hat{C}_{1,3}$	$\hat{b}_9$	3	32	$\hat{C}_{3,5}$	$\hat{b}_{19}$	1
31	$\hat{C}_{1,4}$	$\hat{b}_{10}$	2	32	$\hat{C}_{4,2}$	$\hat{b}_{20}$	2
31	$\hat{C}_{1,5}$	$\hat{b}_{11}$	2	32	$\hat{C}_{4,3}$	$\hat{b}_{21}$	2
31	$\hat{C}_{2,2}$	$\hat{b}_{12}$	3	32	$\hat{C}_{4,4}$	$\hat{b}_{22}$	1

$\hat{L}$	$\hat{C}_{i,k}$	$\hat{b}_m$	$\hat{B}_m$	$\hat{L}$	$\hat{C}_{i,k}$	$\hat{b}_m$	$\hat{B}_m$
32	$\hat{C}_{4,5}$	$\hat{b}_{23}$	1	33	$\hat{C}_{6,4}$	$\hat{b}_{32}$	1
32	$\hat{C}_{5,2}$	$\hat{b}_{24}$	2	33	$\hat{C}_{6,5}$	$\hat{b}_{33}$	1
32	$\hat{C}_{5,3}$	$\hat{b}_{25}$	1	33	$\hat{C}_{6,6}$	$\hat{b}_{34}$	1
32	$\hat{C}_{5,4}$	$\hat{b}_{26}$	1				
32	$\hat{C}_{5,5}$	$\hat{b}_{27}$	1	34	$\hat{C}_{1,2}$	$\hat{b}_8$	3
32	$\hat{C}_{5,6}$	$\hat{b}_{28}$	1	34	$\hat{C}_{1,3}$	$\hat{b}_9$	2
32	$\hat{C}_{6,2}$	$\hat{b}_{29}$	2	34	$\hat{C}_{1,4}$	$\hat{b}_{10}$	2
32	$\hat{C}_{6,3}$	$\hat{b}_{30}$	1	34	$\hat{C}_{1,5}$	$\hat{b}_{11}$	2
32	$\hat{C}_{6,4}$	$\hat{b}_{31}$	1	34	$\hat{C}_{2,2}$	$\hat{b}_{12}$	3
32	$\hat{C}_{6,5}$	$\hat{b}_{32}$	1	34	$\hat{C}_{2,3}$	$\hat{b}_{13}$	2
32	$\hat{C}_{6,6}$	$\hat{b}_{33}$	0	34	$\hat{C}_{2,4}$	$\hat{b}_{14}$	2
				34	$\hat{C}_{2,5}$	$\hat{b}_{15}$	2
33	$\hat{C}_{1,2}$	$\hat{b}_8$	3	34	$\hat{C}_{3,2}$	$\hat{b}_{16}$	3
33	$\hat{C}_{1,3}$	$\hat{b}_9$	3	34	$\hat{C}_{3,3}$	$\hat{b}_{17}$	2
33	$\hat{C}_{1,4}$	$\hat{b}_{10}$	2	34	$\hat{C}_{3,4}$	$\hat{b}_{18}$	2
33	$\hat{C}_{1,5}$	$\hat{b}_{11}$	2	34	$\hat{C}_{3,5}$	$\hat{b}_{19}$	1
33	$\hat{C}_{2,2}$	$\hat{b}_{12}$	3	34	$\hat{C}_{3,6}$	$\hat{b}_{20}$	1
33	$\hat{C}_{2,3}$	$\hat{b}_{13}$	3	34	$\hat{C}_{4,2}$	$\hat{b}_{21}$	2
33	$\hat{C}_{2,4}$	$\hat{b}_{14}$	2	34	$\hat{C}_{4,3}$	$\hat{b}_{22}$	2
33	$\hat{C}_{2,5}$	$\hat{b}_{15}$	2	34	$\hat{C}_{4,4}$	$\hat{b}_{23}$	1
33	$\hat{C}_{3,2}$	$\hat{b}_{16}$	3	34	$\hat{C}_{4,5}$	$\hat{b}_{24}$	1
33	$\hat{C}_{3,3}$	$\hat{b}_{17}$	2	34	$\hat{C}_{4,6}$	$\hat{b}_{25}$	1
33	$\hat{C}_{3,4}$	$\hat{b}_{18}$	1	34	$\hat{C}_{5,2}$	$\hat{b}_{26}$	2
33	$\hat{C}_{3,5}$	$\hat{b}_{19}$	1	34	$\hat{C}_{5,3}$	$\hat{b}_{27}$	1
33	$\hat{C}_{4,2}$	$\hat{b}_{20}$	2	34	$\hat{C}_{5,4}$	$\hat{b}_{28}$	1
33	$\hat{C}_{4,3}$	$\hat{b}_{21}$	2	34	$\hat{C}_{5,5}$	$\hat{b}_{29}$	1
33	$\hat{C}_{4,4}$	$\hat{b}_{22}$	1	34	$\hat{C}_{5,6}$	$\hat{b}_{30}$	1
33	$\hat{C}_{4,5}$	$\hat{b}_{23}$	1	34	$\hat{C}_{6,2}$	$\hat{b}_{31}$	2
33	$\hat{C}_{4,6}$	$\hat{b}_{24}$	1	34	$\hat{C}_{6,3}$	$\hat{b}_{32}$	1
33	$\hat{C}_{5,2}$	$\hat{b}_{25}$	2	34	$\hat{C}_{6,4}$	$\hat{b}_{33}$	1
33	$\hat{C}_{5,3}$	$\hat{b}_{26}$	1	34	$\hat{C}_{6,5}$	$\hat{b}_{34}$	1
33	$\hat{C}_{5,4}$	$\hat{b}_{27}$	1	34	$\hat{C}_{6,6}$	$\hat{b}_{35}$	0
33	$\hat{C}_{5,5}$	$\hat{b}_{28}$	1				
33	$\hat{C}_{5,6}$	$\hat{b}_{29}$	1	35	$\hat{C}_{1,2}$	$\hat{b}_8$	3
33	$\hat{C}_{6,2}$	$\hat{b}_{30}$	2	35	$\hat{C}_{1,3}$	$\hat{b}_9$	2
33	$\hat{C}_{6,3}$	$\hat{b}_{31}$	1	35	$\hat{C}_{1,4}$	$\hat{b}_{10}$	2

$\hat{L}$	$\hat{C}_{i,k}$	$\hat{b}_m$	$\hat{B}_m$	$\hat{L}$	$\hat{C}_{i,k}$	$\hat{b}_m$	$\hat{B}_m$
35	$\hat{C}_{1,5}$	$\hat{b}_{11}$	2	36	$\hat{C}_{2,6}$	$\hat{b}_{17}$	1
35	$\hat{C}_{2,2}$	$\hat{b}_{12}$	3	36	$\hat{C}_{3,2}$	$\hat{b}_{18}$	3
35	$\hat{C}_{2,3}$	$\hat{b}_{13}$	2	36	$\hat{C}_{3,3}$	$\hat{b}_{19}$	2
35	$\hat{C}_{2,4}$	$\hat{b}_{14}$	2	36	$\hat{C}_{3,4}$	$\hat{b}_{20}$	1
35	$\hat{C}_{2,5}$	$\hat{b}_{15}$	2	36	$\hat{C}_{3,5}$	$\hat{b}_{21}$	1
35	$\hat{C}_{2,6}$	$\hat{b}_{16}$	2	36	$\hat{C}_{3,6}$	$\hat{b}_{22}$	1
35	$\hat{C}_{3,2}$	$\hat{b}_{17}$	3	36	$\hat{C}_{4,2}$	$\hat{b}_{23}$	2
35	$\hat{C}_{3,3}$	$\hat{b}_{18}$	2	36	$\hat{C}_{4,3}$	$\hat{b}_{24}$	2
35	$\hat{C}_{3,4}$	$\hat{b}_{19}$	1	36	$\hat{C}_{4,4}$	$\hat{b}_{25}$	1
35	$\hat{C}_{3,5}$	$\hat{b}_{20}$	1	36	$\hat{C}_{4,5}$	$\hat{b}_{26}$	1
35	$\hat{C}_{3,6}$	$\hat{b}_{21}$	1	36	$\hat{C}_{4,6}$	$\hat{b}_{27}$	1
35	$\hat{C}_{4,2}$	$\hat{b}_{22}$	2	36	$\hat{C}_{5,2}$	$\hat{b}_{28}$	2
35	$\hat{C}_{4,3}$	$\hat{b}_{23}$	2	36	$\hat{C}_{5,3}$	$\hat{b}_{29}$	1
35	$\hat{C}_{4,4}$	$\hat{b}_{24}$	1	36	$\hat{C}_{5,4}$	$\hat{b}_{30}$	1
35	$\hat{C}_{4,5}$	$\hat{b}_{25}$	1	36	$\hat{C}_{5,5}$	$\hat{b}_{31}$	1
35	$\hat{C}_{4,6}$	$\hat{b}_{26}$	1	36	$\hat{C}_{5,6}$	$\hat{b}_{32}$	0
35	$\hat{C}_{5,2}$	$\hat{b}_{27}$	2	36	$\hat{C}_{6,2}$	$\hat{b}_{33}$	2
35	$\hat{C}_{5,3}$	$\hat{b}_{28}$	1	36	$\hat{C}_{6,3}$	$\hat{b}_{34}$	1
35	$\hat{C}_{5,4}$	$\hat{b}_{29}$	1	36	$\hat{C}_{6,4}$	$\hat{b}_{35}$	1
35	$\hat{C}_{5,5}$	$\hat{b}_{30}$	1	36	$\hat{C}_{6,5}$	$\hat{b}_{36}$	1
35	$\hat{C}_{5,6}$	$\hat{b}_{31}$	0	36	$\hat{C}_{6,6}$	$\hat{b}_{37}$	0
35	$\hat{C}_{6,2}$	$\hat{b}_{32}$	2				
35	$\hat{C}_{6,3}$	$\hat{b}_{33}$	1	37	$\hat{C}_{1,2}$	$\hat{b}_8$	3
35	$\hat{C}_{6,4}$	$\hat{b}_{34}$	1	37	$\hat{C}_{1,3}$	$\hat{b}_9$	2
35	$\hat{C}_{6,5}$	$\hat{b}_{35}$	1	37	$\hat{C}_{1,4}$	$\hat{b}_{10}$	2
35	$\hat{C}_{6,6}$	$\hat{b}_{36}$	0	37	$\hat{C}_{1,5}$	$\hat{b}_{11}$	2
				37	$\hat{C}_{1,6}$	$\hat{b}_{12}$	1
36	$\hat{C}_{1,2}$	$\hat{b}_8$	3	37	$\hat{C}_{2,2}$	$\hat{b}_{13}$	3
36	$\hat{C}_{1,3}$	$\hat{b}_9$	2	37	$\hat{C}_{2,3}$	$\hat{b}_{14}$	2
36	$\hat{C}_{1,4}$	$\hat{b}_{10}$	2	37	$\hat{C}_{2,4}$	$\hat{b}_{15}$	2
36	$\hat{C}_{1,5}$	$\hat{b}_{11}$	2	37	$\hat{C}_{2,5}$	$\hat{b}_{16}$	2
36	$\hat{C}_{1,6}$	$\hat{b}_{12}$	1	37	$\hat{C}_{2,6}$	$\hat{b}_{17}$	2
36	$\hat{C}_{2,2}$	$\hat{b}_{13}$	3	37	$\hat{C}_{3,2}$	$\hat{b}_{18}$	3
36	$\hat{C}_{2,3}$	$\hat{b}_{14}$	2	37	$\hat{C}_{3,3}$	$\hat{b}_{19}$	2
36	$\hat{C}_{2,4}$	$\hat{b}_{15}$	2	37	$\hat{C}_{3,4}$	$\hat{b}_{20}$	1
36	$\hat{C}_{2,5}$	$\hat{b}_{16}$	2	37	$\hat{C}_{3,5}$	$\hat{b}_{21}$	1

$\hat{L}$	$\hat{C}_{i,k}$	$\hat{b}_m$	$\hat{B}_m$	$\hat{L}$	$\hat{C}_{i,k}$	$\hat{b}_m$	$\hat{B}_m$
37	$\hat{C}_{3,6}$	$\hat{b}_{22}$	1	38	$\hat{C}_{4,5}$	$\hat{b}_{26}$	1
37	$\hat{C}_{4,2}$	$\hat{b}_{23}$	2	38	$\hat{C}_{4,6}$	$\hat{b}_{27}$	1
37	$\hat{C}_{4,3}$	$\hat{b}_{24}$	1	38	$\hat{C}_{5,2}$	$\hat{b}_{28}$	2
37	$\hat{C}_{4,4}$	$\hat{b}_{25}$	1	38	$\hat{C}_{5,3}$	$\hat{b}_{29}$	1
37	$\hat{C}_{4,5}$	$\hat{b}_{26}$	1	38	$\hat{C}_{5,4}$	$\hat{b}_{30}$	1
37	$\hat{C}_{4,6}$	$\hat{b}_{27}$	1	38	$\hat{C}_{5,5}$	$\hat{b}_{31}$	1
37	$\hat{C}_{5,2}$	$\hat{b}_{28}$	2	38	$\hat{C}_{5,6}$	$\hat{b}_{32}$	1
37	$\hat{C}_{5,3}$	$\hat{b}_{29}$	1	38	$\hat{C}_{5,7}$	$\hat{b}_{33}$	0
37	$\hat{C}_{5,4}$	$\hat{b}_{30}$	1	38	$\hat{C}_{6,2}$	$\hat{b}_{34}$	2
37	$\hat{C}_{5,5}$	$\hat{b}_{31}$	1	38	$\hat{C}_{6,3}$	$\hat{b}_{35}$	1
37	$\hat{C}_{5,6}$	$\hat{b}_{32}$	0	38	$\hat{C}_{6,4}$	$\hat{b}_{36}$	1
37	$\hat{C}_{6,2}$	$\hat{b}_{33}$	2	38	$\hat{C}_{6,5}$	$\hat{b}_{37}$	1
37	$\hat{C}_{6,3}$	$\hat{b}_{34}$	1	38	$\hat{C}_{6,6}$	$\hat{b}_{38}$	1
37	$\hat{C}_{6,4}$	$\hat{b}_{35}$	1	38	$\hat{C}_{6,7}$	$\hat{b}_{39}$	0
37	$\hat{C}_{6,5}$	$\hat{b}_{36}$	1				
37	$\hat{C}_{6,6}$	$\hat{b}_{37}$	1	39	$\hat{C}_{1,2}$	$\hat{b}_8$	3
37	$\hat{C}_{6,7}$	$\hat{b}_{38}$	0	39	$\hat{C}_{1,3}$	$\hat{b}_9$	2
				39	$\hat{C}_{1,4}$	$\hat{b}_{10}$	2
38	$\hat{C}_{1,2}$	$\hat{b}_8$	3	39	$\hat{C}_{1,5}$	$\hat{b}_{11}$	2
38	$\hat{C}_{1,3}$	$\hat{b}_9$	2	39	$\hat{C}_{1,6}$	$\hat{b}_{12}$	1
38	$\hat{C}_{1,4}$	$\hat{b}_{10}$	2	39	$\hat{C}_{2,2}$	$\hat{b}_{13}$	3
38	$\hat{C}_{1,5}$	$\hat{b}_{11}$	2	39	$\hat{C}_{2,3}$	$\hat{b}_{14}$	2
38	$\hat{C}_{1,6}$	$\hat{b}_{12}$	1	39	$\hat{C}_{2,4}$	$\hat{b}_{15}$	2
38	$\hat{C}_{2,2}$	$\hat{b}_{13}$	3	39	$\hat{C}_{2,5}$	$\hat{b}_{16}$	2
38	$\hat{C}_{2,3}$	$\hat{b}_{14}$	2	39	$\hat{C}_{2,6}$	$\hat{b}_{17}$	1
38	$\hat{C}_{2,4}$	$\hat{b}_{15}$	2	39	$\hat{C}_{3,2}$	$\hat{b}_{18}$	3
38	$\hat{C}_{2,5}$	$\hat{b}_{16}$	2	39	$\hat{C}_{3,3}$	$\hat{b}_{19}$	2
38	$\hat{C}_{2,6}$	$\hat{b}_{17}$	1	39	$\hat{C}_{3,4}$	$\hat{b}_{20}$	1
38	$\hat{C}_{3,2}$	$\hat{b}_{18}$	3	39	$\hat{C}_{3,5}$	$\hat{b}_{21}$	1
38	$\hat{C}_{3,3}$	$\hat{b}_{19}$	2	39	$\hat{C}_{3,6}$	$\hat{b}_{22}$	1
38	$\hat{C}_{3,4}$	$\hat{b}_{20}$	1	39	$\hat{C}_{4,2}$	$\hat{b}_{23}$	2
38	$\hat{C}_{3,5}$	$\hat{b}_{21}$	1	39	$\hat{C}_{4,3}$	$\hat{b}_{24}$	2
38	$\hat{C}_{3,6}$	$\hat{b}_{22}$	1	39	$\hat{C}_{4,4}$	$\hat{b}_{25}$	1
38	$\hat{C}_{4,2}$	$\hat{b}_{23}$	2	39	$\hat{C}_{4,5}$	$\hat{b}_{26}$	1
38	$\hat{C}_{4,3}$	$\hat{b}_{24}$	1	39	$\hat{C}_{4,6}$	$\hat{b}_{27}$	1
38	$\hat{C}_{4,4}$	$\hat{b}_{25}$	1	39	$\hat{C}_{4,7}$	$\hat{b}_{28}$	0

$\hat{L}$	$\hat{C}_{i,k}$	$\hat{b}_m$	$\hat{B}_m$	$\hat{L}$	$\hat{C}_{i,k}$	$\hat{b}_m$	$\hat{B}_m$
39	$\hat{C}_{5,2}$	$\hat{b}_{29}$	2	40	$\hat{C}_{5,3}$	$\hat{b}_{31}$	1
39	$\hat{C}_{5,3}$	$\hat{b}_{30}$	1	40	$\hat{C}_{5,4}$	$\hat{b}_{32}$	1
39	$\hat{C}_{5,4}$	$\hat{b}_{31}$	1	40	$\hat{C}_{5,5}$	$\hat{b}_{33}$	1
39	$\hat{C}_{5,5}$	$\hat{b}_{32}$	1	40	$\hat{C}_{5,6}$	$\hat{b}_{34}$	1
39	$\hat{C}_{5,6}$	$\hat{b}_{33}$	1	40	$\hat{C}_{5,7}$	$\hat{b}_{35}$	0
39	$\hat{C}_{5,7}$	$\hat{b}_{34}$	0	40	$\hat{C}_{6,2}$	$\hat{b}_{36}$	2
39	$\hat{C}_{6,2}$	$\hat{b}_{35}$	2	40	$\hat{C}_{6,3}$	$\hat{b}_{37}$	1
39	$\hat{C}_{6,3}$	$\hat{b}_{36}$	1	40	$\hat{C}_{6,4}$	$\hat{b}_{38}$	1
39	$\hat{C}_{6,4}$	$\hat{b}_{37}$	1	40	$\hat{C}_{6,5}$	$\hat{b}_{39}$	1
39	$\hat{C}_{6,5}$	$\hat{b}_{38}$	1	40	$\hat{C}_{6,6}$	$\hat{b}_{40}$	0
39	$\hat{C}_{6,6}$	$\hat{b}_{39}$	0	40	$\hat{C}_{6,7}$	$\hat{b}_{41}$	0
39	$\hat{C}_{6,7}$	$\hat{b}_{40}$	0				
				41	$\hat{C}_{1,2}$	$\hat{b}_8$	3
40	$\hat{C}_{1,2}$	$\hat{b}_8$	3	41	$\hat{C}_{1,3}$	$\hat{b}_9$	2
40	$\hat{C}_{1,3}$	$\hat{b}_9$	2	41	$\hat{C}_{1,4}$	$\hat{b}_{10}$	2
40	$\hat{C}_{1,4}$	$\hat{b}_{10}$	2	41	$\hat{C}_{1,5}$	$\hat{b}_{11}$	1
40	$\hat{C}_{1,5}$	$\hat{b}_{11}$	2	41	$\hat{C}_{1,6}$	$\hat{b}_{12}$	1
40	$\hat{C}_{1,6}$	$\hat{b}_{12}$	1	41	$\hat{C}_{2,2}$	$\hat{b}_{13}$	3
40	$\hat{C}_{2,2}$	$\hat{b}_{13}$	3	41	$\hat{C}_{2,3}$	$\hat{b}_{14}$	2
40	$\hat{C}_{2,3}$	$\hat{b}_{14}$	2	41	$\hat{C}_{2,4}$	$\hat{b}_{15}$	2
40	$\hat{C}_{2,4}$	$\hat{b}_{15}$	2	41	$\hat{C}_{2,5}$	$\hat{b}_{16}$	2
40	$\hat{C}_{2,5}$	$\hat{b}_{16}$	1	41	$\hat{C}_{2,6}$	$\hat{b}_{17}$	1
40	$\hat{C}_{2,6}$	$\hat{b}_{17}$	1	41	$\hat{C}_{2,7}$	$\hat{b}_{18}$	1
40	$\hat{C}_{3,2}$	$\hat{b}_{18}$	3	41	$\hat{C}_{3,2}$	$\hat{b}_{19}$	3
40	$\hat{C}_{3,3}$	$\hat{b}_{19}$	2	41	$\hat{C}_{3,3}$	$\hat{b}_{20}$	2
40	$\hat{C}_{3,4}$	$\hat{b}_{20}$	1	41	$\hat{C}_{3,4}$	$\hat{b}_{21}$	1
40	$\hat{C}_{3,5}$	$\hat{b}_{21}$	1	41	$\hat{C}_{3,5}$	$\hat{b}_{22}$	1
40	$\hat{C}_{3,6}$	$\hat{b}_{22}$	1	41	$\hat{C}_{3,6}$	$\hat{b}_{23}$	1
40	$\hat{C}_{3,7}$	$\hat{b}_{23}$	1	41	$\hat{C}_{3,7}$	$\hat{b}_{24}$	1
40	$\hat{C}_{4,2}$	$\hat{b}_{24}$	2	41	$\hat{C}_{4,2}$	$\hat{b}_{25}$	2
40	$\hat{C}_{4,3}$	$\hat{b}_{25}$	2	41	$\hat{C}_{4,3}$	$\hat{b}_{26}$	2
40	$\hat{C}_{4,4}$	$\hat{b}_{26}$	1	41	$\hat{C}_{4,4}$	$\hat{b}_{27}$	1
40	$\hat{C}_{4,5}$	$\hat{b}_{27}$	1	41	$\hat{C}_{4,5}$	$\hat{b}_{28}$	1
40	$\hat{C}_{4,6}$	$\hat{b}_{28}$	1	41	$\hat{C}_{4,6}$	$\hat{b}_{29}$	1
40	$\hat{C}_{4,7}$	$\hat{b}_{29}$	0	41	$\hat{C}_{4,7}$	$\hat{b}_{30}$	0
40	$\hat{C}_{5,2}$	$\hat{b}_{30}$	2	41	$\hat{C}_{5,2}$	$\hat{b}_{31}$	2

$\hat{L}$	$\hat{C}_{i,k}$	$\hat{b}_m$	$\hat{B}_m$	$\hat{L}$	$\hat{C}_{i,k}$	$\hat{b}_m$	$\hat{B}_m$
41	$\hat{C}_{5,3}$	$\hat{b}_{32}$	1	42	$\hat{C}_{5,2}$	$\hat{b}_{32}$	2
41	$\hat{C}_{5,4}$	$\hat{b}_{33}$	1	42	$\hat{C}_{5,3}$	$\hat{b}_{33}$	1
41	$\hat{C}_{5,5}$	$\hat{b}_{34}$	1	42	$\hat{C}_{5,4}$	$\hat{b}_{34}$	1
41	$\hat{C}_{5,6}$	$\hat{b}_{35}$	1	42	$\hat{C}_{5,5}$	$\hat{b}_{35}$	1
41	$\hat{C}_{5,7}$	$\hat{b}_{36}$	0	42	$\hat{C}_{5,6}$	$\hat{b}_{36}$	0
41	$\hat{C}_{6,2}$	$\hat{b}_{37}$	2	42	$\hat{C}_{5,7}$	$\hat{b}_{37}$	0
41	$\hat{C}_{6,3}$	$\hat{b}_{38}$	1	42	$\hat{C}_{6,2}$	$\hat{b}_{38}$	2
41	$\hat{C}_{6,4}$	$\hat{b}_{39}$	1	42	$\hat{C}_{6,3}$	$\hat{b}_{39}$	1
41	$\hat{C}_{6,5}$	$\hat{b}_{40}$	1	42	$\hat{C}_{6,4}$	$\hat{b}_{40}$	1
41	$\hat{C}_{6,6}$	$\hat{b}_{41}$	0	42	$\hat{C}_{6,5}$	$\hat{b}_{41}$	1
41	$\hat{C}_{6,7}$	$\hat{b}_{42}$	0	42	$\hat{C}_{6,6}$	$\hat{b}_{42}$	0
				42	$\hat{C}_{6,7}$	$\hat{b}_{43}$	0
42	$\hat{C}_{1,2}$	$\hat{b}_8$	3				
42	$\hat{C}_{1,3}$	$\hat{b}_9$	2	43	$\hat{C}_{1,2}$	$\hat{b}_8$	3
42	$\hat{C}_{1,4}$	$\hat{b}_{10}$	2	43	$\hat{C}_{1,3}$	$\hat{b}_9$	2
42	$\hat{C}_{1,5}$	$\hat{b}_{11}$	2	43	$\hat{C}_{1,4}$	$\hat{b}_{10}$	2
42	$\hat{C}_{1,6}$	$\hat{b}_{12}$	1	43	$\hat{C}_{1,5}$	$\hat{b}_{11}$	2
42	$\hat{C}_{1,7}$	$\hat{b}_{13}$	1	43	$\hat{C}_{1,6}$	$\hat{b}_{12}$	1
42	$\hat{C}_{2,2}$	$\hat{b}_{14}$	3	43	$\hat{C}_{1,7}$	$\hat{b}_{13}$	1
42	$\hat{C}_{2,3}$	$\hat{b}_{15}$	2	43	$\hat{C}_{2,2}$	$\hat{b}_{14}$	3
42	$\hat{C}_{2,4}$	$\hat{b}_{16}$	2	43	$\hat{C}_{2,3}$	$\hat{b}_{15}$	2
42	$\hat{C}_{2,5}$	$\hat{b}_{17}$	2	43	$\hat{C}_{2,4}$	$\hat{b}_{16}$	2
42	$\hat{C}_{2,6}$	$\hat{b}_{18}$	1	43	$\hat{C}_{2,5}$	$\hat{b}_{17}$	2
42	$\hat{C}_{2,7}$	$\hat{b}_{19}$	1	43	$\hat{C}_{2,6}$	$\hat{b}_{18}$	1
42	$\hat{C}_{3,2}$	$\hat{b}_{20}$	2	43	$\hat{C}_{2,7}$	$\hat{b}_{19}$	1
42	$\hat{C}_{3,3}$	$\hat{b}_{21}$	2	43	$\hat{C}_{3,2}$	$\hat{b}_{20}$	2
42	$\hat{C}_{3,4}$	$\hat{b}_{22}$	1	43	$\hat{C}_{3,3}$	$\hat{b}_{21}$	2
42	$\hat{C}_{3,5}$	$\hat{b}_{23}$	1	43	$\hat{C}_{3,4}$	$\hat{b}_{22}$	1
42	$\hat{C}_{3,6}$	$\hat{b}_{24}$	1	43	$\hat{C}_{3,5}$	$\hat{b}_{23}$	1
42	$\hat{C}_{3,7}$	$\hat{b}_{25}$	1	43	$\hat{C}_{3,6}$	$\hat{b}_{24}$	1
42	$\hat{C}_{4,2}$	$\hat{b}_{26}$	2	43	$\hat{C}_{3,7}$	$\hat{b}_{25}$	1
42	$\hat{C}_{4,3}$	$\hat{b}_{27}$	2	43	$\hat{C}_{4,2}$	$\hat{b}_{26}$	2
42	$\hat{C}_{4,4}$	$\hat{b}_{28}$	1	43	$\hat{C}_{4,3}$	$\hat{b}_{27}$	1
42	$\hat{C}_{4,5}$	$\hat{b}_{29}$	1	43	$\hat{C}_{4,4}$	$\hat{b}_{28}$	1
42	$\hat{C}_{4,6}$	$\hat{b}_{30}$	1	43	$\hat{C}_{4,5}$	$\hat{b}_{29}$	1
42	$\hat{C}_{4,7}$	$\hat{b}_{31}$	0	43	$\hat{C}_{4,6}$	$\hat{b}_{30}$	1

$\hat{L}$	$\hat{C}_{i,k}$	$\hat{b}_m$	$\hat{B}_m$	$\hat{L}$	$\hat{C}_{i,k}$	$\hat{b}_m$	$\hat{B}_m$
43	$\hat{C}_{4,7}$	$\hat{b}_{31}$	0	44	$\hat{C}_{4,5}$	$\hat{b}_{29}$	1
43	$\hat{C}_{5,2}$	$\hat{b}_{32}$	2	44	$\hat{C}_{4,6}$	$\hat{b}_{30}$	1
43	$\hat{C}_{5,3}$	$\hat{b}_{33}$	1	44	$\hat{C}_{4,7}$	$\hat{b}_{31}$	0
43	$\hat{C}_{5,4}$	$\hat{b}_{34}$	1	44	$\hat{C}_{5,2}$	$\hat{b}_{32}$	2
43	$\hat{C}_{5,5}$	$\hat{b}_{35}$	1	44	$\hat{C}_{5,3}$	$\hat{b}_{33}$	1
43	$\hat{C}_{5,6}$	$\hat{b}_{36}$	0	44	$\hat{C}_{5,4}$	$\hat{b}_{34}$	1
43	$\hat{C}_{5,7}$	$\hat{b}_{37}$	0	44	$\hat{C}_{5,5}$	$\hat{b}_{35}$	1
43	$\hat{C}_{6,2}$	$\hat{b}_{38}$	2	44	$\hat{C}_{5,6}$	$\hat{b}_{36}$	1
43	$\hat{C}_{6,3}$	$\hat{b}_{39}$	1	44	$\hat{C}_{5,7}$	$\hat{b}_{37}$	0
43	$\hat{C}_{6,4}$	$\hat{b}_{40}$	1	44	$\hat{C}_{5,8}$	$\hat{b}_{38}$	0
43	$\hat{C}_{6,5}$	$\hat{b}_{41}$	1	44	$\hat{C}_{6,2}$	$\hat{b}_{39}$	2
43	$\hat{C}_{6,6}$	$\hat{b}_{42}$	1	44	$\hat{C}_{6,3}$	$\hat{b}_{40}$	1
43	$\hat{C}_{6,7}$	$\hat{b}_{43}$	0	44	$\hat{C}_{6,4}$	$\hat{b}_{41}$	1
43	$\hat{C}_{6,8}$	$\hat{b}_{44}$	0	44	$\hat{C}_{6,5}$	$\hat{b}_{42}$	1
				44	$\hat{C}_{6,6}$	$\hat{b}_{43}$	1
44	$\hat{C}_{1,2}$	$\hat{b}_8$	3	44	$\hat{C}_{6,7}$	$\hat{b}_{44}$	0
44	$\hat{C}_{1,3}$	$\hat{b}_9$	2	44	$\hat{C}_{6,8}$	$\hat{b}_{45}$	0
44	$\hat{C}_{1,4}$	$\hat{b}_{10}$	2				
44	$\hat{C}_{1,5}$	$\hat{b}_{11}$	1	45	$\hat{C}_{1,2}$	$\hat{b}_8$	3
44	$\hat{C}_{1,6}$	$\hat{b}_{12}$	1	45	$\hat{C}_{1,3}$	$\hat{b}_9$	2
44	$\hat{C}_{1,7}$	$\hat{b}_{13}$	1	45	$\hat{C}_{1,4}$	$\hat{b}_{10}$	2
44	$\hat{C}_{2,2}$	$\hat{b}_{14}$	3	45	$\hat{C}_{1,5}$	$\hat{b}_{11}$	1
44	$\hat{C}_{2,3}$	$\hat{b}_{15}$	2	45	$\hat{C}_{1,6}$	$\hat{b}_{12}$	1
44	$\hat{C}_{2,4}$	$\hat{b}_{16}$	2	45	$\hat{C}_{1,7}$	$\hat{b}_{13}$	1
44	$\hat{C}_{2,5}$	$\hat{b}_{17}$	2	45	$\hat{C}_{2,2}$	$\hat{b}_{14}$	3
44	$\hat{C}_{2,6}$	$\hat{b}_{18}$	1	45	$\hat{C}_{2,3}$	$\hat{b}_{15}$	2
44	$\hat{C}_{2,7}$	$\hat{b}_{19}$	1	45	$\hat{C}_{2,4}$	$\hat{b}_{16}$	2
44	$\hat{C}_{3,2}$	$\hat{b}_{20}$	2	45	$\hat{C}_{2,5}$	$\hat{b}_{17}$	1
44	$\hat{C}_{3,3}$	$\hat{b}_{21}$	2	45	$\hat{C}_{2,6}$	$\hat{b}_{18}$	1
44	$\hat{C}_{3,4}$	$\hat{b}_{22}$	1	45	$\hat{C}_{2,7}$	$\hat{b}_{19}$	1
44	$\hat{C}_{3,5}$	$\hat{b}_{23}$	1	45	$\hat{C}_{3,2}$	$\hat{b}_{20}$	2
44	$\hat{C}_{3,6}$	$\hat{b}_{24}$	1	45	$\hat{C}_{3,3}$	$\hat{b}_{21}$	2
44	$\hat{C}_{3,7}$	$\hat{b}_{25}$	1	45	$\hat{C}_{3,4}$	$\hat{b}_{22}$	1
44	$\hat{C}_{4,2}$	$\hat{b}_{26}$	2	45	$\hat{C}_{3,5}$	$\hat{b}_{23}$	1
44	$\hat{C}_{4,3}$	$\hat{b}_{27}$	1	45	$\hat{C}_{3,6}$	$\hat{b}_{24}$	1
44	$\hat{C}_{4,4}$	$\hat{b}_{28}$	1	45	$\hat{C}_{3,7}$	$\hat{b}_{25}$	1

$\hat{L}$	$\hat{C}_{i,k}$	$\hat{b}_m$	$\hat{B}_m$	$\hat{L}$	$\hat{C}_{i,k}$	$\hat{b}_m$	$\hat{B}_m$
45	$\hat{C}_{4,2}$	$\hat{b}_{26}$	2	46	$\hat{C}_{3,4}$	$\hat{b}_{22}$	1
45	$\hat{C}_{4,3}$	$\hat{b}_{27}$	2	46	$\hat{C}_{3,5}$	$\hat{b}_{23}$	1
45	$\hat{C}_{4,4}$	$\hat{b}_{28}$	1	46	$\hat{C}_{3,6}$	$\hat{b}_{24}$	1
45	$\hat{C}_{4,5}$	$\hat{b}_{29}$	1	46	$\hat{C}_{3,7}$	$\hat{b}_{25}$	1
45	$\hat{C}_{4,6}$	$\hat{b}_{30}$	1	46	$\hat{C}_{3,8}$	$\hat{b}_{26}$	1
45	$\hat{C}_{4,7}$	$\hat{b}_{31}$	0	46	$\hat{C}_{4,2}$	$\hat{b}_{27}$	2
45	$\hat{C}_{4,8}$	$\hat{b}_{32}$	0	46	$\hat{C}_{4,3}$	$\hat{b}_{28}$	2
45	$\hat{C}_{5,2}$	$\hat{b}_{33}$	2	46	$\hat{C}_{4,4}$	$\hat{b}_{29}$	1
45	$\hat{C}_{5,3}$	$\hat{b}_{34}$	1	46	$\hat{C}_{4,5}$	$\hat{b}_{30}$	1
45	$\hat{C}_{5,4}$	$\hat{b}_{35}$	1	46	$\hat{C}_{4,6}$	$\hat{b}_{31}$	1
45	$\hat{C}_{5,5}$	$\hat{b}_{36}$	1	46	$\hat{C}_{4,7}$	$\hat{b}_{32}$	0
45	$\hat{C}_{5,6}$	$\hat{b}_{37}$	1	46	$\hat{C}_{4,8}$	$\hat{b}_{33}$	0
45	$\hat{C}_{5,7}$	$\hat{b}_{38}$	0	46	$\hat{C}_{5,2}$	$\hat{b}_{34}$	2
45	$\hat{C}_{5,8}$	$\hat{b}_{39}$	0	46	$\hat{C}_{5,3}$	$\hat{b}_{35}$	1
45	$\hat{C}_{6,2}$	$\hat{b}_{40}$	2	46	$\hat{C}_{5,4}$	$\hat{b}_{36}$	1
45	$\hat{C}_{6,3}$	$\hat{b}_{41}$	1	46	$\hat{C}_{5,5}$	$\hat{b}_{37}$	1
45	$\hat{C}_{6,4}$	$\hat{b}_{42}$	1	46	$\hat{C}_{5,6}$	$\hat{b}_{38}$	1
45	$\hat{C}_{6,5}$	$\hat{b}_{43}$	1	46	$\hat{C}_{5,7}$	$\hat{b}_{39}$	0
45	$\hat{C}_{6,6}$	$\hat{b}_{44}$	1	46	$\hat{C}_{5,8}$	$\hat{b}_{40}$	0
45	$\hat{C}_{6,7}$	$\hat{b}_{45}$	0	46	$\hat{C}_{6,2}$	$\hat{b}_{41}$	2
45	$\hat{C}_{6,8}$	$\hat{b}_{46}$	0	46	$\hat{C}_{6,3}$	$\hat{b}_{42}$	1
				46	$\hat{C}_{6,4}$	$\hat{b}_{43}$	1
46	$\hat{C}_{1,2}$	$\hat{b}_8$	3	46	$\hat{C}_{6,5}$	$\hat{b}_{44}$	1
46	$\hat{C}_{1,3}$	$\hat{b}_9$	2	46	$\hat{C}_{6,6}$	$\hat{b}_{45}$	1
46	$\hat{C}_{1,4}$	$\hat{b}_{10}$	2	46	$\hat{C}_{6,7}$	$\hat{b}_{46}$	0
46	$\hat{C}_{1,5}$	$\hat{b}_{11}$	1	46	$\hat{C}_{6,8}$	$\hat{b}_{47}$	0
46	$\hat{C}_{1,6}$	$\hat{b}_{12}$	1				
46	$\hat{C}_{1,7}$	$\hat{b}_{13}$	1	47	$\hat{C}_{1,2}$	$\hat{b}_8$	3
46	$\hat{C}_{2,2}$	$\hat{b}_{14}$	3	47	$\hat{C}_{1,3}$	$\hat{b}_9$	2
46	$\hat{C}_{2,3}$	$\hat{b}_{15}$	2	47	$\hat{C}_{1,4}$	$\hat{b}_{10}$	2
46	$\hat{C}_{2,4}$	$\hat{b}_{16}$	2	47	$\hat{C}_{1,5}$	$\hat{b}_{11}$	1
46	$\hat{C}_{2,5}$	$\hat{b}_{17}$	1	47	$\hat{C}_{1,6}$	$\hat{b}_{12}$	1
46	$\hat{C}_{2,6}$	$\hat{b}_{18}$	1	47	$\hat{C}_{1,7}$	$\hat{b}_{13}$	1
46	$\hat{C}_{2,7}$	$\hat{b}_{19}$	1	47	$\hat{C}_{2,2}$	$\hat{b}_{14}$	3
46	$\hat{C}_{3,2}$	$\hat{b}_{20}$	2	47	$\hat{C}_{2,3}$	$\hat{b}_{15}$	2
46	$\hat{C}_{3,3}$	$\hat{b}_{21}$	2	47	$\hat{C}_{2,4}$	$\hat{b}_{16}$	2

$\hat{L}$	$\hat{C}_{i,k}$	$\hat{b}_m$	$\hat{B}_m$	$\hat{L}$	$\hat{C}_{i,k}$	$\hat{b}_m$	$\hat{B}_m$
47	$\hat{C}_{2,5}$	$\hat{b}_{17}$	1	48	$\hat{C}_{1,5}$	$\hat{b}_{11}$	1
47	$\hat{C}_{2,6}$	$\hat{b}_{18}$	1	48	$\hat{C}_{1,6}$	$\hat{b}_{12}$	1
47	$\hat{C}_{2,7}$	$\hat{b}_{19}$	1	48	$\hat{C}_{1,7}$	$\hat{b}_{13}$	1
47	$\hat{C}_{2,8}$	$\hat{b}_{20}$	1	48	$\hat{C}_{1,8}$	$\hat{b}_{14}$	1
47	$\hat{C}_{3,2}$	$\hat{b}_{21}$	2	48	$\hat{C}_{2,2}$	$\hat{b}_{15}$	3
47	$\hat{C}_{3,3}$	$\hat{b}_{22}$	2	48	$\hat{C}_{2,3}$	$\hat{b}_{16}$	2
47	$\hat{C}_{3,4}$	$\hat{b}_{23}$	1	48	$\hat{C}_{2,4}$	$\hat{b}_{17}$	2
47	$\hat{C}_{3,5}$	$\hat{b}_{24}$	1	48	$\hat{C}_{2,5}$	$\hat{b}_{18}$	1
47	$\hat{C}_{3,6}$	$\hat{b}_{25}$	1	48	$\hat{C}_{2,6}$	$\hat{b}_{19}$	1
47	$\hat{C}_{3,7}$	$\hat{b}_{26}$	1	48	$\hat{C}_{2,7}$	$\hat{b}_{20}$	1
47	$\hat{C}_{3,8}$	$\hat{b}_{27}$	1	48	$\hat{C}_{2,8}$	$\hat{b}_{21}$	1
47	$\hat{C}_{4,2}$	$\hat{b}_{28}$	2	48	$\hat{C}_{3,2}$	$\hat{b}_{22}$	2
47	$\hat{C}_{4,3}$	$\hat{b}_{29}$	2	48	$\hat{C}_{3,3}$	$\hat{b}_{23}$	2
47	$\hat{C}_{4,4}$	$\hat{b}_{30}$	1	48	$\hat{C}_{3,4}$	$\hat{b}_{24}$	1
47	$\hat{C}_{4,5}$	$\hat{b}_{31}$	1	48	$\hat{C}_{3,5}$	$\hat{b}_{25}$	1
47	$\hat{C}_{4,6}$	$\hat{b}_{32}$	1	48	$\hat{C}_{3,6}$	$\hat{b}_{26}$	1
47	$\hat{C}_{4,7}$	$\hat{b}_{33}$	0	48	$\hat{C}_{3,7}$	$\hat{b}_{27}$	1
47	$\hat{C}_{4,8}$	$\hat{b}_{34}$	0	48	$\hat{C}_{3,8}$	$\hat{b}_{28}$	1
47	$\hat{C}_{5,2}$	$\hat{b}_{35}$	2	48	$\hat{C}_{4,2}$	$\hat{b}_{29}$	2
47	$\hat{C}_{5,3}$	$\hat{b}_{36}$	1	48	$\hat{C}_{4,3}$	$\hat{b}_{30}$	2
47	$\hat{C}_{5,4}$	$\hat{b}_{37}$	1	48	$\hat{C}_{4,4}$	$\hat{b}_{31}$	1
47	$\hat{C}_{5,5}$	$\hat{b}_{38}$	1	48	$\hat{C}_{4,5}$	$\hat{b}_{32}$	1
47	$\hat{C}_{5,6}$	$\hat{b}_{39}$	1	48	$\hat{C}_{4,6}$	$\hat{b}_{33}$	1
47	$\hat{C}_{5,7}$	$\hat{b}_{40}$	0	48	$\hat{C}_{4,7}$	$\hat{b}_{34}$	0
47	$\hat{C}_{5,8}$	$\hat{b}_{41}$	0	48	$\hat{C}_{4,8}$	$\hat{b}_{35}$	0
47	$\hat{C}_{6,2}$	$\hat{b}_{42}$	2	48	$\hat{C}_{5,2}$	$\hat{b}_{36}$	2
47	$\hat{C}_{6,3}$	$\hat{b}_{43}$	1	48	$\hat{C}_{5,3}$	$\hat{b}_{37}$	1
47	$\hat{C}_{6,4}$	$\hat{b}_{44}$	1	48	$\hat{C}_{5,4}$	$\hat{b}_{38}$	1
47	$\hat{C}_{6,5}$	$\hat{b}_{45}$	1	48	$\hat{C}_{5,5}$	$\hat{b}_{39}$	1
47	$\hat{C}_{6,6}$	$\hat{b}_{46}$	0	48	$\hat{C}_{5,6}$	$\hat{b}_{40}$	0
47	$\hat{C}_{6,7}$	$\hat{b}_{47}$	0	48	$\hat{C}_{5,7}$	$\hat{b}_{41}$	0
47	$\hat{C}_{6,8}$	$\hat{b}_{48}$	0	48	$\hat{C}_{5,8}$	$\hat{b}_{42}$	0
				48	$\hat{C}_{6,2}$	$\hat{b}_{43}$	2
48	$\hat{C}_{1,2}$	$\hat{b}_8$	3	48	$\hat{C}_{6,3}$	$\hat{b}_{44}$	1
48	$\hat{C}_{1,3}$	$\hat{b}_9$	2	48	$\hat{C}_{6,4}$	$\hat{b}_{45}$	1
48	$\hat{C}_{1,4}$	$\hat{b}_{10}$	2	48	$\hat{C}_{6,5}$	$\hat{b}_{46}$	1

$\hat{L}$	$\hat{C}_{i,k}$	$\hat{b}_m$	$\hat{B}_m$	$\hat{L}$	$\hat{C}_{i,k}$	$\hat{b}_m$	$\hat{B}_m$
48	$\hat{C}_{6,6}$	$\hat{b}_{47}$	0	49	$\hat{C}_{5,6}$	$\hat{b}_{40}$	0
48	$\hat{C}_{6,7}$	$\hat{b}_{48}$	0	49	$\hat{C}_{5,7}$	$\hat{b}_{41}$	0
48	$\hat{C}_{6,8}$	$\hat{b}_{49}$	0	49	$\hat{C}_{5,8}$	$\hat{b}_{42}$	0
				49	$\hat{C}_{6,2}$	$\hat{b}_{43}$	2
49	$\hat{C}_{1,2}$	$\hat{b}_8$	3	49	$\hat{C}_{6,3}$	$\hat{b}_{44}$	1
49	$\hat{C}_{1,3}$	$\hat{b}_9$	2	49	$\hat{C}_{6,4}$	$\hat{b}_{45}$	1
49	$\hat{C}_{1,4}$	$\hat{b}_{10}$	2	49	$\hat{C}_{6,5}$	$\hat{b}_{46}$	1
49	$\hat{C}_{1,5}$	$\hat{b}_{11}$	1	49	$\hat{C}_{6,6}$	$\hat{b}_{47}$	1
49	$\hat{C}_{1,6}$	$\hat{b}_{12}$	1	49	$\hat{C}_{6,7}$	$\hat{b}_{48}$	0
49	$\hat{C}_{1,7}$	$\hat{b}_{13}$	1	49	$\hat{C}_{6,8}$	$\hat{b}_{49}$	0
49	$\hat{C}_{1,8}$	$\hat{b}_{14}$	1	49	$\hat{C}_{6,9}$	$\hat{b}_{50}$	0
49	$\hat{C}_{2,2}$	$\hat{b}_{15}$	3				
49	$\hat{C}_{2,3}$	$\hat{b}_{16}$	2	50	$\hat{C}_{1,2}$	$\hat{b}_8$	3
49	$\hat{C}_{2,4}$	$\hat{b}_{17}$	2	50	$\hat{C}_{1,3}$	$\hat{b}_9$	2
49	$\hat{C}_{2,5}$	$\hat{b}_{18}$	1	50	$\hat{C}_{1,4}$	$\hat{b}_{10}$	2
49	$\hat{C}_{2,6}$	$\hat{b}_{19}$	1	50	$\hat{C}_{1,5}$	$\hat{b}_{11}$	1
49	$\hat{C}_{2,7}$	$\hat{b}_{20}$	1	50	$\hat{C}_{1,6}$	$\hat{b}_{12}$	1
49	$\hat{C}_{2,8}$	$\hat{b}_{21}$	1	50	$\hat{C}_{1,7}$	$\hat{b}_{13}$	1
49	$\hat{C}_{3,2}$	$\hat{b}_{22}$	2	50	$\hat{C}_{1,8}$	$\hat{b}_{14}$	1
49	$\hat{C}_{3,3}$	$\hat{b}_{23}$	2	50	$\hat{C}_{2,2}$	$\hat{b}_{15}$	3
49	$\hat{C}_{3,4}$	$\hat{b}_{24}$	1	50	$\hat{C}_{2,3}$	$\hat{b}_{16}$	2
49	$\hat{C}_{3,5}$	$\hat{b}_{25}$	1	50	$\hat{C}_{2,4}$	$\hat{b}_{17}$	2
49	$\hat{C}_{3,6}$	$\hat{b}_{26}$	1	50	$\hat{C}_{2,5}$	$\hat{b}_{18}$	1
49	$\hat{C}_{3,7}$	$\hat{b}_{27}$	1	50	$\hat{C}_{2,6}$	$\hat{b}_{19}$	1
49	$\hat{C}_{3,8}$	$\hat{b}_{28}$	0	50	$\hat{C}_{2,7}$	$\hat{b}_{20}$	1
49	$\hat{C}_{4,2}$	$\hat{b}_{29}$	2	50	$\hat{C}_{2,8}$	$\hat{b}_{21}$	1
49	$\hat{C}_{4,3}$	$\hat{b}_{30}$	2	50	$\hat{C}_{3,2}$	$\hat{b}_{22}$	2
49	$\hat{C}_{4,4}$	$\hat{b}_{31}$	1	50	$\hat{C}_{3,3}$	$\hat{b}_{23}$	2
49	$\hat{C}_{4,5}$	$\hat{b}_{32}$	1	50	$\hat{C}_{3,4}$	$\hat{b}_{24}$	1
49	$\hat{C}_{4,6}$	$\hat{b}_{33}$	1	50	$\hat{C}_{3,5}$	$\hat{b}_{25}$	1
49	$\hat{C}_{4,7}$	$\hat{b}_{34}$	0	50	$\hat{C}_{3,6}$	$\hat{b}_{26}$	1
49	$\hat{C}_{4,8}$	$\hat{b}_{35}$	0	50	$\hat{C}_{3,7}$	$\hat{b}_{27}$	1
49	$\hat{C}_{5,2}$	$\hat{b}_{36}$	2	50	$\hat{C}_{3,8}$	$\hat{b}_{28}$	0
49	$\hat{C}_{5,3}$	$\hat{b}_{37}$	1	50	$\hat{C}_{4,2}$	$\hat{b}_{29}$	2
49	$\hat{C}_{5,4}$	$\hat{b}_{38}$	1	50	$\hat{C}_{4,3}$	$\hat{b}_{30}$	2
49	$\hat{C}_{5,5}$	$\hat{b}_{39}$	1	50	$\hat{C}_{4,4}$	$\hat{b}_{31}$	1

$\hat{L}$	$\hat{C}_{i,k}$	$\hat{b}_m$	$\hat{B}_m$	$\hat{L}$	$\hat{C}_{i,k}$	$\hat{b}_m$	$\hat{B}_m$
50	$\hat{C}_{4,5}$	$\hat{b}_{32}$	1	51	$\hat{C}_{3,3}$	$\hat{b}_{23}$	2
50	$\hat{C}_{4,6}$	$\hat{b}_{33}$	1	51	$\hat{C}_{3,4}$	$\hat{b}_{24}$	1
50	$\hat{C}_{4,7}$	$\hat{b}_{34}$	0	51	$\hat{C}_{3,5}$	$\hat{b}_{25}$	1
50	$\hat{C}_{4,8}$	$\hat{b}_{35}$	0	51	$\hat{C}_{3,6}$	$\hat{b}_{26}$	1
50	$\hat{C}_{5,2}$	$\hat{b}_{36}$	2	51	$\hat{C}_{3,7}$	$\hat{b}_{27}$	1
50	$\hat{C}_{5,3}$	$\hat{b}_{37}$	1	51	$\hat{C}_{3,8}$	$\hat{b}_{28}$	0
50	$\hat{C}_{5,4}$	$\hat{b}_{38}$	1	51	$\hat{C}_{4,2}$	$\hat{b}_{29}$	2
50	$\hat{C}_{5,5}$	$\hat{b}_{39}$	1	51	$\hat{C}_{4,3}$	$\hat{b}_{30}$	2
50	$\hat{C}_{5,6}$	$\hat{b}_{40}$	1	51	$\hat{C}_{4,4}$	$\hat{b}_{31}$	1
50	$\hat{C}_{5,7}$	$\hat{b}_{41}$	0	51	$\hat{C}_{4,5}$	$\hat{b}_{32}$	1
50	$\hat{C}_{5,8}$	$\hat{b}_{42}$	0	51	$\hat{C}_{4,6}$	$\hat{b}_{33}$	1
50	$\hat{C}_{5,9}$	$\hat{b}_{43}$	0	51	$\hat{C}_{4,7}$	$\hat{b}_{34}$	0
50	$\hat{C}_{6,2}$	$\hat{b}_{44}$	2	51	$\hat{C}_{4,8}$	$\hat{b}_{35}$	0
50	$\hat{C}_{6,3}$	$\hat{b}_{45}$	1	51	$\hat{C}_{4,9}$	$\hat{b}_{36}$	0
50	$\hat{C}_{6,4}$	$\hat{b}_{46}$	1	51	$\hat{C}_{5,2}$	$\hat{b}_{37}$	2
50	$\hat{C}_{6,5}$	$\hat{b}_{47}$	1	51	$\hat{C}_{5,3}$	$\hat{b}_{38}$	1
50	$\hat{C}_{6,6}$	$\hat{b}_{48}$	0	51	$\hat{C}_{5,4}$	$\hat{b}_{39}$	1
50	$\hat{C}_{6,7}$	$\hat{b}_{49}$	0	51	$\hat{C}_{5,5}$	$\hat{b}_{40}$	1
50	$\hat{C}_{6,8}$	$\hat{b}_{50}$	0	51	$\hat{C}_{5,6}$	$\hat{b}_{41}$	1
50	$\hat{C}_{6,9}$	$\hat{b}_{51}$	0	51	$\hat{C}_{5,7}$	$\hat{b}_{42}$	0
				51	$\hat{C}_{5,8}$	$\hat{b}_{43}$	0
51	$\hat{C}_{1,2}$	$\hat{b}_8$	3	51	$\hat{C}_{5,9}$	$\hat{b}_{44}$	0
51	$\hat{C}_{1,3}$	$\hat{b}_9$	2	51	$\hat{C}_{6,2}$	$\hat{b}_{45}$	2
51	$\hat{C}_{1,4}$	$\hat{b}_{10}$	2	51	$\hat{C}_{6,3}$	$\hat{b}_{46}$	1
51	$\hat{C}_{1,5}$	$\hat{b}_{11}$	1	51	$\hat{C}_{6,4}$	$\hat{b}_{47}$	1
51	$\hat{C}_{1,6}$	$\hat{b}_{12}$	1	51	$\hat{C}_{6,5}$	$\hat{b}_{48}$	1
51	$\hat{C}_{1,7}$	$\hat{b}_{13}$	1	51	$\hat{C}_{6,6}$	$\hat{b}_{49}$	1
51	$\hat{C}_{1,8}$	$\hat{b}_{14}$	1	51	$\hat{C}_{6,7}$	$\hat{b}_{50}$	0
51	$\hat{C}_{2,2}$	$\hat{b}_{15}$	3	51	$\hat{C}_{6,8}$	$\hat{b}_{51}$	0
51	$\hat{C}_{2,3}$	$\hat{b}_{16}$	2	51	$\hat{C}_{6,9}$	$\hat{b}_{52}$	0
51	$\hat{C}_{2,4}$	$\hat{b}_{17}$	1				
51	$\hat{C}_{2,5}$	$\hat{b}_{18}$	1	52	$\hat{C}_{1,2}$	$\hat{b}_8$	3
51	$\hat{C}_{2,6}$	$\hat{b}_{19}$	1	52	$\hat{C}_{1,3}$	$\hat{b}_9$	2
51	$\hat{C}_{2,7}$	$\hat{b}_{20}$	1	52	$\hat{C}_{1,4}$	$\hat{b}_{10}$	1
51	$\hat{C}_{2,8}$	$\hat{b}_{21}$	1	52	$\hat{C}_{1,5}$	$\hat{b}_{11}$	1
51	$\hat{C}_{3,2}$	$\hat{b}_{22}$	2	52	$\hat{C}_{1,6}$	$\hat{b}_{12}$	1

$\hat{L}$	$\hat{C}_{i,k}$	$\hat{b}_m$	$\hat{B}_m$	$\hat{L}$	$\hat{C}_{i,k}$	$\hat{b}_m$	$\hat{B}_m$
52	$\hat{C}_{1,7}$	$\hat{b}_{13}$	1	52	$\hat{C}_{6,5}$	$\hat{b}_{49}$	1
52	$\hat{C}_{1,8}$	$\hat{b}_{14}$	1	52	$\hat{C}_{6,6}$	$\hat{b}_{50}$	1
52	$\hat{C}_{2,2}$	$\hat{b}_{15}$	3	52	$\hat{C}_{6,7}$	$\hat{b}_{51}$	0
52	$\hat{C}_{2,3}$	$\hat{b}_{16}$	2	52	$\hat{C}_{6,8}$	$\hat{b}_{52}$	0
52	$\hat{C}_{2,4}$	$\hat{b}_{17}$	2	52	$\hat{C}_{6,9}$	$\hat{b}_{53}$	0
52	$\hat{C}_{2,5}$	$\hat{b}_{18}$	1				
52	$\hat{C}_{2,6}$	$\hat{b}_{19}$	1	53	$\hat{C}_{1,2}$	$\hat{b}_8$	3
52	$\hat{C}_{2,7}$	$\hat{b}_{20}$	1	53	$\hat{C}_{1,3}$	$\hat{b}_9$	2
52	$\hat{C}_{2,8}$	$\hat{b}_{21}$	1	53	$\hat{C}_{1,4}$	$\hat{b}_{10}$	1
52	$\hat{C}_{3,2}$	$\hat{b}_{22}$	2	53	$\hat{C}_{1,5}$	$\hat{b}_{11}$	1
52	$\hat{C}_{3,3}$	$\hat{b}_{23}$	2	53	$\hat{C}_{1,6}$	$\hat{b}_{12}$	1
52	$\hat{C}_{3,4}$	$\hat{b}_{24}$	1	53	$\hat{C}_{1,7}$	$\hat{b}_{13}$	1
52	$\hat{C}_{3,5}$	$\hat{b}_{25}$	1	53	$\hat{C}_{1,8}$	$\hat{b}_{14}$	1
52	$\hat{C}_{3,6}$	$\hat{b}_{26}$	1	53	$\hat{C}_{2,2}$	$\hat{b}_{15}$	3
52	$\hat{C}_{3,7}$	$\hat{b}_{27}$	1	53	$\hat{C}_{2,3}$	$\hat{b}_{16}$	2
52	$\hat{C}_{3,8}$	$\hat{b}_{28}$	1	53	$\hat{C}_{2,4}$	$\hat{b}_{17}$	2
52	$\hat{C}_{3,9}$	$\hat{b}_{29}$	0	53	$\hat{C}_{2,5}$	$\hat{b}_{18}$	1
52	$\hat{C}_{4,2}$	$\hat{b}_{30}$	2	53	$\hat{C}_{2,6}$	$\hat{b}_{19}$	1
52	$\hat{C}_{4,3}$	$\hat{b}_{31}$	2	53	$\hat{C}_{2,7}$	$\hat{b}_{20}$	1
52	$\hat{C}_{4,4}$	$\hat{b}_{32}$	1	53	$\hat{C}_{2,8}$	$\hat{b}_{21}$	1
52	$\hat{C}_{4,5}$	$\hat{b}_{33}$	1	53	$\hat{C}_{2,9}$	$\hat{b}_{22}$	1
52	$\hat{C}_{4,6}$	$\hat{b}_{34}$	1	53	$\hat{C}_{3,2}$	$\hat{b}_{23}$	2
52	$\hat{C}_{4,7}$	$\hat{b}_{35}$	0	53	$\hat{C}_{3,3}$	$\hat{b}_{24}$	2
52	$\hat{C}_{4,8}$	$\hat{b}_{36}$	0	53	$\hat{C}_{3,4}$	$\hat{b}_{25}$	1
52	$\hat{C}_{4,9}$	$\hat{b}_{37}$	0	53	$\hat{C}_{3,5}$	$\hat{b}_{26}$	1
52	$\hat{C}_{5,2}$	$\hat{b}_{38}$	2	53	$\hat{C}_{3,6}$	$\hat{b}_{27}$	1
52	$\hat{C}_{5,3}$	$\hat{b}_{39}$	1	53	$\hat{C}_{3,7}$	$\hat{b}_{28}$	1
52	$\hat{C}_{5,4}$	$\hat{b}_{40}$	1	53	$\hat{C}_{3,8}$	$\hat{b}_{29}$	1
52	$\hat{C}_{5,5}$	$\hat{b}_{41}$	1	53	$\hat{C}_{3,9}$	$\hat{b}_{30}$	0
52	$\hat{C}_{5,6}$	$\hat{b}_{42}$	1	53	$\hat{C}_{4,2}$	$\hat{b}_{31}$	2
52	$\hat{C}_{5,7}$	$\hat{b}_{43}$	0	53	$\hat{C}_{4,3}$	$\hat{b}_{32}$	2
52	$\hat{C}_{5,8}$	$\hat{b}_{44}$	0	53	$\hat{C}_{4,4}$	$\hat{b}_{33}$	1
52	$\hat{C}_{5,9}$	$\hat{b}_{45}$	0	53	$\hat{C}_{4,5}$	$\hat{b}_{34}$	1
52	$\hat{C}_{6,2}$	$\hat{b}_{46}$	2	53	$\hat{C}_{4,6}$	$\hat{b}_{35}$	1
52	$\hat{C}_{6,3}$	$\hat{b}_{47}$	1	53	$\hat{C}_{4,7}$	$\hat{b}_{36}$	0
52	$\hat{C}_{6,4}$	$\hat{b}_{48}$	1	53	$\hat{C}_{4,8}$	$\hat{b}_{37}$	0

$\hat{L}$	$\hat{C}_{i,k}$	$\hat{b}_m$	$\hat{B}_m$	$\hat{L}$	$\hat{C}_{i,k}$	$\hat{b}_m$	$\hat{B}_m$
53	$\hat{C}_{4,9}$	$\hat{b}_{38}$	0	54	$\hat{C}_{3,4}$	$\hat{b}_{26}$	1
53	$\hat{C}_{5,2}$	$\hat{b}_{39}$	2	54	$\hat{C}_{3,5}$	$\hat{b}_{27}$	1
53	$\hat{C}_{5,3}$	$\hat{b}_{40}$	1	54	$\hat{C}_{3,6}$	$\hat{b}_{28}$	1
53	$\hat{C}_{5,4}$	$\hat{b}_{41}$	1	54	$\hat{C}_{3,7}$	$\hat{b}_{29}$	1
53	$\hat{C}_{5,5}$	$\hat{b}_{42}$	1	54	$\hat{C}_{3,8}$	$\hat{b}_{30}$	1
53	$\hat{C}_{5,6}$	$\hat{b}_{43}$	1	54	$\hat{C}_{3,9}$	$\hat{b}_{31}$	0
53	$\hat{C}_{5,7}$	$\hat{b}_{44}$	0	54	$\hat{C}_{4,2}$	$\hat{b}_{32}$	2
53	$\hat{C}_{5,8}$	$\hat{b}_{45}$	0	54	$\hat{C}_{4,3}$	$\hat{b}_{33}$	2
53	$\hat{C}_{5,9}$	$\hat{b}_{46}$	0	54	$\hat{C}_{4,4}$	$\hat{b}_{34}$	1
53	$\hat{C}_{6,2}$	$\hat{b}_{47}$	2	54	$\hat{C}_{4,5}$	$\hat{b}_{35}$	1
53	$\hat{C}_{6,3}$	$\hat{b}_{48}$	1	54	$\hat{C}_{4,6}$	$\hat{b}_{36}$	1
53	$\hat{C}_{6,4}$	$\hat{b}_{49}$	1	54	$\hat{C}_{4,7}$	$\hat{b}_{37}$	0
53	$\hat{C}_{6,5}$	$\hat{b}_{50}$	1	54	$\hat{C}_{4,8}$	$\hat{b}_{38}$	0
53	$\hat{C}_{6,6}$	$\hat{b}_{51}$	0	54	$\hat{C}_{4,9}$	$\hat{b}_{39}$	0
53	$\hat{C}_{6,7}$	$\hat{b}_{52}$	0	54	$\hat{C}_{5,2}$	$\hat{b}_{40}$	2
53	$\hat{C}_{6,8}$	$\hat{b}_{53}$	0	54	$\hat{C}_{5,3}$	$\hat{b}_{41}$	1
53	$\hat{C}_{6,9}$	$\hat{b}_{54}$	0	54	$\hat{C}_{5,4}$	$\hat{b}_{42}$	1
				54	$\hat{C}_{5,5}$	$\hat{b}_{43}$	1
54	$\hat{C}_{1,2}$	$\hat{b}_8$	3	54	$\hat{C}_{5,6}$	$\hat{b}_{44}$	1
54	$\hat{C}_{1,3}$	$\hat{b}_9$	2	54	$\hat{C}_{5,7}$	$\hat{b}_{45}$	0
54	$\hat{C}_{1,4}$	$\hat{b}_{10}$	2	54	$\hat{C}_{5,8}$	$\hat{b}_{46}$	0
54	$\hat{C}_{1,5}$	$\hat{b}_{11}$	1	54	$\hat{C}_{5,9}$	$\hat{b}_{47}$	0
54	$\hat{C}_{1,6}$	$\hat{b}_{12}$	1	54	$\hat{C}_{6,2}$	$\hat{b}_{48}$	2
54	$\hat{C}_{1,7}$	$\hat{b}_{13}$	1	54	$\hat{C}_{6,3}$	$\hat{b}_{49}$	1
54	$\hat{C}_{1,8}$	$\hat{b}_{14}$	1	54	$\hat{C}_{6,4}$	$\hat{b}_{50}$	1
54	$\hat{C}_{1,9}$	$\hat{b}_{15}$	0	54	$\hat{C}_{6,5}$	$\hat{b}_{51}$	1
54	$\hat{C}_{2,2}$	$\hat{b}_{16}$	3	54	$\hat{C}_{6,6}$	$\hat{b}_{52}$	0
54	$\hat{C}_{2,3}$	$\hat{b}_{17}$	2	54	$\hat{C}_{6,7}$	$\hat{b}_{53}$	0
54	$\hat{C}_{2,4}$	$\hat{b}_{18}$	2	54	$\hat{C}_{6,8}$	$\hat{b}_{54}$	0
54	$\hat{C}_{2,5}$	$\hat{b}_{19}$	1	54	$\hat{C}_{6,9}$	$\hat{b}_{55}$	0
54	$\hat{C}_{2,6}$	$\hat{b}_{20}$	1				
54	$\hat{C}_{2,7}$	$\hat{b}_{21}$	1	55	$\hat{C}_{1,2}$	$\hat{b}_8$	3
54	$\hat{C}_{2,8}$	$\hat{b}_{22}$	1	55	$\hat{C}_{1,3}$	$\hat{b}_9$	2
54	$\hat{C}_{2,9}$	$\hat{b}_{23}$	0	55	$\hat{C}_{1,4}$	$\hat{b}_{10}$	2
54	$\hat{C}_{3,2}$	$\hat{b}_{24}$	2	55	$\hat{C}_{1,5}$	$\hat{b}_{11}$	1
54	$\hat{C}_{3,3}$	$\hat{b}_{25}$	2	55	$\hat{C}_{1,6}$	$\hat{b}_{12}$	1

$\hat{L}$	$\hat{C}_{i,k}$	$\hat{b}_m$	$\hat{B}_m$	$\hat{L}$	$\hat{C}_{i,k}$	$\hat{b}_m$	$\hat{B}_m$
55	$\hat{C}_{1,7}$	$\hat{b}_{13}$	1	55	$\hat{C}_{6,3}$	$\hat{b}_{49}$	1
55	$\hat{C}_{1,8}$	$\hat{b}_{14}$	1	55	$\hat{C}_{6,4}$	$\hat{b}_{50}$	1
55	$\hat{C}_{1,9}$	$\hat{b}_{15}$	0	55	$\hat{C}_{6,5}$	$\hat{b}_{51}$	1
55	$\hat{C}_{2,2}$	$\hat{b}_{16}$	3	55	$\hat{C}_{6,6}$	$\hat{b}_{52}$	1
55	$\hat{C}_{2,3}$	$\hat{b}_{17}$	2	55	$\hat{C}_{6,7}$	$\hat{b}_{53}$	0
55	$\hat{C}_{2,4}$	$\hat{b}_{18}$	2	55	$\hat{C}_{6,8}$	$\hat{b}_{54}$	0
55	$\hat{C}_{2,5}$	$\hat{b}_{19}$	1	55	$\hat{C}_{6,9}$	$\hat{b}_{55}$	0
55	$\hat{C}_{2,6}$	$\hat{b}_{20}$	1	55	$\hat{C}_{6,10}$	$\hat{b}_{56}$	0
55	$\hat{C}_{2,7}$	$\hat{b}_{21}$	1				
55	$\hat{C}_{2,8}$	$\hat{b}_{22}$	1	56	$\hat{C}_{1,2}$	$\hat{b}_8$	3
55	$\hat{C}_{2,9}$	$\hat{b}_{23}$	0	56	$\hat{C}_{1,3}$	$\hat{b}_9$	2
55	$\hat{C}_{3,2}$	$\hat{b}_{24}$	2	56	$\hat{C}_{1,4}$	$\hat{b}_{10}$	2
55	$\hat{C}_{3,3}$	$\hat{b}_{25}$	2	56	$\hat{C}_{1,5}$	$\hat{b}_{11}$	1
55	$\hat{C}_{3,4}$	$\hat{b}_{26}$	1	56	$\hat{C}_{1,6}$	$\hat{b}_{12}$	1
55	$\hat{C}_{3,5}$	$\hat{b}_{27}$	1	56	$\hat{C}_{1,7}$	$\hat{b}_{13}$	1
55	$\hat{C}_{3,6}$	$\hat{b}_{28}$	1	56	$\hat{C}_{1,8}$	$\hat{b}_{14}$	1
55	$\hat{C}_{3,7}$	$\hat{b}_{29}$	1	56	$\hat{C}_{1,9}$	$\hat{b}_{15}$	0
55	$\hat{C}_{3,8}$	$\hat{b}_{30}$	1	56	$\hat{C}_{2,2}$	$\hat{b}_{16}$	3
55	$\hat{C}_{3,9}$	$\hat{b}_{31}$	0	56	$\hat{C}_{2,3}$	$\hat{b}_{17}$	2
55	$\hat{C}_{4,2}$	$\hat{b}_{32}$	2	56	$\hat{C}_{2,4}$	$\hat{b}_{18}$	2
55	$\hat{C}_{4,3}$	$\hat{b}_{33}$	2	56	$\hat{C}_{2,5}$	$\hat{b}_{19}$	1
55	$\hat{C}_{4,4}$	$\hat{b}_{34}$	1	56	$\hat{C}_{2,6}$	$\hat{b}_{20}$	1
55	$\hat{C}_{4,5}$	$\hat{b}_{35}$	1	56	$\hat{C}_{2,7}$	$\hat{b}_{21}$	1
55	$\hat{C}_{4,6}$	$\hat{b}_{36}$	1	56	$\hat{C}_{2,8}$	$\hat{b}_{22}$	1
55	$\hat{C}_{4,7}$	$\hat{b}_{37}$	0	56	$\hat{C}_{2,9}$	$\hat{b}_{23}$	0
55	$\hat{C}_{4,8}$	$\hat{b}_{38}$	0	56	$\hat{C}_{3,2}$	$\hat{b}_{24}$	2
55	$\hat{C}_{4,9}$	$\hat{b}_{39}$	0	56	$\hat{C}_{3,3}$	$\hat{b}_{25}$	2
55	$\hat{C}_{5,2}$	$\hat{b}_{40}$	2	56	$\hat{C}_{3,4}$	$\hat{b}_{26}$	1
55	$\hat{C}_{5,3}$	$\hat{b}_{41}$	1	56	$\hat{C}_{3,5}$	$\hat{b}_{27}$	1
55	$\hat{C}_{5,4}$	$\hat{b}_{42}$	1	56	$\hat{C}_{3,6}$	$\hat{b}_{28}$	1
55	$\hat{C}_{5,5}$	$\hat{b}_{43}$	1	56	$\hat{C}_{3,7}$	$\hat{b}_{29}$	1
55	$\hat{C}_{5,6}$	$\hat{b}_{44}$	0	56	$\hat{C}_{3,8}$	$\hat{b}_{30}$	1
55	$\hat{C}_{5,7}$	$\hat{b}_{45}$	0	56	$\hat{C}_{3,9}$	$\hat{b}_{31}$	0
55	$\hat{C}_{5,8}$	$\hat{b}_{46}$	0	56	$\hat{C}_{4,2}$	$\hat{b}_{32}$	2
55	$\hat{C}_{5,9}$	$\hat{b}_{47}$	0	56	$\hat{C}_{4,3}$	$\hat{b}_{33}$	2
55	$\hat{C}_{6,2}$	$\hat{b}_{48}$	2	56	$\hat{C}_{4,4}$	$\hat{b}_{34}$	1

$\hat{L}$	$\hat{C}_{i,k}$	$\hat{b}_m$	$\hat{B}_m$
56	$\hat{C}_{4,5}$	$\hat{b}_{35}$	1
56	$\hat{C}_{4,6}$	$\hat{b}_{36}$	1
56	$\hat{C}_{4,7}$	$\hat{b}_{37}$	0
56	$\hat{C}_{4,8}$	$\hat{b}_{38}$	0
56	$\hat{C}_{4,9}$	$\hat{b}_{39}$	0
56	$\hat{C}_{5,2}$	$\hat{b}_{40}$	2
56	$\hat{C}_{5,3}$	$\hat{b}_{41}$	1
56	$\hat{C}_{5,4}$	$\hat{b}_{42}$	1
56	$\hat{C}_{5,5}$	$\hat{b}_{43}$	1
56	$\hat{C}_{5,6}$	$\hat{b}_{44}$	1
56	$\hat{C}_{5,7}$	$\hat{b}_{45}$	0
56	$\hat{C}_{5,8}$	$\hat{b}_{46}$	0
56	$\hat{C}_{5,9}$	$\hat{b}_{47}$	0
56	$\hat{C}_{5,10}$	$\hat{b}_{48}$	0
56	$\hat{C}_{6,2}$	$\hat{b}_{49}$	2
56	$\hat{C}_{6,3}$	$\hat{b}_{50}$	1
56	$\hat{C}_{6,4}$	$\hat{b}_{51}$	1
56	$\hat{C}_{6,5}$	$\hat{b}_{52}$	1
56	$\hat{C}_{6,6}$	$\hat{b}_{53}$	0
56	$\hat{C}_{6,7}$	$\hat{b}_{54}$	0
56	$\hat{C}_{6,8}$	$\hat{b}_{55}$	0
56	$\hat{C}_{6,9}$	$\hat{b}_{56}$	0
56	$\hat{C}_{6,10}$	$\hat{b}_{57}$	0

Annex H: Bit Frame Format

Symbol	Bit 1	Bit 0	Symbol	Bit 1	Bit 0
0	$c_0(18)$	$c_1(23)$	36	$c_0(6)$	$c_1(11)$
1	$c_2(22)$	$c_3(22)$	37	$c_2(10)$	$c_3(10)$
2	$c_4(14)$	$c_5(14)$	38	$c_4(2)$	$c_5(2)$
3	$c_0(17)$	$c_1(22)$	39	$c_0(5)$	$c_1(10)$
4	$c_2(21)$	$c_3(21)$	40	$c_2(9)$	$c_3(9)$
5	$c_4(13)$	$c_5(13)$	41	$c_4(1)$	$c_5(1)$
6	$c_0(16)$	$c_1(21)$	42	$c_0(4)$	$c_1(9)$
7	$c_2(20)$	$c_3(20)$	43	$c_2(8)$	$c_3(8)$
8	$c_4(12)$	$c_5(12)$	44	$c_4(0)$	$c_5(0)$
9	$c_0(15)$	$c_1(20)$	45	$c_0(3)$	$c_1(8)$
10	$c_2(19)$	$c_3(19)$	46	$c_2(7)$	$c_3(7)$
11	$c_4(11)$	$c_5(11)$	47	$c_6(15)$	$c_6(6)$
12	$c_0(14)$	$c_1(19)$	48	$c_0(2)$	$c_1(7)$
13	$c_2(18)$	$c_3(18)$	49	$c_2(6)$	$c_3(6)$
14	$c_4(10)$	$c_5(10)$	50	$c_6(14)$	$c_6(5)$
15	$c_0(13)$	$c_1(18)$	51	$c_0(1)$	$c_1(6)$
16	$c_2(17)$	$c_3(17)$	52	$c_2(5)$	$c_3(5)$
17	$c_4(9)$	$c_5(9)$	53	$c_6(13)$	$c_6(4)$
18	$c_0(12)$	$c_1(17)$	54	$c_0(0)$	$c_1(5)$
19	$c_2(16)$	$c_3(16)$	55	$c_2(4)$	$c_3(4)$
20	$c_4(8)$	$c_5(8)$	56	$c_6(12)$	$c_6(3)$
21	$c_0(11)$	$c_1(16)$	57	$c_6(22)$	$c_1(4)$
22	$c_2(15)$	$c_3(15)$	58	$c_2(3)$	$c_3(3)$
23	$c_4(7)$	$c_5(7)$	59	$c_6(11)$	$c_6(2)$
24	$c_0(10)$	$c_1(15)$	60	$c_6(21)$	$c_1(3)$
25	$c_2(14)$	$c_3(14)$	61	$c_2(2)$	$c_3(2)$
26	$c_4(6)$	$c_5(6)$	62	$c_6(10)$	$c_6(1)$
27	$c_0(9)$	$c_1(14)$	63	$c_6(20)$	$c_1(2)$
28	$c_2(13)$	$c_3(13)$	64	$c_2(1)$	$c_3(1)$
29	$c_4(5)$	$c_5(5)$	65	$c_6(9)$	$c_6(0)$
30	$c_0(8)$	$c_1(13)$	66	$c_6(19)$	$c_1(1)$
31	$c_2(12)$	$c_3(12)$	67	$c_2(0)$	$c_3(0)$
32	$c_4(4)$	$c_5(4)$	68	$c_6(8)$	$c_6(18)$
33	$c_0(7)$	$c_1(12)$	69	$c_1(0)$	$c_6(17)$
34	$c_2(11)$	$c_3(11)$	70	$c_6(16)$	$c_6(7)$
35	$c_4(3)$	$c_5(3)$			

Annex I: Speech Synthesis Window

n	$w_S(n)$	n	$w_S(n)$	n	$w_S(n)$	n	$w_S(n)$	n	$w_S(n)$
-105	0.000000	-74	0.620000	-43	1.000000	-12	1.000000	19	1.000000
-104	0.020000	-73	0.640000	-42	1.000000	-11	1.000000	20	1.000000
-103	0.040000	-72	0.660000	-41	1.000000	-10	1.000000	21	1.000000
-102	0.060000	-71	0.680000	-40	1.000000	-9	1.000000	22	1.000000
-101	0.080000	-70	0.700000	-39	1.000000	-8	1.000000	23	1.000000
-100	0.100000	-69	0.720000	-38	1.000000	-7	1.000000	24	1.000000
-99	0.120000	-68	0.740000	-37	1.000000	-6	1.000000	25	1.000000
-98	0.140000	-67	0.760000	-36	1.000000	-5	1.000000	26	1.000000
-97	0.160000	-66	0.780000	-35	1.000000	-4	1.000000	27	1.000000
-96	0.180000	-65	0.800000	-34	1.000000	-3	1.000000	28	1.000000
-95	0.200000	-64	0.820000	-33	1.000000	-2	1.000000	29	1.000000
-94	0.220000	-63	0.840000	-32	1.000000	-1	1.000000	30	1.000000
-93	0.240000	-62	0.860000	-31	1.000000	0	1.000000	31	1.000000
-92	0.260000	-61	0.880000	-30	1.000000	1	1.000000	32	1.000000
-91	0.280000	-60	0.900000	-29	1.000000	2	1.000000	33	1.000000
-90	0.300000	-59	0.920000	-28	1.000000	3	1.000000	34	1.000000
-89	0.320000	-58	0.940000	-27	1.000000	4	1.000000	35	1.000000
-88	0.340000	-57	0.960000	-26	1.000000	5	1.000000	36	1.000000
-87	0.360000	-56	0.980000	-25	1.000000	6	1.000000	37	1.000000
-86	0.380000	-55	1.000000	-24	1.000000	7	1.000000	38	1.000000
-85	0.400000	-54	1.000000	-23	1.000000	8	1.000000	39	1.000000
-84	0.420000	-53	1.000000	-22	1.000000	9	1.000000	40	1.000000
-83	0.440000	-52	1.000000	-21	1.000000	10	1.000000	41	1.000000
-82	0.460000	-51	1.000000	-20	1.000000	11	1.000000	42	1.000000
-81	0.480000	-50	1.000000	-19	1.000000	12	1.000000	43	1.000000
-80	0.500000	-49	1.000000	-18	1.000000	13	1.000000	44	1.000000
-79	0.520000	-48	1.000000	-17	1.000000	14	1.000000	45	1.000000
-78	0.540000	-47	1.000000	-16	1.000000	15	1.000000	46	1.000000
-77	0.560000	-46	1.000000	-15	1.000000	16	1.000000	47	1.000000
-76	0.580000	-45	1.000000	-14	1.000000	17	1.000000	48	1.000000
-75	0.600000	-44	1.000000	-13	1.000000	18	1.000000	49	1.000000

n	$w_S(n)$	n	$w_S(n)$
50	1.000000	81	0.480000
51	1.000000	82	0.460000
52	1.000000	83	0.440000
53	1.000000	84	0.420000
54	1.000000	85	0.400000
55	1.000000	86	0.380000
56	0.980000	87	0.360000
57	0.960000	88	0.340000
58	0.940000	89	0.320000
59	0.920000	90	0.300000
60	0.900000	91	0.280000
61	0.880000	92	0.260000
62	0.860000	93	0.240000
63	0.840000	94	0.220000
64	0.820000	95	0.200000
65	0.800000	96	0.180000
66	0.780000	97	0.160000
67	0.760000	98	0.140000
68	0.740000	99	0.120000
69	0.720000	100	0.100000
70	0.700000	101	0.080000
71	0.680000	102	0.060000
72	0.660000	103	0.040000
73	0.640000	104	0.020000
74	0.620000	105	0.000000
75	0.600000		
76	0.580000		
77	0.560000		
78	0.540000		
79	0.520000		
80	0.500000		

Annex J: Log Magnitude Prediction Residual Block Lengths

$\hat{L}$	$\hat{J}_1$	$\hat{J}_2$	$\hat{J}_3$	$\hat{J}_4$	$\hat{J}_5$	$\hat{J}_6$	$\hat{L}$	$\hat{J}_1$	$\hat{J}_2$	$\hat{J}_3$	$\hat{J}_4$	$\hat{J}_5$	$\hat{J}_6$
9	1	1	1	2	2	2	34	5	5	6	6	6	6
10	1	1	2	2	2	2	35	5	6	6	6	6	6
11	1	2	2	2	2	2	36	6	6	6	6	6	6
12	2	2	2	2	2	2	37	6	6	6	6	6	7
13	2	2	2	2	2	3	38	6	6	6	6	7	7
14	2	2	2	2	3	3	39	6	6	6	7	7	7
15	2	2	2	3	3	3	40	6	6	7	7	7	7
16	2	2	3	3	3	3	41	6	7	7	7	7	7
17	2	3	3	3	3	3	42	7	7	7	7	7	7
18	3	3	3	3	3	3	43	7	7	7	7	7	8
19	3	3	3	3	3	4	44	7	7	7	7	8	8
20	3	3	3	3	4	4	45	7	7	7	8	8	8
21	3	3	3	4	4	4	46	7	7	8	8	8	8
22	3	3	4	4	4	4	47	7	8	8	8	8	8
23	3	4	4	4	4	4	48	8	8	8	8	8	8
24	4	4	4	4	4	4	49	8	8	8	8	8	9
25	4	4	4	4	4	5	50	8	8	8	8	9	9
26	4	4	4	4	5	5	51	8	8	8	9	9	9
27	4	4	4	5	5	5	52	8	8	9	9	9	9
28	4	4	5	5	5	5	53	8	9	9	9	9	9
29	4	5	5	5	5	5	54	9	9	9	9	9	9
30	5	5	5	5	5	5	55	9	9	9	9	9	10
31	5	5	5	5	5	6	56	9	9	9	9	10	10
32	5	5	5	5	6	6							
33	5	5	5	6	6	6							

Annex K: Flow Charts

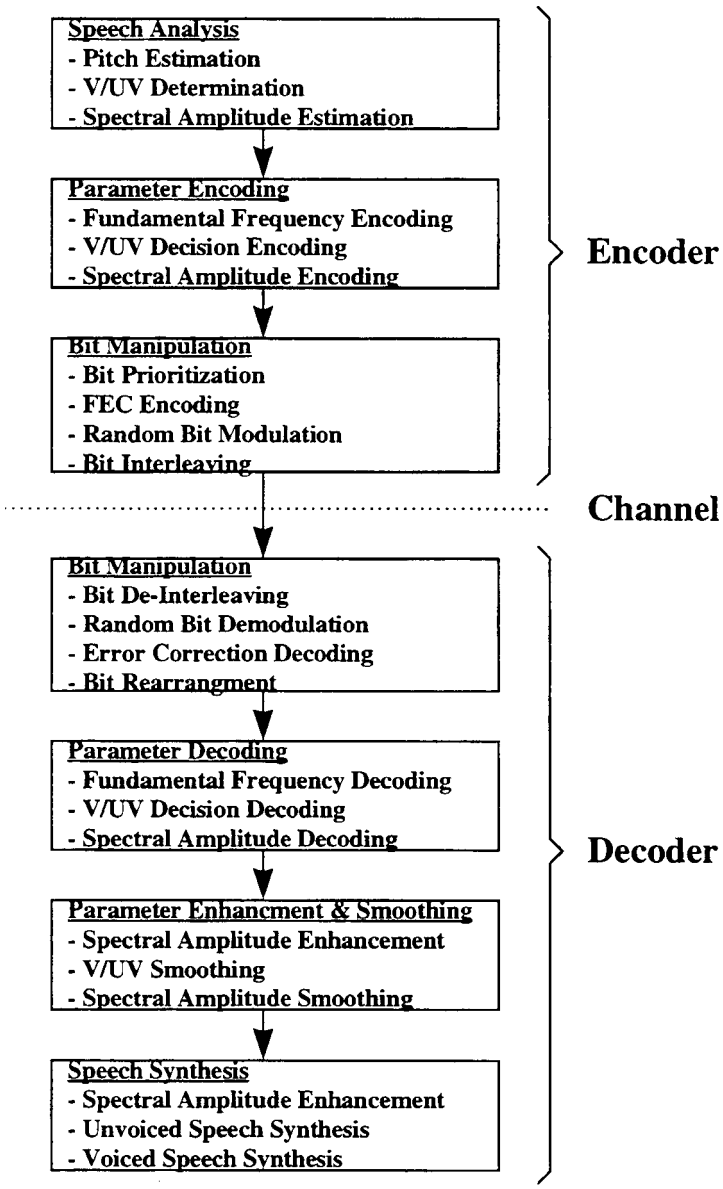

Flow Chart 1: IMBE Voice Coder

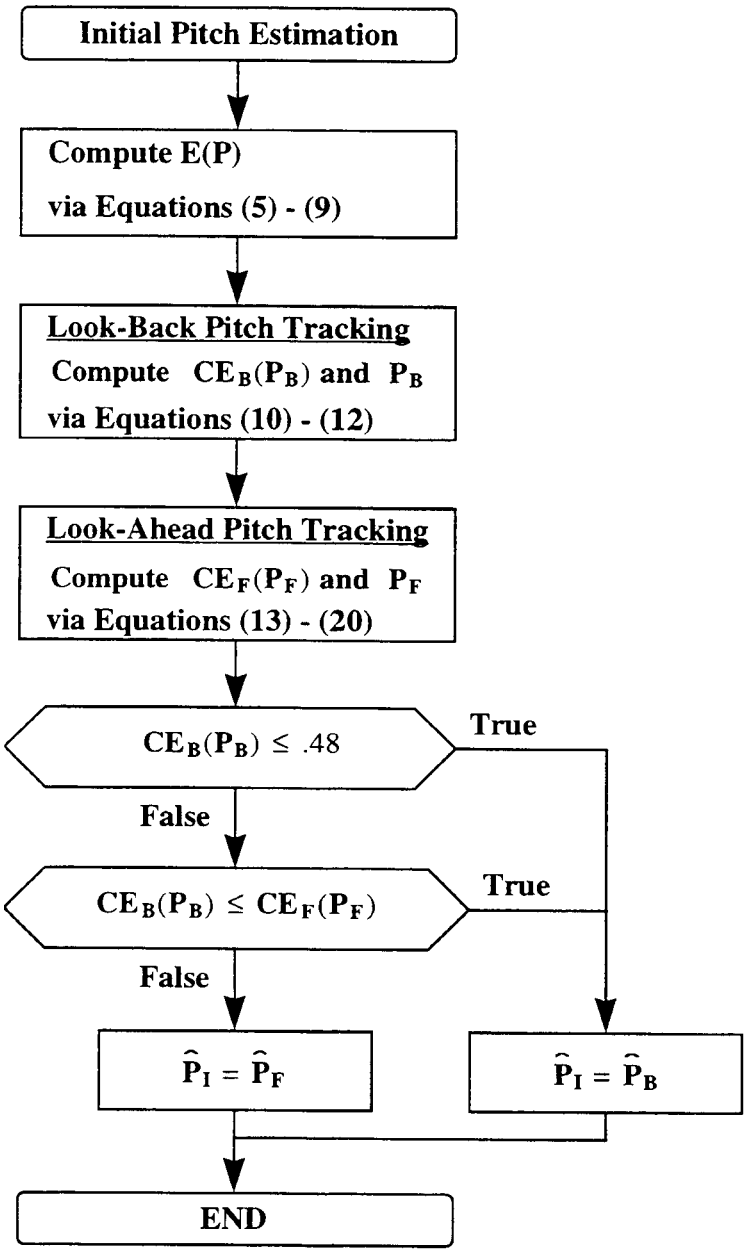

Flow Chart 2: Initial Pitch Estimation

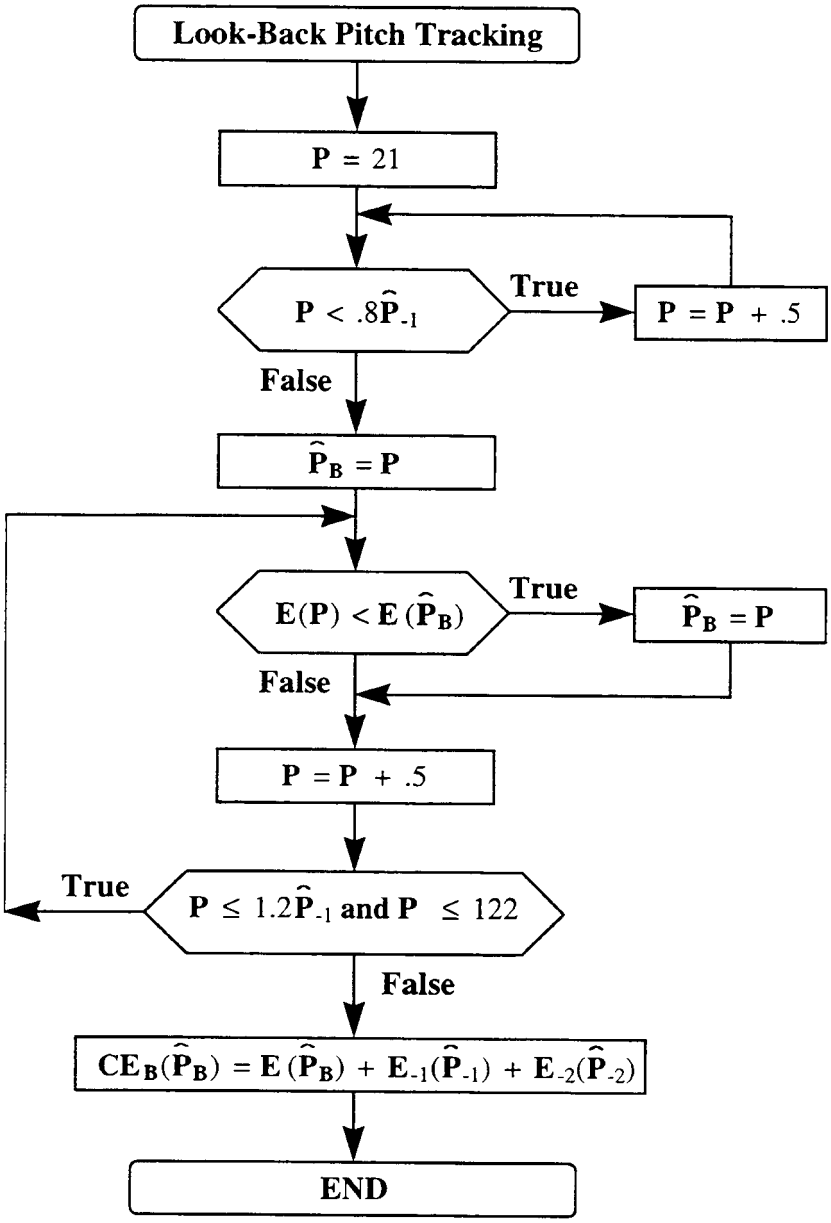

Flow Chart 3: Look-Back Pitch Tracking

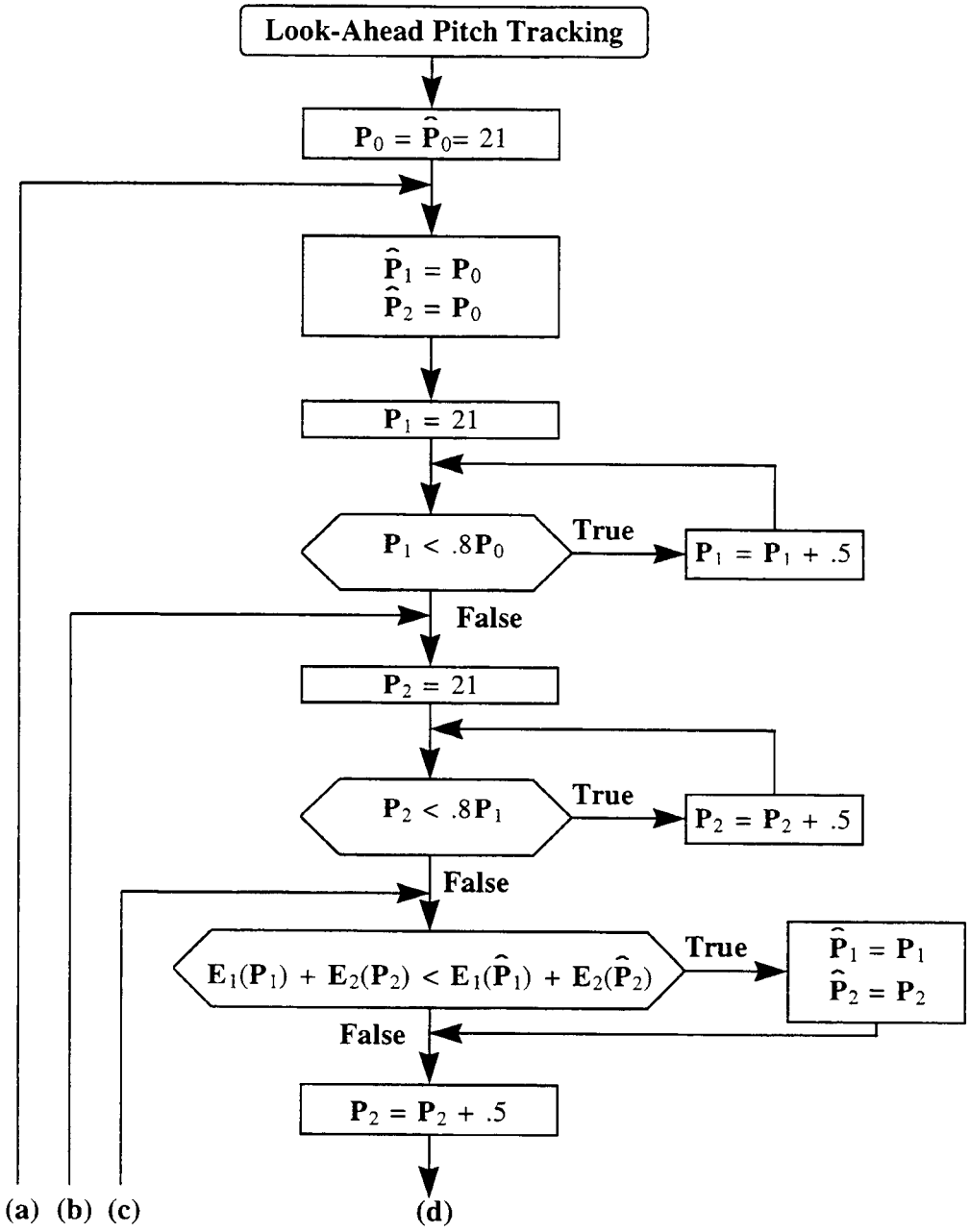

Flow Chart 4: Look-Ahead Pitch Tracking (1 of 3)

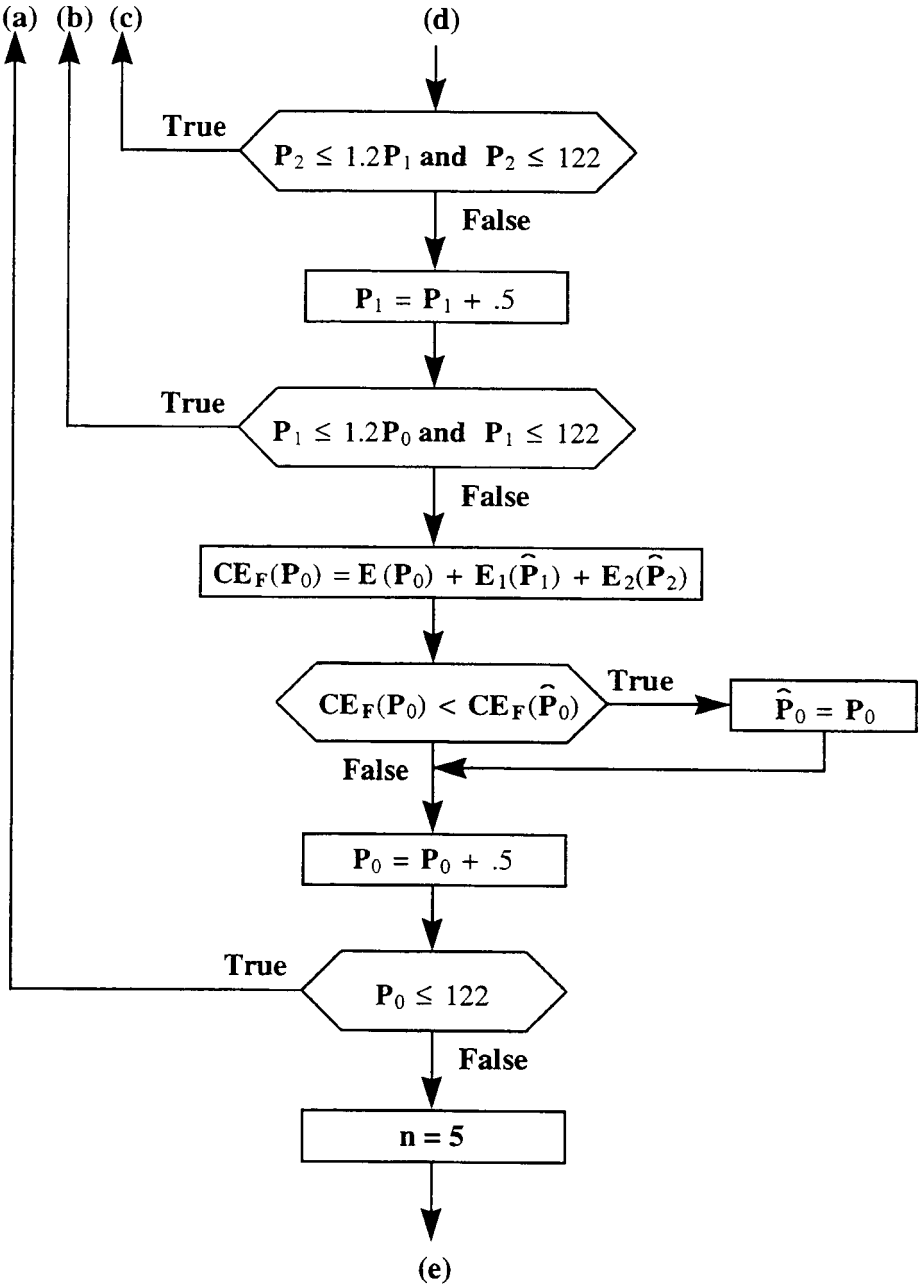

Flow Chart 4: Look-Ahead Pitch Tracking (2 of 3)

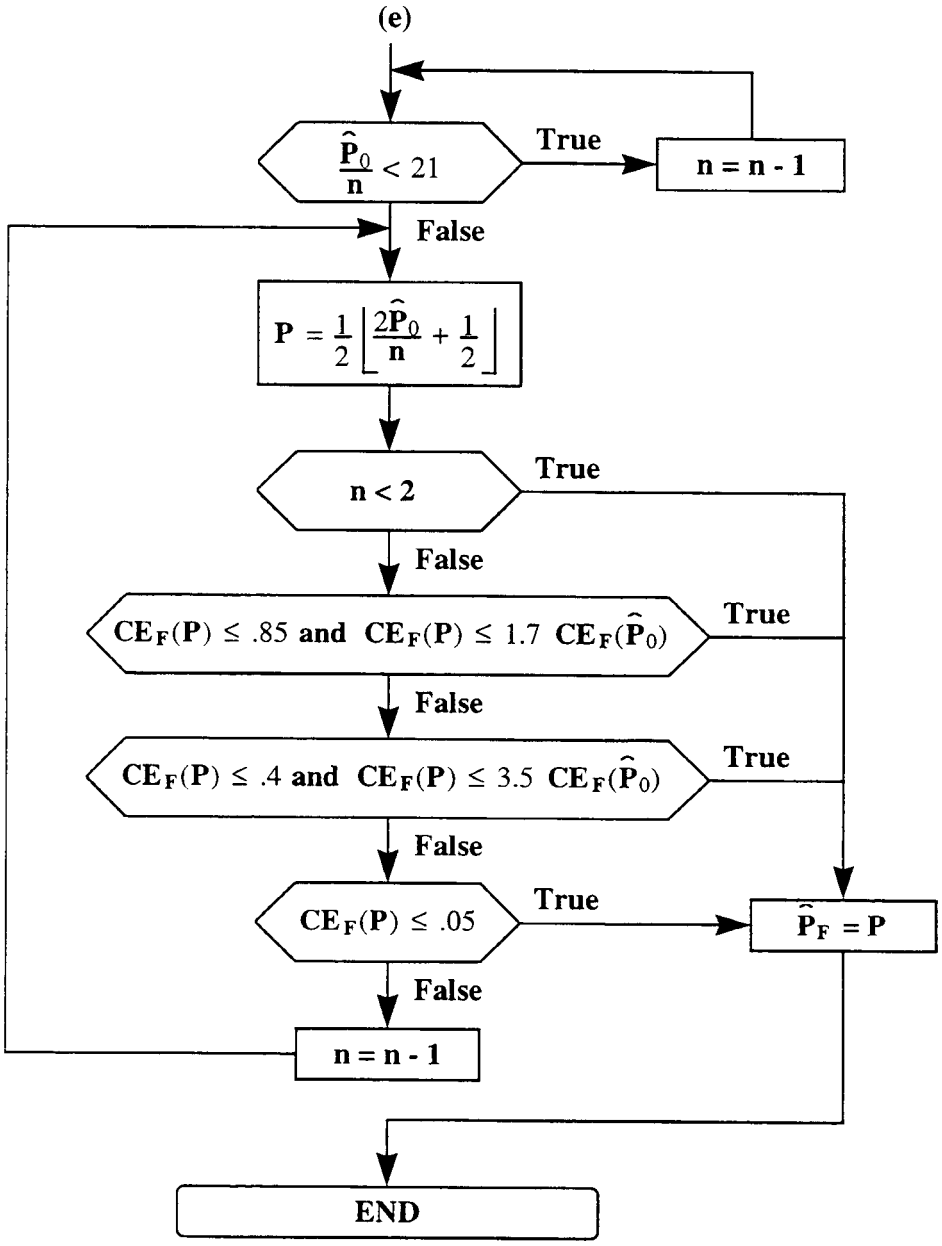

Flow Chart 4: Look-Ahead Pitch Tracking (3 of 3)

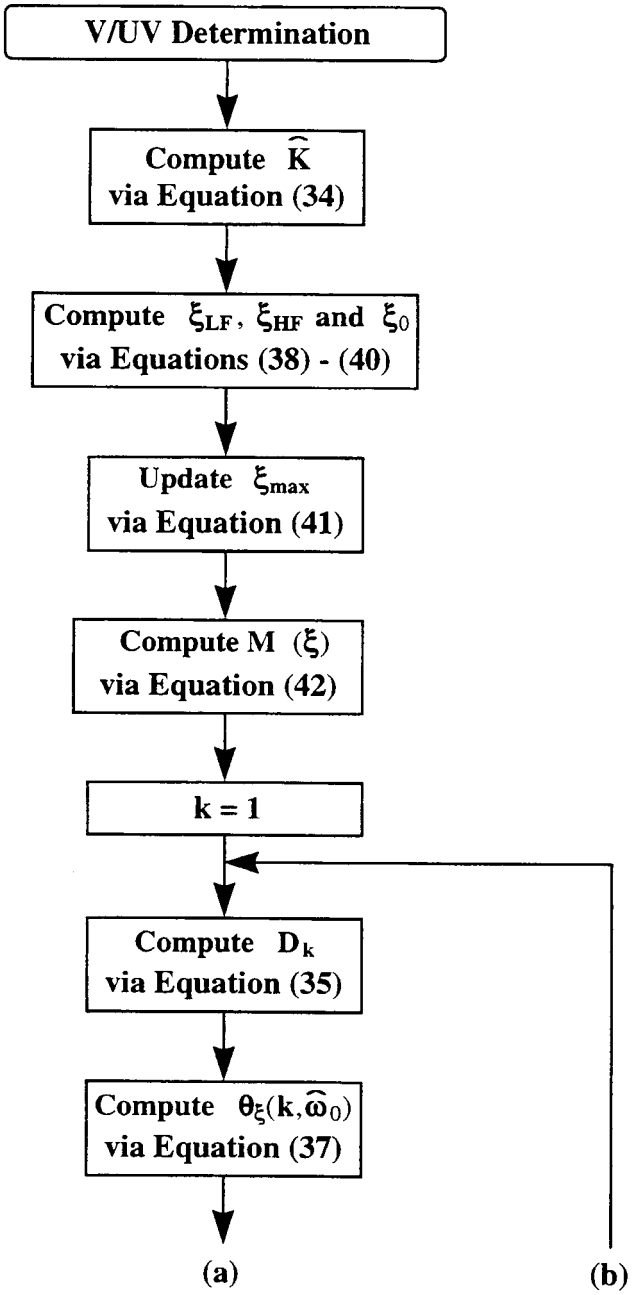

Flow Chart 5: V/UV Determination (1 of 2)

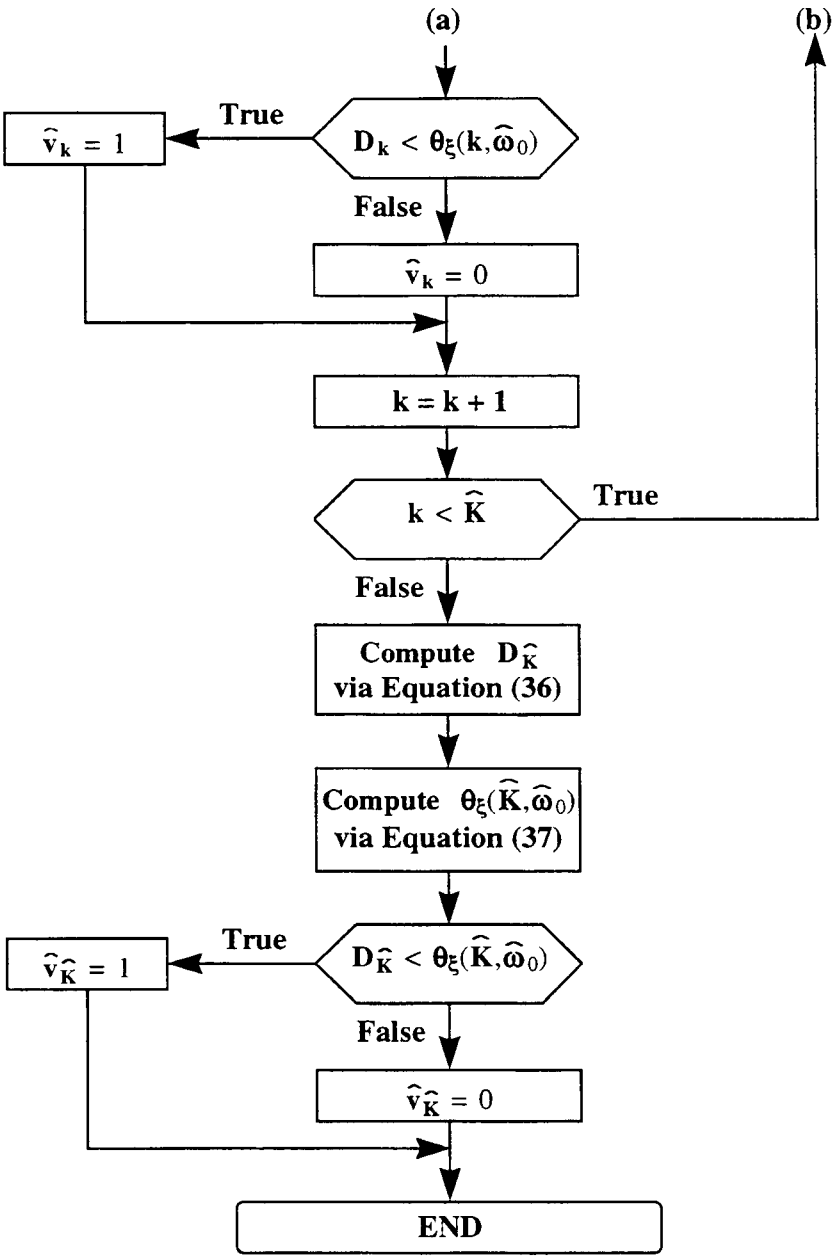

Flow Chart 5: V/UV Determination (2 of 2)

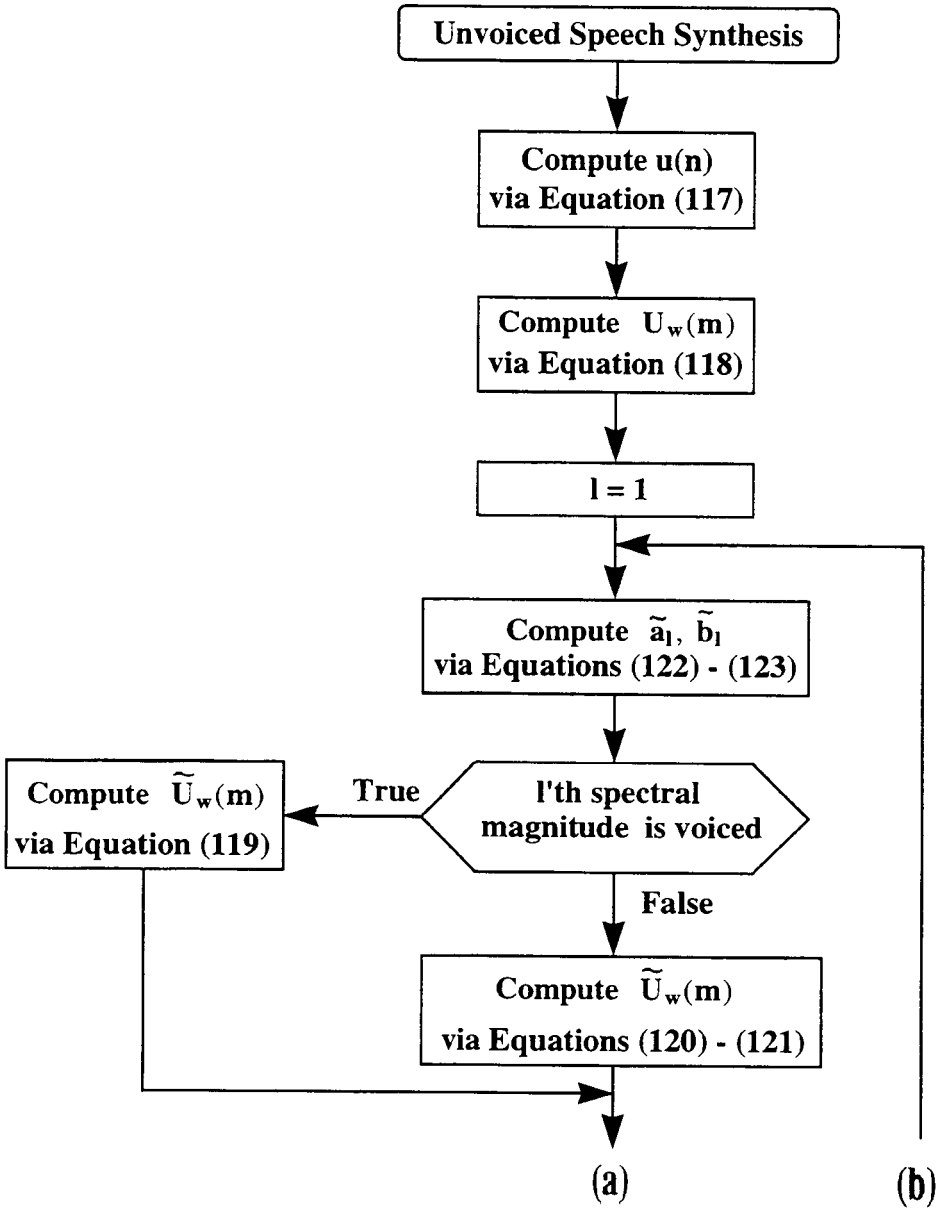

Flow Chart 6: Unvoiced Speech Synthesis (1 of 2)

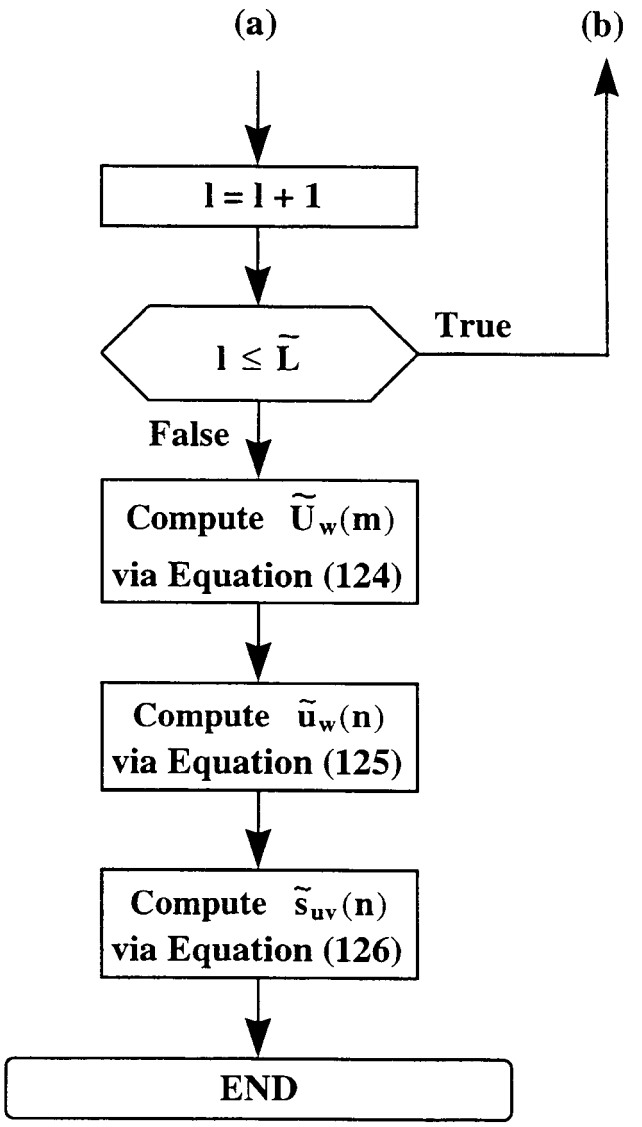

Flow Chart 6: Unvoiced Speech Synthesis (2 of 2)

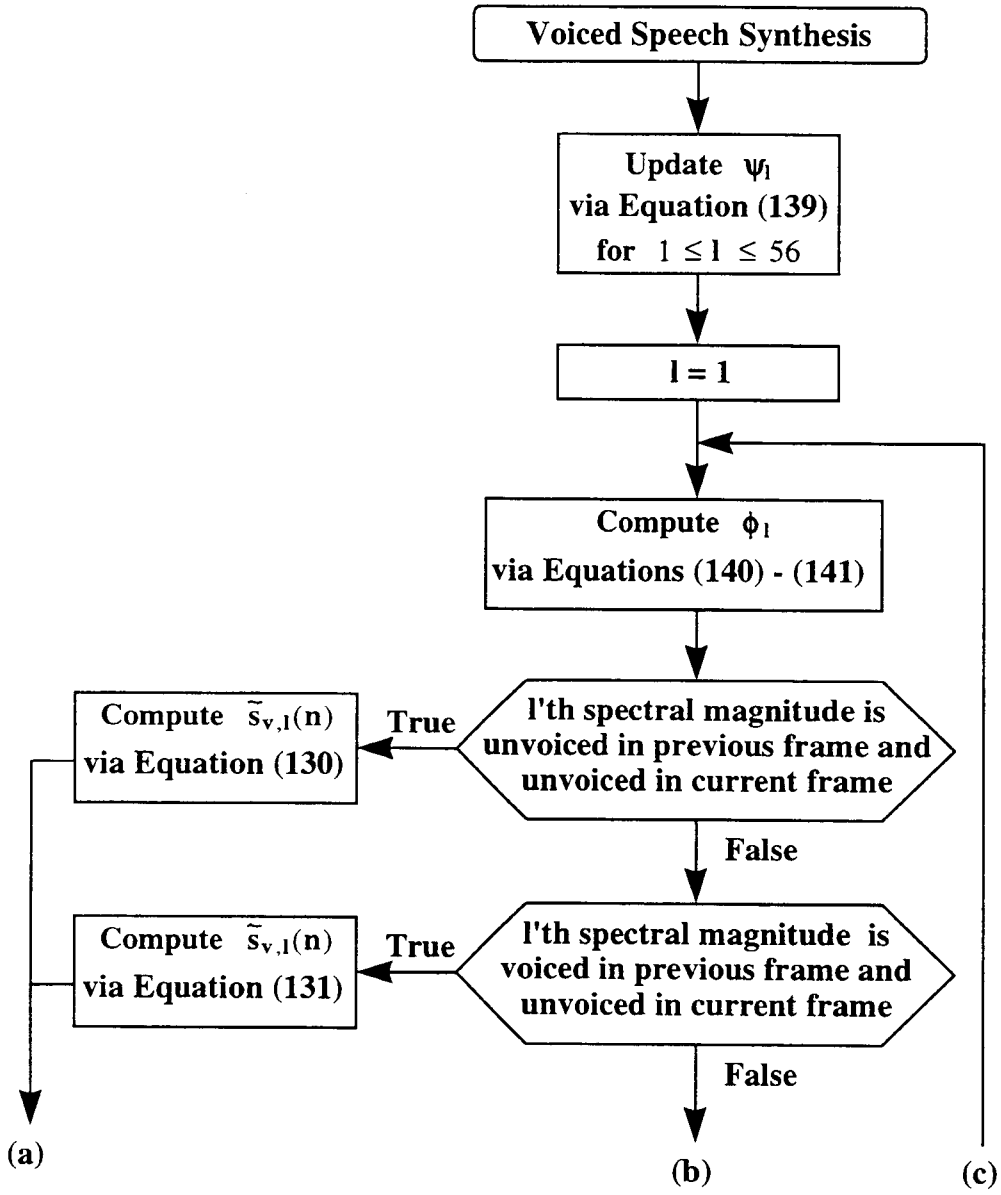

Flow Chart 7: Voiced Speech Synthesis (1 of 2)

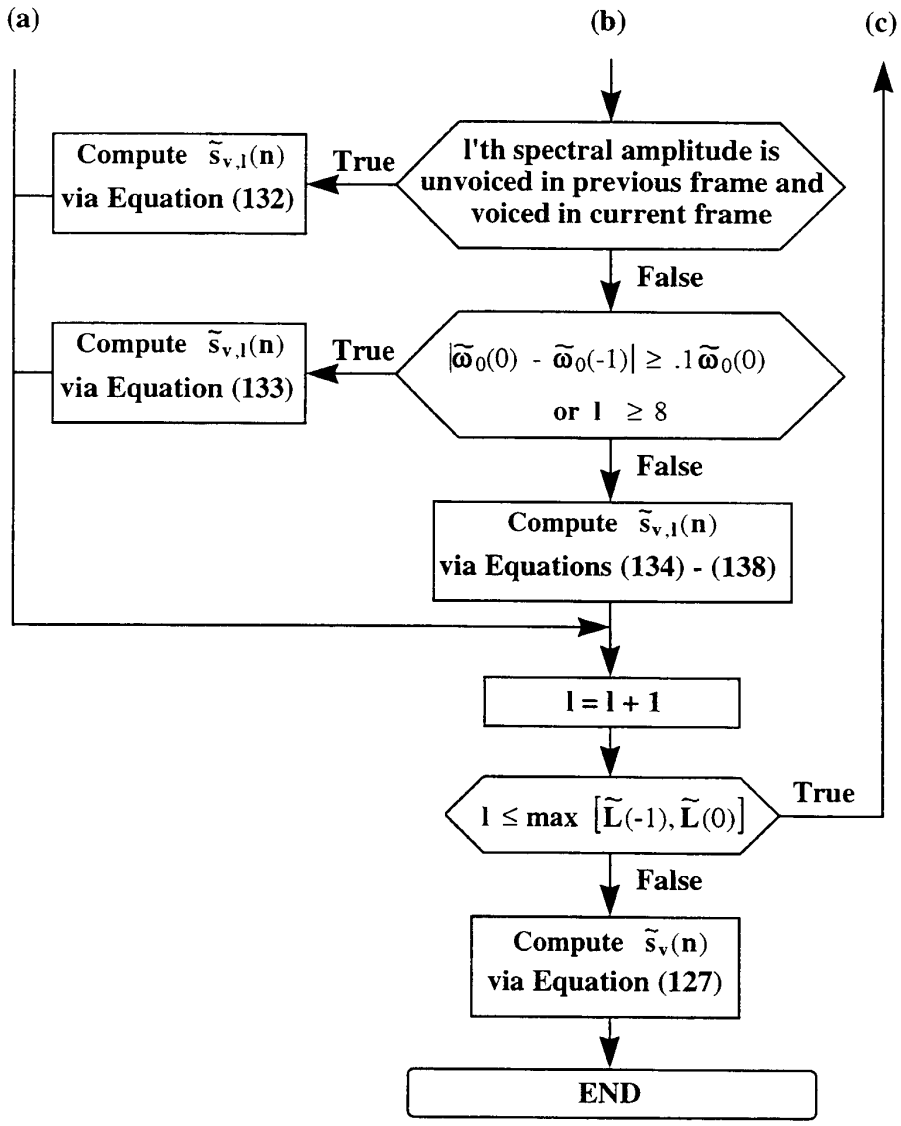

Flow Chart 7: Voiced Speech Synthesis (2 of 2)

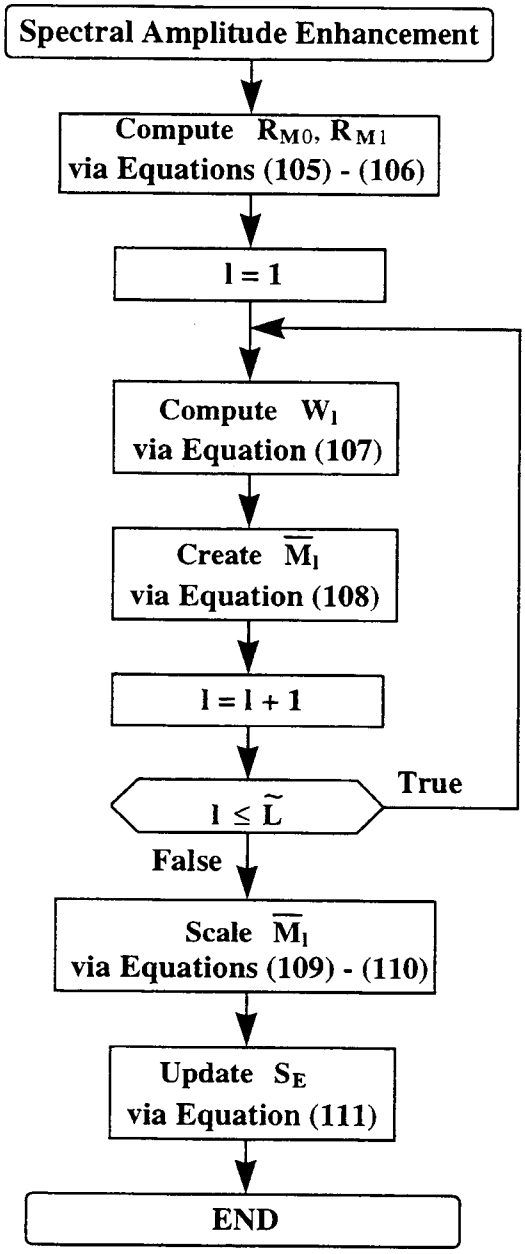

Flow Chart 8: Spectral Amplitude Enhancement

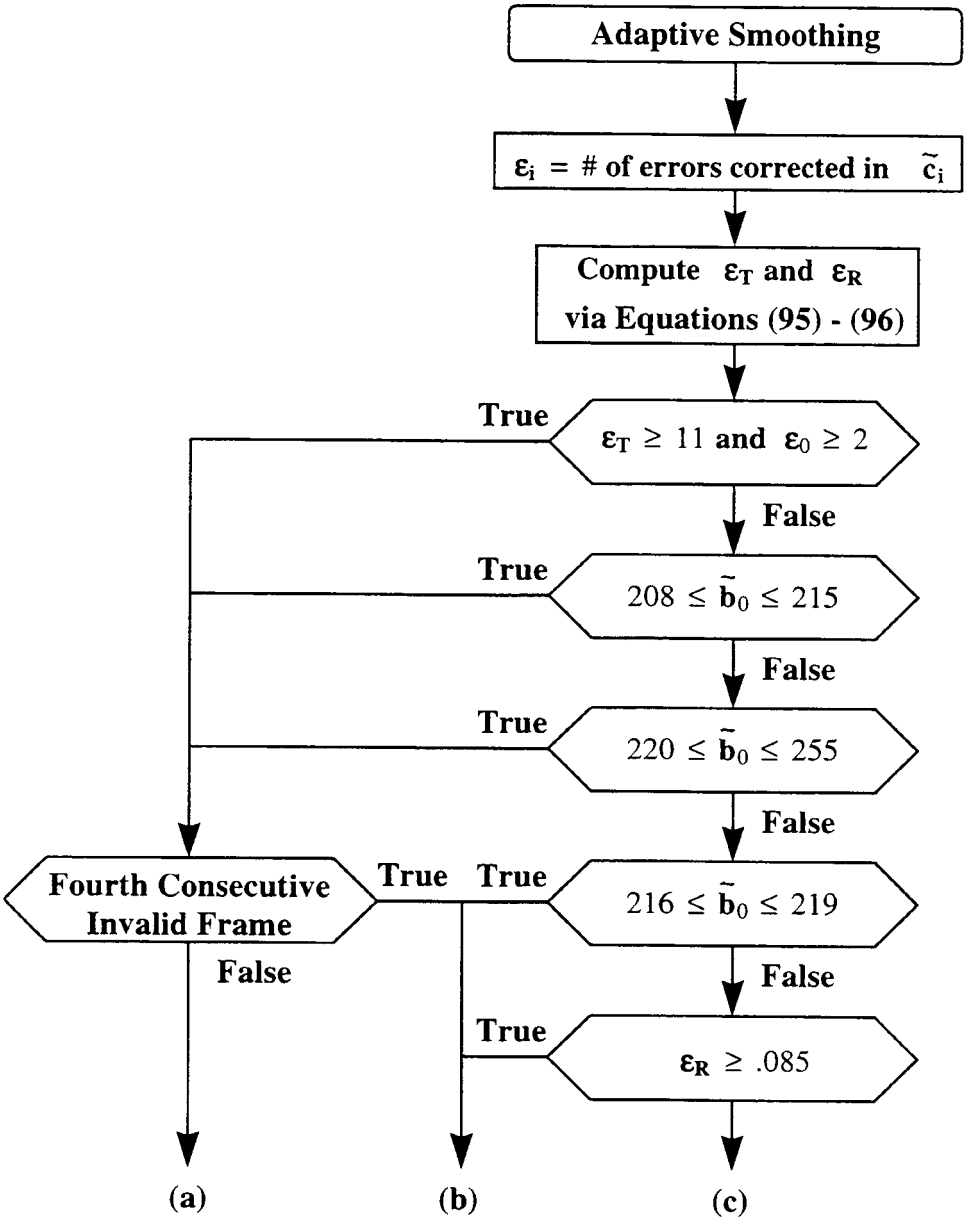

Flow Chart 9: Adaptive Smoothing (1 of 2)

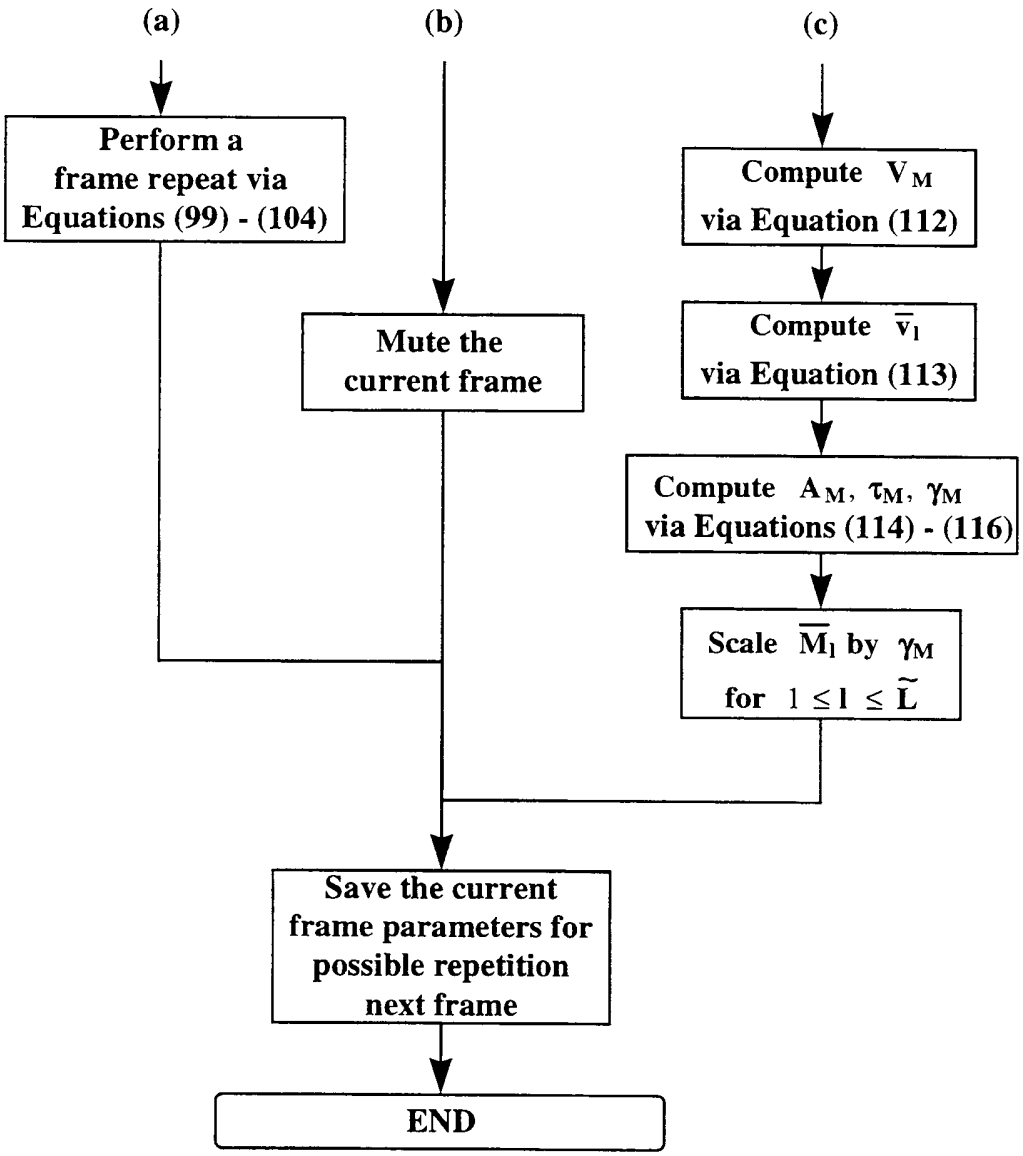

Flow Chart 9: Adaptive Smoothing (2 of 2)

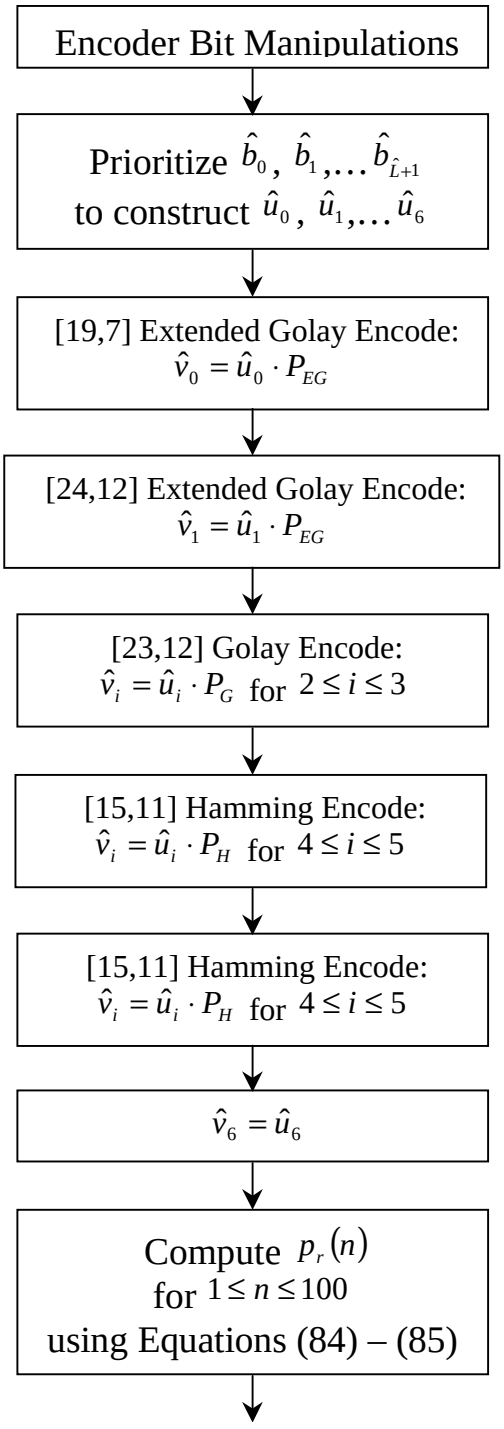

(a)

Flow Chart 10: Encoder Bit Manipulations (1 of 2)

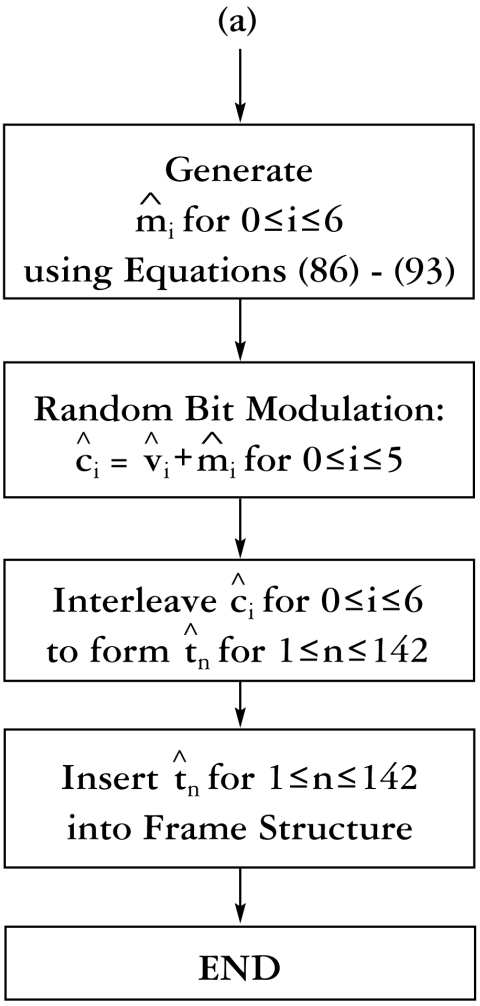

Flow Chart 10: Encoder Bit Manipulations (2 of 2)

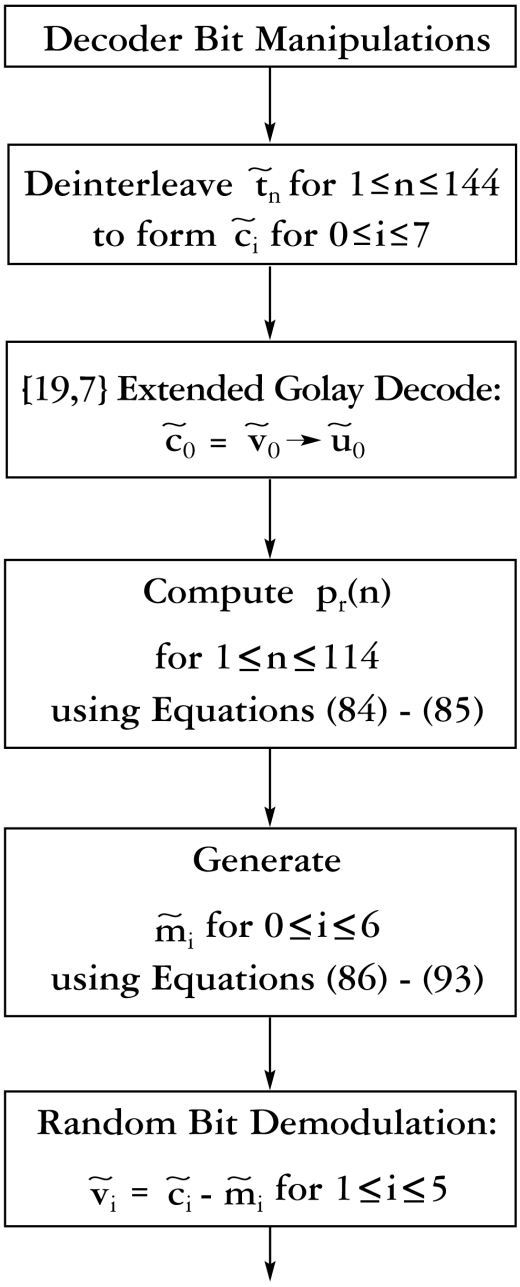

Flow Chart 11: Decoder Bit Manipulations (1 of 2)

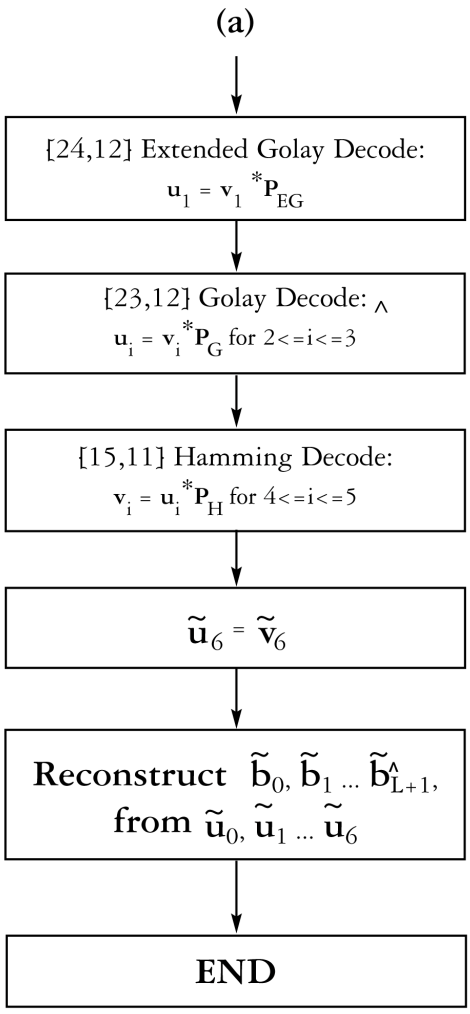

Flow Chart 11: Decoder Bit Manipulations (2 of 2)

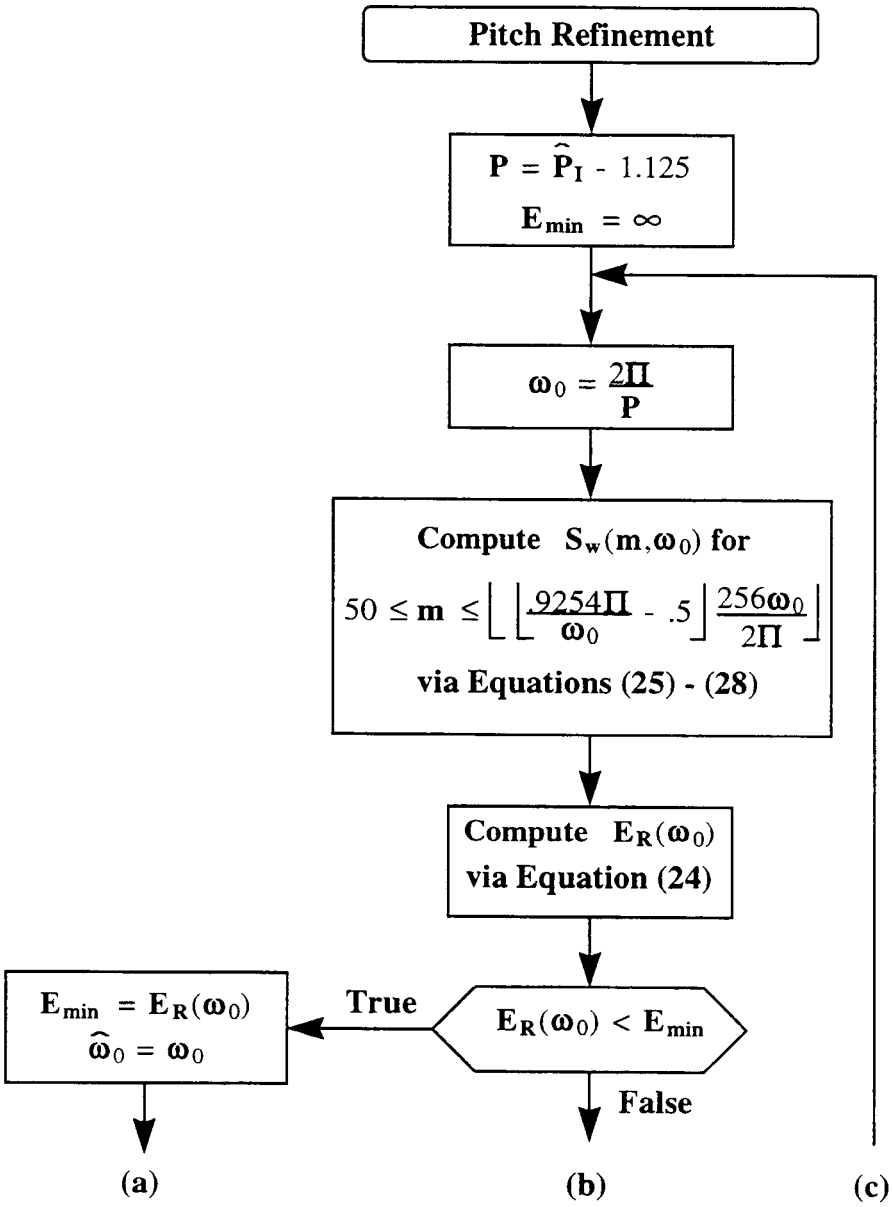

Flow Chart 12: Pitch Refinement (1 of 2)

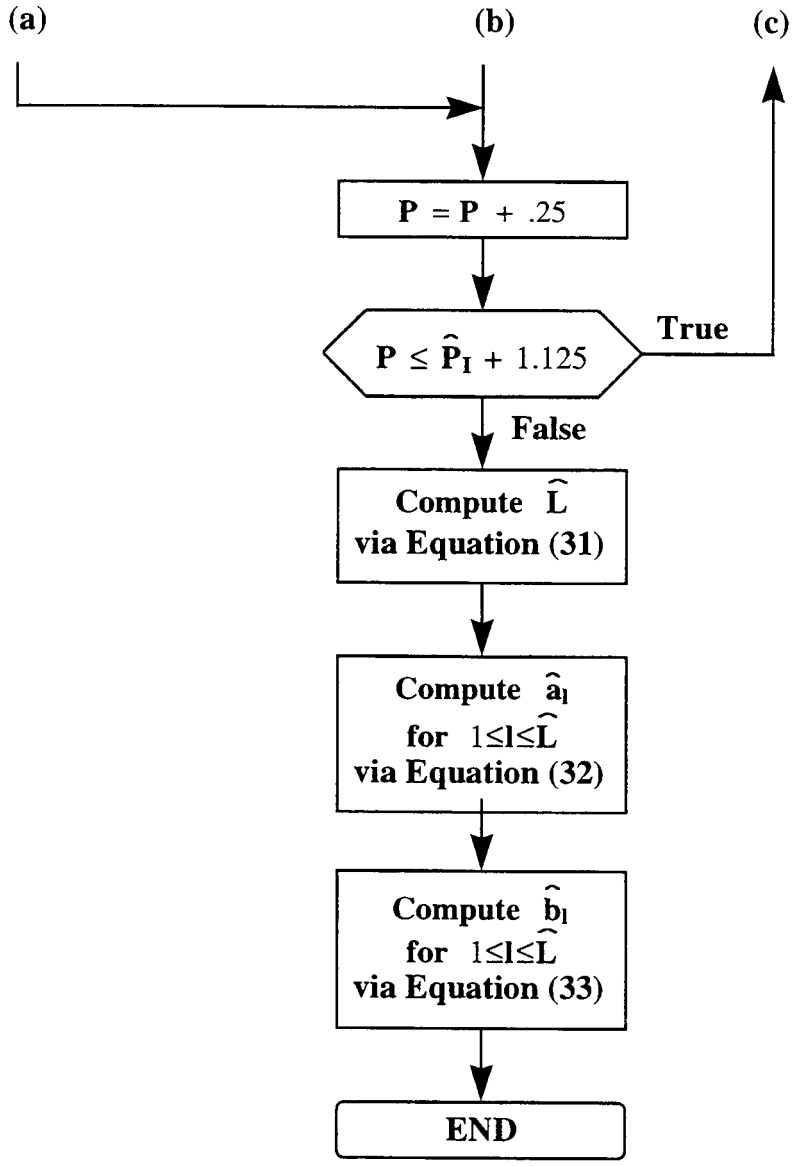

Flow Chart 12: Pitch Refinement (2 of 2)

References

[1] L. B. Almeida and F. M. Silva, "Variable Frequency Synthesis: An Improved Harmonic Coding Scheme," *Proc. ICASSP 84*, San Diego, CA, pp. 289-292, March 1984.

[2] J. P. Campbell et. al., "The new 4800 bps Voice Coding Standard," *Proc. Mil. Speech Tech. 89*, Washington D.C., pp. 64-70, Nov. 1989.

[3] D. W. Griffin and J. S. Lim, "Multiband Excitation Vocoder," *IEEE Transactions on ASSP*, Vol. 36, No. 8, August 1988.

[4] D. W. Griffin and J. S. Lim, "Signal Estimation From Modified Short-Time Fourier Transform," *IEEE Transactions on ASSP*, Vol. 32, No. 2, pp. 236-243, April 1984.

[5] J. C. Hardwick and J. S. Lim, "A 4800 bps Improved Multi-Band Excitation Speech Coder," *Proc. of IEEE Workshop on Speech Coding for Tele.*, Vancouver, B.C., Canada, Sept 5-8, 1989.

[6] J. C. Hardwick, "A 4.8 Kbps Multi-Band Excitation Speech Coder," *S.M. Thesis*, E.E.C.S Department, M.I.T., May 1988.

[7] N. Jayant and P. Noll, *Digital Coding of Waveforms*, Prentice-Hall, 1984.

[8] A. Levesque and A. Michelson, *Error-Control Techniques for Digital Communication*, Wiley, 1985.

[9] Lin and Costello, *Error Control Coding: Fundamentals and Applications*, Prentice-Hall, 1983.

[10] W. Press et. al., *Numerical Recipes in C*, Cambridge University Press, 1988.

[11] A. Oppenheim and R. Schafer, *Discrete Time Signal Processing*, Prentice-Hall, 1989.